Turun yliopisto
University of Turku

UNRAVELING THE FUNCTIONAL DIVERGENCE OF MEMBRANE-BOUND PYROPHOSPHATASES

Heidi Luoto

TURUN YLIOPISTON JULKAISUJA – ANNALES UNIVERSITATIS TURKUENSIS
Sarja - ser. AI osa - tom. 513 | Astronomica - Chemica - Physica - Mathematica | Turku 2015

University of Turku

Faculty of Mathematics and Natural Sciences
Department of Biochemistry

Supervised by

Professor, Ph.D., Reijo Lahti
Department of Biochemistry
University of Turku
Turku, Finland

Ph.D. Anssi Malinen
Department of Biochemistry,
University of Turku
Turku, Finland

Professor, Ph.D., Alexander A. Baykov
A.N. Belozersky Institute of Physico-Chemical Biology
Moscow State University
Moscow, Russia

Reviewed by

Associate Professor, Ph.D., Blanca Barquera
Department of Biological Sciences
Rensselaer Polytechnic Institute
Troy, NY, the United States

Head of laboratory, Ph.D. Manuela M. Pereira
Instituto de Tecnologia Química e Biológica
Universidade Nova de Lisboa
Oeiras, Portugal

Opponent

Professor, Ph.D., Volker Müller
Molecular Microbiology & Bioenergetics
Institute of Molecular Biosciences
Goethe-University Frankfurt
Frankfurt, Germany

The originality of this thesis has been checked in accordance with the University of Turku quality assurance system using the Turnitin OriginalityCheck service.

ISBN 978-951-29-6093-4 (PRINT)
ISBN 978-951-29-6094-1 (PDF)
ISSN 0082-7002
Painosalama Oy - Turku, Finland 2015

The End is the New Beginning

To my Dear Family and Friends

CONTENTS

LIST OF ORIGINAL PUBLICATIONS

The thesis is based on the following publications, referred in the text by Roman numerals.

I Luoto, H. H., Belogurov, G. A., Baykov, A. A., Lahti, R., Malinen, A. M. 2011. Na^+-translocating membrane pyrophosphatases are widespread in the microbial world and evolutionarily preceded H^+-translocating pyrophosphatases. *J. Biol. Chem.* **286**:21633–21642, doi: 10.1074/jbc.M111.244483.

II Luoto, H. H., Baykov, A. A., Lahti, R., Malinen, A. M. 2013. Membrane-integral pyrophosphatase subfamily capable of translocating both Na^+ and H^+. *Proc. Natl. Acad. Sci. USA* **110**:1255–1260. doi: 10.1073/pnas.1217816110.

III Luoto, H. H., Nordbo, E., Baykov, A. A., Lahti, R. & Malinen, A. M. 2013. Membrane Na^+-pyrophosphatases can transport protons at low sodium concentrations. *J. Biol. Chem.* **288**:35489–35499, doi: 10.1074/jbc.M113.510909.

IV Luoto, H. H., Nordbo, E., Malinen, A. M., Baykov, A. A. & Lahti, R. 2015. Evolutionary divergent, Na^+-regulated H^+-transporting membrane-bound pyrophosphatases. *Biochem. J.* **467**:281–291, doi: 10.1042/BJ20141434

ABSTRACT

Inorganic pyrophosphatases (PPases) are enzymes that hydrolyze pyrophosphate (PP_i) which is produced as a byproduct in many important growth related processes e.g. in the biosynthesis of DNA, proteins and lipids. PPases can be either soluble or membrane-bound. Membrane-bound PPases (mPPases) are ion transporters that couple the energy released during PP_i hydrolysis to Na^+ or H^+ transport.

When I started the project, only three Na^+-transporting mPPases were known to exist. In this study, I aimed to confirm if Na^+-transport is a common function of mPPases. Furthermore, the amino acid residues responsible for determining the transporter specificity were unknown. I constructed a phylogenetic tree for mPPases and selected the representative bacterial and archaeal mPPases to be investigated. I expressed different prokaryotic mPPases in *Escherichia coli*, isolated these as inverted membrane vesicles and characterized their functions. In the first project I identified four new Na^+-PPases, two K^+-dependent H^+-PPases and one K^+-independent mPPase. The residues determining the transporter specificity were identified by site-directed mutagenesis. I showed that the conserved glutamate residues are important for specificity, though are not the only residues that influence it. This research clarified the ion transport specificities throughout the mPPase phylogenetic tree, and revealed that Na^+ transport is a widespread function of mPPases. In addition, it became clear that the transporter specificity can be predicted from the amino acid sequence in combination with a phylogenetic analysis.

In the second project, I identified a novel class of mPPases, which is capable of transporting both Na^+ and H^+ ions and is mainly found in bacteria of the human gastrointestinal tract. The physiological role of these novel enzymes may be to help the bacteria survive in the demanding conditions of the host.

In the third project, I characterized the *Chlorobium limicola* Na^+-PPase and found that this and related mPPases are able to transport H^+ ions at subphysiological Na^+ concentrations. In addition, the H^+-transport activity was shown to be a common function of all studied Na^+-PPases at low Na^+ concentrations. I observed that mutating gate-lysine to asparagine eliminated the H^+ but not the Na^+ ion transport function, indicating the important role of the residue in the transport of H^+.

In the fourth project, I characterized the unknown and evolutionary divergent mPPase clade of the phylogenetic tree. The enzymes belonging to this clade are able to transport H^+ ions and, based on their sequence, were expected to be K^+- and Na^+-independent. The sequences of membrane-bound PPase are usually highly conserved, but the enzymes belonging to this clade are more divergent and usually contain 100−150 extra amino acid residues compared to other known mPPases. Despite the vast sequence differences, these mPPases have the full set of important residues and, surprisingly, are regulated by Na^+ and K^+ ions. These enzymes are mainly of bacterial origin.

TIIVISTELMÄ

Pyrofosfataasit (PPaasit) ovat entsyymejä, jotka vapauttavat energiaa pyrofosfaatti-nimisestä (PP_i) molekyylistä. Nämä entsyymit voivat olla soluissa liukoisina tai membraaneihin kiinnittyneinä. Membraanilla kiinni olevien PPaasien (mPPaasien) tehtävänä on siirtää Na^+- tai H^+-ioneja kalvon läpi PP_i:sta vapautetun energian avulla, tai ne voivat muodostaa pyrofosfaattia ionigradienttien avulla. Täten mPPaasit toimivat tärkeinä solun energiatalouden säätelijöinä. Lisäksi, nämä entsyymit ovat bioteknologisesti tärkeitä työkaluja, joiden avulla voidaan tuottaa kasvilinjoja, jotka ovat satoisia ja jotka kasvavat hyvin haastavissa olosuhteissa, kuten suolaisessa ympäristössä. Koska mPPaaseja ei ole ihmisellä, mutta koska niitä on esimerkiksi malariaa aiheuttavalla alkueliöllä, on niiden toiminnan tunteminen tärkeää myös lääkeaineiden suunnittelun kannalta.

Kun aloitin väitöstutkimukseni, Na^+-ioneja siirtävät mPPaasit oli vasta löydetty, eikä tiedetty, onko Na^+-ionin siirto yleinen mPPaasien toiminto. Halusin myös selvittää, mitkä aminohapot säätelevät mPPaasien ionien siirron spesifisyyttä. Tutkimuksen alussa rakensin mPPaasien evoluutiota kuvaavan fylogeneettisen puun ja valitsin puun tutkimattomista osista esitumallisten mPPaaseja tutkimuksen kohteeksi. Ilmensin mPPaasit *Escherichia coli* -soluissa ja eristin ne kalvovesikkeleihin. Vesikkeleistä tutkin entsyymin toimintaa. Ensimmäisessä osatyössä löysin neljä uutta Na^+-PPaasia, kaksi uutta K^+-riippuvaista H^+-PPaasia ja K^+-riippumattoman mPPaasin. Tutkin ionin siirrossa tarvittavia aminohappoja mutaatioanalyysin avulla ja osoitin, että evoluutiossa hyvin säilyneet glutamaatti-aminohapot ovat tärkeitä ionin siirrossa. Osoitin myös, että Na^+-ionin siirto on mPPaasien yleinen toiminto ja kehitin menetelmän, jonka avulla mPPaasien ionin siirron spesifisyys voidaan luotettavasti ennustaa aminohapposekvenssin ja fylogeneettisen analyysin perusteella.

Toisessa osatyössä löysin uuden mPPaasi-perheen, jonka jäsenet pystyvät pumppaamaan sekä Na^+- että H^+-ioneja. mPPaasien on aiemmin havaittu toimivan bakteerien stessiensietokyvyn säätelyssä ja nämä uudet mPPaasit ovat pääosin peräisin ihmisen ruuansulatuskanavan bakteereilta. Na^+,H^+-PPaasien tehtävänä on mahdollisesti lisätä bakteerien kykyä selviytyä ruuansulatuskanavan haastavissa olosuhteissa.

Kolmannessa osatyössä tutkin *Chlorobium limicola* -bakteerin Na^+-PPaasin toimintaa ja havaitsin, että se pystyy siirtämään H^+-ioneja matalissa Na^+-ionipitoisuuksissa. Tutkimuksessa tehtiin myös mutaatioanalyysi, ja havaittiin, että membraani-PPaaseilla tietty, evolutiossa hyvin säilynyt lysiini aminohappo on välttämätön Na^+-PPaasien H^+ ionien siirrossa.

Membraani-PPaasit ovat säilyneet evoluution kuluessa hyvin samanlaisina, mutta on olemassa yksi mPPaasien alaperhe, joka poikkeaa muista perheistä aminohappojärjestykseltään. Havaitsin näitä mPPaaseja olevan 46 bakteerilla ja yhdellä arkkibakteerilla ja osoitin niiden toimivan K^+- ja Na^+-ioneilla säädeltävinä H^+-PPaaseina. Väitöskirjatutkimukseni kokeellisten tulosten ja mPPaasien fylogenetiikan perusteella kehitin mallin, joka kuvaa mPPaasien evoluutiota.

ABBREVIATIONS

ABA	Abscisic acid
ACMA	9-Amino-6-chloro-2-methoxyacridine
Ac-PPase	*Anaerostipes caccae* Na^+-pyrophosphatase
Am-PPase	*Akkermansia muciniphila* Na^+,H^+-pyrophosphatase
AVP	*Arabidopsis thaliana* H^+-pyrophosphatase
Aw-PPase	*Acetobacterium woodii* Na^+-pyrophosphatase
AMDP	Aminomethylenediphosphonate
AO	Acridine orange
ATP	Adenosine triphosphate
BA	6-Benzyladenine
BPB	4-Bromophenacyl bromide
Bv-PPase	*Bacteroides vulgatus* Na^+,H^+-pyrophosphatase
CAPSO	3-(Cyclohexylamino)-2-hydroxy-1-propanesulfonic acid
CBS	Cystathionine-beta-synthase
CCCP	Carbonyl cyanide 3-chlorophenylhydrazone
Cf-PPase	*Cellulomonas fimi* divergent H^+-pyrophosphatase
Ch-PPase	*Carboxydothermus hydrogenoformans* H^+-pyrophosphatase
Cl-PPase	*Chlorobium limicola* Na^+-pyrophosphatase
Cl-PPase(2)	*Chlorobium limicola* divergent H^+-pyrophosphatase
Clep-PPase	*Clostridium leptum* Na^+,H^+-pyrophosphatase
Clen-PPase	*Clostridium lentocellum* Na^+,H^+-pyrophosphatase
Cs-PPase	*Clostridium* sp.7_2_43FAA Na^+-pyrophosphatase
Ctet-PPase	*Clostridium tetani*_E88 Na^+-pyrophosphatase
Ct-PPase	*Clostridium thermocellum* membrane-bound pyrophosphatase
Da-PPase	*Desulfuromonas acetoxidans* Na^+-pyrophosphatase
DEPC	Diethyl pyrocarbonate
DCCD	*N,N'*-Dicyclohexylcarbodiimid
DDM	Dodecyl-β-maltopyranoside
DM	Decyl-β-maltopyranoside
$DiBAC_4(3)$	Bis-(1,3-dibutylbarbituric acid)trimethine oxonol
D-thio-M	Decyl-β-thiomaltopyranoside

EGTA	Ethylene glycol-bis(2-aminoethylether)-*N,N,N',N'*-tetraacetic acid
EDTA	Ethylenediaminetetraacetic acid
ER	Endoplasmic reticulum
ETH157	*N,N'*-Dibenzyl-*N,N'*-diphenyl-1,2-phenylenedioxydiacetamide
Fj-PPase	*Flavobacterium johnsoniae* H^+-pyrophosphatase
FRET	Fluorescent resonance energy transfer
GA	Gibberellic acid
HAD	Haloacid dehalogenase
H^+-PPase	H^+ transporting membrane-bound pyrophosphatase
IDP	Imidodiphosphate
IMV	Inverted membrane vesicle
IPTG	Isopropyl β-D-1-tiogalactopyranoside
JA	Jasmonic acid
KF	Potassium fluoride
Lb-PPase	*Leptospira biflexa* H^+-pyrophosphatase
LUCA	Last universal common ancestor
MDA	Malonidialdehyde
MES	2-(*N*-Morpholino)ethanesulfonic acid
Mm-PPase	*Methanosarcina mazei* Na^+-pyrophosphatase
Mt-PPase	*Moorella thermoacetica* Na^+-pyrophosphatase
MOPS	3-(*N*-Morpholino)propanesulfonic acid
Na^+-PPase	Na^+ transporting membrane-bound pyrophosphatase
NEM	*N*-Ethylmaleimide
NG	Nonyl-β-glucoside
NM	Nonyl-β-maltopyranoside
NO	Nitric oxide
OGNPG	Octyl glucose neopentyl glycol
OVP	*Oryza sativa* H^+-pyrophosphatase
Pa-PPase	*Pyrobaculum aerophilum* H^+-pyrophosphatase
PEG	Polyethyleneglycol
P_i	Phosphate
PM	Plasma membrane
PP_i	Pyrophosphate

Po-PPase	*Prevotella oralis* Na^+,H^+-pyrophosphatase
PPase	Pyrophosphatase
PSV	Protein storage vacuole
RT	Room temperature
Sc-PPase	*Streptomyces coelicolor* H^+-pyrophosphatase
SDS	Sodium dodecylsulphate
S.D.	Standard deviation
S.E.	Standard error
TAPS	*N*-[Tris(hydroxymethyl)methyl]-3 aminopropanesulfonic acid
Tm-PPase	*Thermotoga maritima* Na^+-pyrophosphatase
TM	Transmembrane helix
TMA hydroxide	Tetramethylammonium hydroxide
TMA chloride	Tetramethylammonium chloride
TMA_4•PP_i	Tetramethylammonium pyrophosphate
UDM	Undecyl-β-maltopyranoside
Vb-PPase	*Verrucomicrobiae bacterium* Na^+-pyrophosphatase
Vr-PPase	*Vigna radiata* H^+-pyrophosphatase

ABBREVIATIONS OF THE AMINO ACID RESIDUES

A	Ala	Alanine
C	Cys	Cysteine
D	Asp	Aspartic acid
E	Glu	Glutamic acid
F	Phe	Phenylalanine
G	Gly	Glycine
H	His	Histidine
I	Ile	Isoleucine
K	Lys	Lysine
L	Leu	Leucine
M	Met	Methionine
N	Asn	Asparagine
P	Pro	Proline
Q	Gln	Glutamine
R	Arg	Arginine
S	Ser	Serine
T	Thr	Threonine
V	Val	Valine
W	Trp	Tryptophan
Y	Tyr	Tyrosine

1. INTRODUCTION

This doctoral thesis focuses on membrane-bound pyrophosphatases (mPPases) - their function and evolution. First, I will briefly describe pyrophosphate (PP_i), the substrate of PPases, and then review the information available on PPases, focusing on membrane-bound PPases and their role in cellular bioenergetics. I will also summarize the available functional, structural, mechanistical and physiological information on mPPases. In the later sections, I will concentrate on the observations I made during my PhD studies. The most important results of this thesis was the discovery of a novel group of mPPases capable of transporting both Na^+ and H^+ ions under physiological conditions.

1.1 Pyrophosphate (PP_i)

Pyrophosphate (PP_i) is a byproduct of almost 200 biologically important synthesis reactions (e.g. DNA, RNA, protein, amide and lipid synthesis), which are coupled to the conversion of a nucleotide triphosphate (NTP) into a nucleoside monophosphate and PP_i (1). PP_i can also be synthesized *in vivo* from phosphate, driven by ion gradients, and photosynthetic bacteria synthesize PP_i in the chromatophore membrane (1). PP_i is a simple molecule composed of two phosphate (P_i) residues. PP_i may have been produced very early in the evolution of life, before ATP (2), as PP_i is produced abiotically under conditions resembling the conditions of the early Earth (3). In addition to PP_i, phosphates may also form longer chains - triphosphates and longer polyphosphates (4).

The energy released during PP_i hydrolysis ($-\Delta G° = 20–25$ kJ mol^{-1}) is ~60% of the energy released by ATP hydrolysis ($-\Delta G° = 35$ kJ mol^{-1}), and PP_i is used as an alternative energy supply when ATP levels are low (5-7). The maintenance of PP_i/ATP and P_i/PP_i ratios is important for the function and growth of the cell (8, 9). The PP_i/ATP ratios change with the growth phase of the cell (8, 10, 11). PP_i concentration is regulated by several enzymes (12-15) and it is normally 0.5−1.5 mM in the bacterial cytosol (1). In plants, PP_i concentration varies between 0.01 and 0.8 mM (16, 17), but it does not change during dark/light transitions (10, 11). High PP_i concentration is generally toxic to cells, because it inhibits the synthesis of macromolecules (1, 5, 12, 18). PP_i forms complexes with Mg^{2+} ions (1, 19, 20), but it also binds with lower affinity to Ca^{2+} and with much lower affinity to Na^+ and K^+ (21, 22). Important regulators of the PP_i level include soluble pyrophosphatases (PPases) and membrane-bound pyrophosphatases (mPPases) that hydrolyze PP_i (20, 23, 24).

1.2 Pyrophosphatases (PPases)

PPases are enzymes that hydrolyze PP_i into two P_is and release energy as heat or use it for ion transport (7, 23, 24). A total of four different PPase families have been discovered: families I, II, and III of soluble PPases and a superfamily of membrane-bound PPases (mPPases). Family I and II PPases accelerate PP_i hydrolysis by a factor of 10^{10}, when

compared to the uncatalyzed reaction (23). Family II PPases have DHH domains and are members of the DHH phosphodiesterase superfamily (25). Some family II PPases have additional regulatory cystathionine-beta-synthase (CBS) and DRTGG domains (26). Family III PPases belong to a group of soluble haloacid dehalogenases (HAD) (24, 27). mPPases are ion transporters in which PP_i hydrolysis drives Na^+ or H^+ ion transport against the electrochemical gradients (24, 28-31). In addition, both soluble and membrane-bound PPases synthesize PP_i under low PP_i conditions and mPPases couple ion gradients to the synthesis of PP_i (31-35).

PPases are a structurally versatile group of enzymes (Fig. 1). The first family I PPase was discovered in 1928 (36) and its first 3D-structure was solved in 1981 by Harutyunyan *et al*. (37) (Fig. 1A). Family I PPases are generally homodimers in eukaryotes and homohexamers in prokaryotes (23, 38-41). The subunits of eukaryotic family I PPases are larger than their prokaryotic counterparts, but both have very similar and highly conserved active site structures (23, 37, 42-44). Family I enzymes, especially those from *Escherichia coli* and *Saccharomyces cerevisiae*, have been extensively studied by structural, mechanistic and mutational analyses (37, 43-55). Family II PPases were discovered in 1998 (56, 57) and their first 3D-structures were solved in 2001 (58, 59). Family II PPases are homodimers and exist in bacteria, archaea (58, 60, 61) and, very rearly, in eukaryotes (62). These enzymes are found in many pathogenic bacteria, but not in humans, suggesting that they are potential drug targets (63). Some family II PPases are regulated by reversible phosphorylation (64, 65). Family II CBS-PPases, discovered in 2007 by Jämsen *et al*., are regulated by adenine nucleotides (26). Salminen *et al.* (66) showed recently that AMP, ADP and ATP bind cooperatively to bacterial CBS-PPases. CBS-PPases may thus sense the energy state of the cell and regulate cellular PP_i levels accordingly (66). The CBS domain is conserved and found in thousands of various types of proteins in all kingdoms of life (67). Many human hereditary diseases are caused by mutations in CBS domains (26, 68). There is currently only a structural model available for CBS-PPases (69), and so the 3D-structure remains to be solved. Family III PPases, the HAD superfamily, are dimers and are found only in certain bacteria (27, 70) (Fig. 1C). The membrane-bound PPases were discovered almost 50 years ago by Baltscheffsky *et al.* (29, 31), but the first 3D-structures for a H^+-PPase and Na^+-PPase, were solved in 2012 (Fig. 1D) (71, 72).

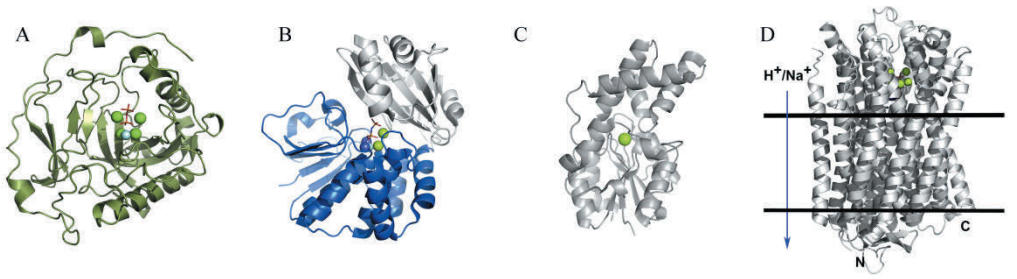

Figure 1. Structures of the subunits of different PPase families show that these enzymes are not structurally related to each other. A. Soluble family I PPase of yeast (1E6A) (47). B. Soluble family II PPase of *B. subtilis* (2HAW) (73). C. Soluble family III PPase of *B. thetaiotamicron* (3QU2) (70). D. Membrane-bound PPase of *Vigna radiata* (4A01) (72). The figure was modified from Kajander *et al*. (24). (Reprinted and adapted from *FEBS Lett.* 587, 13, Kajander, T. *et al.*, Inorganic pyrophosphatases: One substrate, three mechanisms, 1863−9, Copyright (2013), with permission from Elsevier).

All PPases are activated by Mg^{2+} ions, but the soluble family II enzymes, including CBS-PPases, are most active when both Mg^{2+} and a transition metal ion (Mn^{2+} or Co^{2+}) are present (23, 24, 26, 61, 74, 75). In addition, family III enzymes differ from other PPases, because the non-physiological Ni^{2+} activates their function more than Mg^{2+} (27). PPases catalyze PP_i hydrolysis with different velocities as is shown by their k_{cat} values: family I 200−400 s^{-1} (76), family II 1700−3000 s^{-1} (61), family III 0.16−0.22 s^{-1} (27) and membrane-bound PPases 3.5−20 s^{-1} (77-79). Furthermore, family II PPases with CBS domains usually have a lower hydrolysis activity than other family II PPases (26). Family III PPases hydrolyze PP_i at an extremely low rate, suggesting that PP_i hydrolysis may not be their main function and thus, it is still controversial, whether these enzymes should even be called PPases.

The mechanisms of PP_i binding and hydrolysis are quite different for the soluble PPases of families I and II and the membrane-bound PPases, due to differences in the active sites of these enzymes (Fig. 2) (24, 47, 59, 72). The extensively studied family I PPases have an active site containing conserved Asp, Lys and Tyr residues (Fig. 2A) that coordinate the binding of four metal ions (M1−M4) (23, 24, 42). Family I PPases catalyse the hydrolysis of PP_i in a six-state process (23, 47-49, 54, 80). Metal ion binding activates the enzyme, and substrate binding induces isomerization of the enzyme-substrate complex (47, 49, 54, 55). M1 and M2, together with a conserved aspartate residue, enable the formation of the nucleophile that drives PP_i hydrolysis (23, 24, 47). In family II PPases, PP_i hydrolysis site is located between N- and C-terminal domains (58, 59, 73, 74), and histidine residues are required for the coordination of a trimetal center (24, 73, 81). Substrate binding induces a change in the coordination number of one metal ion from five to six, explaining why Mn^{2+} or Co^{2+} is preferred instead of Mg^{2+} (Fig. 2B) (24, 73, 81). In mPPases, PP_i is hydrolyzed at the entrance to the acidic coupling funnel formed by conserved aspartate and lysine residues (30, 71, 72).

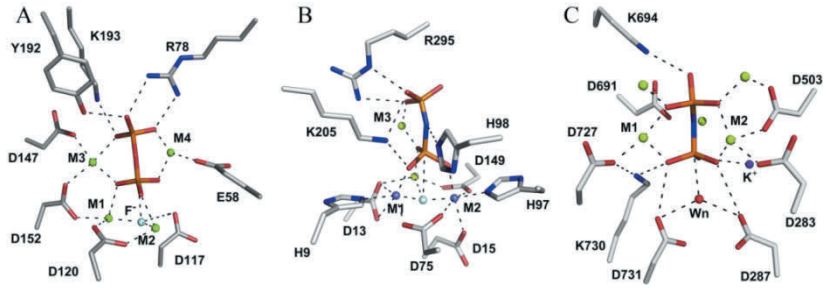

Figure 2. PP_i binding to the active site of soluble and membrane-bound PPases with an attached Mg^{2+} (green), Mn^{2+} (light violet), K^+ (violet), nucleophilic water (Wn, red) and F^- (light blue). A. Soluble family I PPase of yeast, B. Soluble family II PPase of *B. subtilis*, C. Membrane-bound PPase of *V. radiata*. The figure was modified from Kajander *et al.* (24). (Reprinted from *FEBS Lett.* 587, 13, Kajander, T. *et al*., Inorganic pyrophosphatases: One substrate, three mechanisms, 1863−9, Copyright (2013), with permission from Elsevier).

1.3 Bioenergetics and the early evolution of mPPases

The first law of bioenergetics states that living organisms produce a high energy compound, ATP, from molecules imported into the cell (82). The energy stored in ATP can be used

to drive essential cellular processes, including the secondary transport of molecules and temperature control (82, 83). ATP is synthesized by ATP synthase using H^+ ($\Delta\mu_{H}^{+}$) or Na^+ ($\Delta\mu_{Na}^{+}$) transmembrane difference of electrochemical potential as an energy source. The $\Delta\mu_{H}^{+}$ and $\Delta\mu_{Na}^{+}$ have two components a difference in electrical potentials ($\Delta\Psi$) and a difference in the concentrations of protons or sodium ions (ΔpH or ΔpNa) across the membrane (82, 84). H^+-based bioenergetics is common to all kingdoms of life and Na^+-based bioenergetics is used by eukaryotic plasma membranes and certain bacteria (82, 85, 86). Furthermore, bacteria use Na^+-based bioenergetics to be able to live in marine, highly saline or alkaline conditions or at high temperatures (82, 85, 87, 88). Na^+-based bioenergetics is important when energy is limited, and e.g. *Acetobacterium woodii* uses Na^+-based anaerobic caffeate respiration when ATP levels are low (86). In addition, certain pathogenic organisms use Na^+-based bioenergetics to survive in the demanding conditions of the host organism, e.g. *Clostridium tetani* (88-90). Anaerobic archaea prefer Na^+ as a coupling ion in substrate and energy limited conditions (91, 92), because during anaerobic growth the fermentation processes create weak acids that can act as protonophores and destroy H^+ gradients (93, 94). Some organisms, including methanogens, can utilize either H^+ and Na^+ gradients or both in ATP synthesis, depending on environmental conditions (92, 93, 95). Alkalophiles can synthesize ATP by H^+-based bioenergetics and maintain the low cytoplasmic pH compared to outside pH > 9.5 using a Na^+-gradient (96).

In photosynthetic membranes, $\Delta\mu_{H}^{+}$ is created by photosynthetic energy generators, e.g. bacteriochlorophylls or photosystem I and II, or by respiratory chains (82). In mitochondrial membranes and also in the plasma membrane of certain bacteria $\Delta\mu_{H}^{+}$ is created by the NADH:CoQ-oxidoraductase complex (complex I) (97), ubiquinol-cytochrome c oxidoreductase (complex III) and cytochrome c oxidase (complex IV) and is used for ATP synthesis by ATP synthase (82). $\Delta\mu_{H}^{+}$ can also drive the rotation of bacterial flagella and provide energy for bacterial movement (82, 98, 99). In plant vacuoles, the H^+-gradient synthesized by H^+-transporting ATPases and mPPases is used to drive the secondary transport of compounds and the regulation of cytosolic and vacuolar pH (100). $\Delta\mu_{Na}^{+}$ can be generated by Na^+-translocating NADH:quinone-oxidoreductases, Na^+-decarboxylases, O_2 reductases, Na^+-motive methyltransferase complexes, Na^+-motive formylmethanofuran dehydrogenases, Na^+/K^+-ATPases, Na^+-ATPases and Na^+-PPases (82, 85, 86, 90, 94, 97, 101).

The cellular ATP and PP_i levels are interconnected. In many ATP dependent processes PP_i is released as a byproduct, and mPPase may use it further to contribute to the establishment of the membrane potential (82, 102). The $\Delta\mu_{H}^{+}$ created by mPPase-catalyzed PP_i hydrolysis can be employed by an ATP synthase for ATP generation or for other energy conversion processes (31, 103-105). PP_i is required for the maintenance of proton gradients, especially under conditions of low energy e.g. in during intensive growth or in darkness (16, 106-109). It has been shown that e.g. in *A. woodii* 3 mol of PP_i are hydrolyzed to synthesize 1 mol of ATP during caffeate respiration (86). Bacteria may regulate ATPases and mPPases differently during the day and night (110). *Rhodospirillum rubrum* H^+-PPase (Rr-PPase) synthesizes PP_i when grown in light, but

the synthesis is decreased in dark (31, 33, 111, 112). The rate of PP_i synthesis in high light is 25% of the rate of ATP synthesis, but in low light the rate of PP_i synthesis can exceed the rate of ATP synthesis (112).

Various theories have been presented to describe how life emerged on Earth (113-115). PP_i is a simple molecule and the only known alternative for ATP, implying an ancestral role (103, 116). Holm & Baltscheffsky (2) suggested that PP_i may have been formed very early in evolution, and Russell *et al.* (117) showed that PP_i could have been synthesized by PPases under the conditions where life may have originated. PP_i may have first provided the energy for cellular processes and was later replaced by ATP (2, 118). Furthermore, their much simpler structure suggests that mPPases are the predecessors of ATPases in evolution (2, 118). ATPases are present in all kingdoms of life where they are vital for cellular energy-linked functions, unlike the mPPases that provide a backup system for ATPases. mPPases are usually present and active under stressful conditions and in bacteria, archaea and plants that live under environmentally challenging conditions (2, 118, 119).

mPPases may be of an ancient origin, and their amino acid sequence contains the amino acid residues, Gly, Ala, Val and Asp, which are thought to be formed very early in evolution, and which form highly conserved and functionally important motifs in mPPases (116, 120). Furthermore, protein databases do not, based on sequence identity, contain any other enzymes related to mPPases (121). mPPases appear in acidocalcisome organelles that are thought to be present in the last universal common ancestor (LUCA) (122-124). Also evolutionarily old organisms, e.g. the extremophilic archaeon *Candidatus Korarchaeum cryptofilum*, contain mPPases (118).

There are also competing theories about the origin of bioenergetics and especially the specificity of the coupling ion, Na^+ or H^+ (2, 88, 125, 126). Na^+-based bioenergetics may have formed very early in evolution (85, 92) in highly saline environments and may have then been replaced by the more efficient H^+-based bioenergetics on multiple occasions (84, 88, 126). One indication for the "Na^+-first" hypothesis is that Na^+ permeable membranes may be more easily achieved than H^+-permeable membranes, suggesting that membrane evolution has directed the evolution of membrane proteins (84, 88, 126, 127). Further evidence for the Na^+-first hypothesis is that Na^+ is utilized in bacteria living under extreme conditions e.g. at high pH and temperatures, that may resemble the conditions of the early Earth (88). On the protein level, Na^+ binding requires many conserved amino acid residues and has probably evolved only once during evolution of ATP synthases/ATPases (88, 92, 93, 126). Other theories suggest that H^+ ion based bioenergetics was created first (125, 128). Furthermore, enzymes involved in H^+-based bioenergetics are found in evolutionarily old organisms e.g. *C. Korarchaeum cryptofilum* (118). There was a view that, both Na^+ and H^+ ions may have been used as coupling ions in the ancestral cells (129). There are also organisms that can use both Na^+- and H^+-based bioenergetics e.g. methanogens and alkalophiles (92, 95, 96). The evolution of the transporter specificity is also controversial and remains to be clarified.

1.4 Characterization of mPPases

Membrane-bound PPases hydrolyze PP_i and couple the released energy to the active transport of H^+ or Na^+ ions (28) or they form PP_i using $\Delta\mu_{H}^{+}$ or $\Delta\mu_{Na}^{+}$ (29, 31). H^+-PPases were discovered in 1966 (29, 31), but Na^+-PPases were not discovered until 2007 (28). Already before the three-dimensional structures of mPPases were solved it was known that these enzymes are homodimers (130-136) and that high pressure dissociates dimeric H^+-PPases into monomers (137).

Lin *et al*. (72) and Kellosalo *et al.* (71) solved the 3D-structures of a H^+-PPase (at a 2.35 Å resolution, from *Vigna radiata*, [Vr-PPase] Fig. 3A) and a Na^+-PPase (2.6 Å, *Thermotoga maritima,* [Tm-PPase]) in 2012. The enzymes are homodimers with two-fold symmetry, and their monomers are made up of 16 long transmembrane helices (TMs). The dimensions of the complex are 75 Å in height and 85 Å in width, and the long TMs extend 25 Å from the membrane into the cytosol. Each monomer contains all of the residues important for PP_i hydrolysis and ion transport. In addition to the TMs, a mPPase has also two cytosolic α-helices, two luminal/periplasmic helices and two antiparallel β-sheets, and both the N- and C-terminus are oriented away from the cytoplasm (71, 72). The helices form two concentric rings and TMs 5, 6, 11, 12, 15 and 16 are located in the inner ring, and TMs 1, 2, 3, 4, 7, 8, 9, 10, 13, 14 form the outer ring (Fig. 3B). Transmembrane helices 5–6, 9–12 and 13–16 may have arisen via a gene triplication event (120, 138). The outer ring maintains the protein structure and the inner ring creates the funnel-shaped pocket, the coupling-funnel and the ion gate that are responsible for PP_i hydrolysis and ion transport (Fig. 3C). TMs 10, 13 and 15, the loop between TM 12 and 13, and the two short antiparallel β-sheets are involved in forming the monomer-monomer interface. Dimer formation includes interactions between amino acid residues Arg441, Val568, Val570, Tyr587, Arg609 (hydrogen bonds) and Arg441, Glu606 (salt bridges) (Vr-PPase numbering) (71, 72).

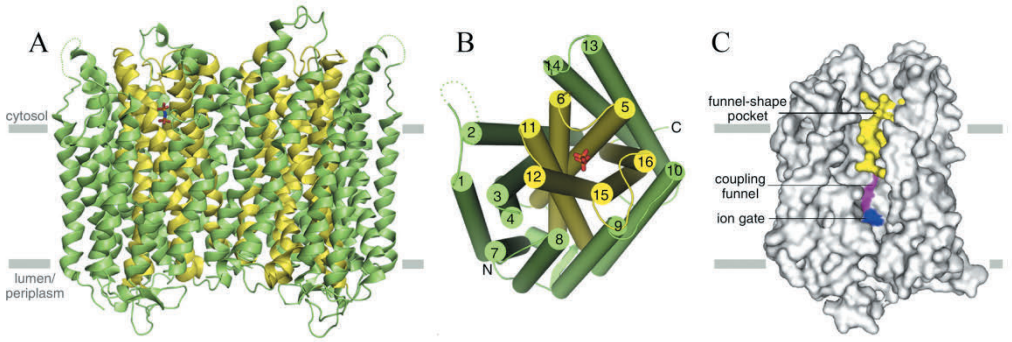

Figure 3. Three-dimensional structure of Vr-PPase. A. Dimeric Vr-PPase, PP_i hydrolysis occurs in the cytoplasmic side of the enzyme and the ions are transported from the cytosol into the periplasm or the lumen, depending on the organism. B. mPPase monomer forms two concentric rings, in which the inner helices (TMS 5, 6, 11, 12, 15, 16) are shown in yellow and the outer helices (TMs 1, 2, 3, 4, 7, 8, 9, 10, 13, 14) in green. C. PP_i is hydrolyzed in the acidic funnel pocket (yellow), and the coupling funnel (pink) and gate amino acid residues (blue) are important for the transport and specificity. Figure was modified from Tsai *et al.* (30). (Reprinted from *Curr. Opin. Struct. Biol*, 27, Tsai, J. Y. *et al.*, Proton/sodium pumping pyrophosphatases: the last of the primary ion pumps, 38−47, Copyrigh (2014), with permission from Elsevier).

1.4.1 Mg^{2+} and Mg_2PP_i binding to mPPases and PP_i hydrolysis

All mPPases require Mg^{2+} for their PP_i hydrolysis activity and the hydrolysis is regulated by Mg^{2+} (28, 31, 75, 124, 139-142). PP_i binds to Mg^{2+} and forms $MgPP_i$ and Mg_2PP_i complexes and the main substrate for mPPases is Mg_2PP_i (75, 143-149). Four Mg^{2+} ions, two free and two complexed with PP_i, are required for the hydrolysis reaction catalyzed by Na^+-PPases (139). Mg^{2+} binds to the enzyme almost independently of Mg_2PP_i binding (139). Based on mersalyl, (a membrane-impermeable cysteine modifying reagent) inactivation data, trypsin and structural studies Mg^{2+} binding to the low-affinity binding site causes a conformational change that is essential for PP_i hydrolysis (Fig. 4) (71, 72, 139). IDP and PP_i binding to mPPase induce similar conformational changes in the enzyme (30, 134). The P_i bound mPPase is in the resting state conformation (30, 134).

Based on the structures of mPPases, six TMs (5, 6, 11, 12, 15 and 16) form the hydrolytic center (Fig. 3A & B) (30, 71), which contained one bound imidodiphosphate (IDP, a PP_i analog) in the structure for Vr-PPase (Fig. 4) revealing the PP_i binding site. The PP_i binding site is highly conserved and acidic containing eleven aspartates and one glutamate residue (Asp253, Asp257, Glu268, Asp269, Asp279, Asp283, Asp287, Asp507, Asp691, Asp723, Asp727 and Asp731). It also contains one asparagine (Asn534), and three lysines (Lys250, Lys730 and Lys694) (Fig. 4) (30, 72).

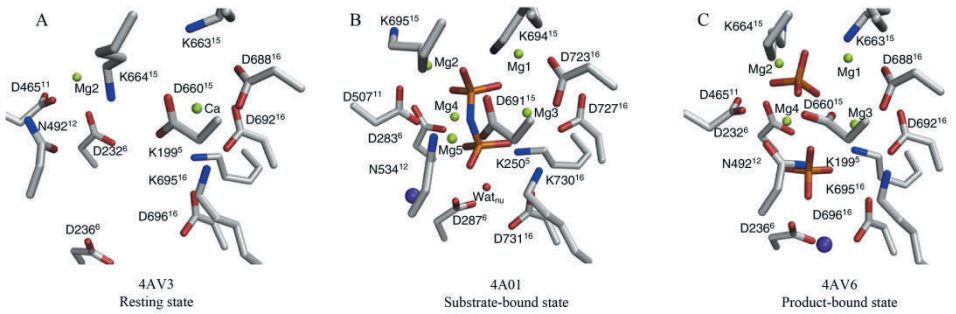

Figure 4. mPPase shown in the resting, substrate bound and product bound states. 4AV3 and 4AV6 are the structures of Tm-PPase at a 2.6 and a 4.0 Å resolution, respectively and 4A01 is Vr-PPase at a 2.35 Å resolution (71, 72, 138). The residues important for Mg^{2+} and imidodiphosphate (IDP, a PP_i analog) and P_i binding are shown and their charges, acidic or basic are coloured in red or blue, respectively. The superscript denotes the TM helix where the amino acid residue is located. Potassium is shown as a violet sphere. The figure was modified from Tsai *et al.* (30). (Reprinted from *Curr. Opin. Struct. Biol,* 27, Tsai, J. Y. *et al.,*Proton/sodium pumping pyrophosphatases: the last of the primary ion pumps, 38−47, Copyrigh (2014), with permission from Elsevier).

The 3D-structure of Tm-Na^+-PPase contained Ca^{2+} and Mg^{2+} ions coordinated to Asp688, Asp692, Asp660, Asp232 and Asp465 (Fig. 4A) (71). Vr-PPase is a K^+-dependent proton pumping enzyme, in which IDP (and PP_i) binding is enabled by five Mg^{2+} ions, one K^+ ion and three lysine amino acids (Lys250, Lys730 and Lys695) (Fig. 4B) (72). The five Mg^{2+} ions are coordinated to six aspartates and one asparagine residues [Mg^{2+}(1): Asp253, Asp257, Mg^{2+}(2): Asp507, Mg^{2+}(3): Asp253, Asp727, Mg^{2+}(4): Asp283, Asp507, Mg^{2+}(5): Asn534, Asp691] as well as water molecules (72). A nucleophilic water is required for the hydrolysis of PP_i (30). The low resolution structure of a Tm-PPase showed the enzyme in the P_i-bound state (Fig. 4C) (30).

In addition to Mg^{2+} other bivalent cations including Zn^{2+}, Co^{2+} and Ca^{2+} activate Rr-H^+-PPase (150, 151), but less efficiently. High concentrations of Zn^{2+} inhibit the enzyme (152). Plant H^+-PPases are inhibited by Ca^{2+}, Co^{2+}, Mn^{2+}, Cu^{2+}, Cd^{2+} and Zn^{2+} as a result of competition with Mg^{2+} (141, 153, 154). Na^+-PPases are specific for Mg^{2+} but Mn^{2+} ions also activate them slightly (139). K^+ modulates Mg^{2+} binding to Na^+-PPases and Mg^{2+} increases Na^+ binding via conformational changes (139). High PP_i and Mg^{2+} concentrations inhibit K^+-dependent H^+-PPases (148). Bivalent cations, especially Mg^{2+}, protect Na^+-PPases against mersalyl inactivation and aminomethylenediphosphonate (AMDP) inhibition (139). Both Mg^{2+} and Zn^{2+} protect Rr-PPases against heat inactivation at 70 °C (149, 155). The pH optimum for H^+-PPase PP_i hydrolysis activity ranges between 6.5−8.5 in bacteria, plants, algaea and protists (28, 150, 152, 156-158). The pH optimum of *M. mazei* Na^+-PPase is 7.5 (28). Interestingly, the pH optimum for PP_i hydrolysis by Rr-PPase is 6.5 (150, 152) and for PP_i synthesis 7.5 (152) suggesting that the enzyme functions in different directions under different environmental conditions.

1.4.2 PP_i synthesis

mPPase mediated PP_i synthesis has been demonstrated by $^{32}P_i/PP_i$ phosphorus exchange (34, 159) and $[^{18}O]P_i/H_2O$ oxygen exchange reactions (35, 111, 160-162). The PP_i synthesis activity of Tm-PPase is very low (0.02%) compared to its PP_i hydrolysis activity. K^+ inhibits PP_i synthesis and activates PP_i hydrolysis in Tm-PPases. As the cytoplasmic K^+ concentration is about 100 mM, Tm-PPase mainly catalyses the hydrolysis of PP_i under physiological conditions (161). Rr-PPase has both PPase and PP_i synthase activities (163, 164). Environmental conditions and the localization of the mPPase determine the direction of the reaction (107, 165-167) (see section 1.5.1.).

1.4.3 The residues important for H^+ and Na^+ ion transport

Both H^+ and Na^+ transport reactions of mPPases are primary and electrogenic processes, which create an inside positive membrane potential difference (28, 86, 168). Based on the available structural information, mPPases transport H^+ or Na^+ ions through the "coupling funnel" located between TMs 5, 6, 11, 12, 15 and 16 (Figs. 3B & C) (71, 72). However, the ion channel and the gate residues, which determine ion transport specificity, are located between TMs 5, 6, 12 and 16. The gate residues, which control ion transport specificity, are Arg242 (TM5), Asp294 (TM6), Glu301 (TM6), Lys742 (TM16) (Vr-PPase numbering) in H^+-PPases and Asp243 (TM6), Glu246 (TM6), Lys707 (TM16) (Tm-PPase numbering) in Na^+-PPases (Figs. 5A & B) (detailed description shown in section 4). The gate was in the closed conformation in both solved 3D-structures (71, 72). Noteworthy, the residues on the periplasmic side of the gate are not as conserved as those on the cytoplasmic side, indicating that tight ion binding sites reside on the cytoplasmic side of the membrane (71).

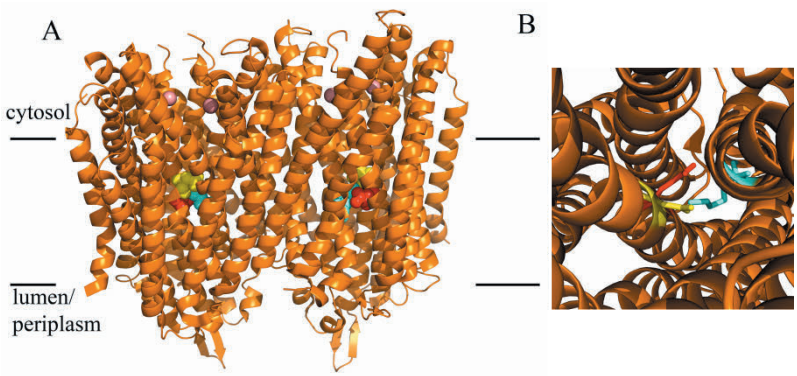

Figure 5. Na^+-transporting Tm-PPase (4AV6) (orange) with gate amino acid residues shown. A. The ion transport specificity is determined by Asp243 (yellow) - Lys707 (cyan) - Glu246 (red) residues. Also two Mg^{2+} ions (pink dots) are bound to the enzyme. B. The conformation of the Na^+ transport gate residues shown. The structure of Tm-PPase was solved by Kellosalo *et al*. (71).

1.4.4 K^+ and Na^+ binding to mPPases

Based on K^+ requirements H^+-PPases are divided into K^+-independent and K^+-dependent H^+-PPases (169, 170). All Na^+-PPases are K^+-dependent enzymes (28, 139). Already in 1991, Davies *et al.* predicted that the K^+ binding site of the *Beta vulgaris* K^+-dependent H^+-PPase is located on the cytosolic side of the protein (171). Belogurov and Lahti showed in 2002 that the K^+ binding site of *Carboxydothermus hydrogenoformans* K^+-dependent H^+-PPase (Ch-PPase) is located near Ala460 (TM12) (170). This alanine residue is highly conserved among K^+-dependent H^+-PPases and is substituted by lysine in K^+-independent H^+-PPases. Positively charged NH_3^+ group of Lys and K^+ were proposed to occupy the same site and activate the enzyme. It was further shown that A460K substitution in Ch-PPase changed the enzyme from K^+-dependent to K^+-independent (170). The 3D-structure of Tm-PPase verified that lysine can replace K^+ at its binding site and K^+ binds next to PP_i in the enzyme active site (Fig. 4C) (30, 71). K^+ was found in an equivalent location in the 3D-structure of a plant H^+-PPase, which is a K^+ dependent enzyme (Fig. 4B) (72).

K^+ binding increases the binding affinity of Na^+-PPases for both Mg^{2+} and Na^+, and the velocity of PP_i hydrolysis even though the enzyme is able to function without added K^+ (139). K^+ binds to the low-affinity Na^+ binding site or to a separate site (28, 139). The bacterial cytoplasm contains about 10-fold more K^+ than Na^+ implying that K^+ ions are attached to K^+-dependent mPPases under physiological conditions (28). Furthermore, Rb^+ can substitute for K^+ ions and activate K^+-dependent H^+-PPases (172-174). In Na^+-PPases, Rb^+ can substitute for K^+ but not Na^+ as the activating ion, and the enzyme is able to transport Na^+ when neither K^+ nor Rb^+ is present (28). There have been speculations on the ability of mPPases to transport K^+ ions (163, 175). Based on $^{86}Rb^+$ transport studies, it was concluded that Na^+-PPases and H^+-PPases are not able to transport K^+ (28, 176). In addition, other monovalent cations are able to activate K^+-dependent Vr-PPase, but to a lesser extent in a decreasing order of $NH_4^+ > Cs^+ > Na^+ > Li^+$ (172). Interestingly, Cs^+ was even more stimulatory than K^+ in one plant H^+-PPase study (163).

In addition to Mg^{2+} Na^+-PPases of *Methanosarcina mazei* (Mm-PPase), *Moorella thermoacetica* (Mt-PPase), *Acetobacterium woodii* (Aw-PPase) and Tm-PPase require Na^+ for activity (28, 86, 139, 161). The maximal activity of Na^+-PPase is increased about 2-fold when both Na^+ and K^+ ions are present at millimolar concentrations (28, 86, 139, 161). A steady state kinetic analysis of PP_i hydrolysis by Na^+-PPase revealed one high-affinity and one low-affinity binding sites for Na^+, and one site for K^+. K^+ binding increases Na^+ binding to the high-affinity binding site by 10-fold (28, 139, 161). This site is highly specific for Na^+, whereas the low-affinity site binds both Na^+ and K^+ (28). Mg^{2+} increases Na^+ binding affinity and Na^+ binding induces conformational changes, which may be important for ion transport (139). Mg^{2+} and Na^+ ions bind in a positively cooperative manner and almost independently of substrate (Mg_2PP_i) to Mm-PPase. The cooperativity of Mg^{2+} binding is lost when Na^+ replaces one Mg^{2+} ion and gives rise to the inactive $ENa_3MgMg_2PP_i$ complex (139). Tm-PPase differs from other Na^+-PPases by having a low affinity binding site for Na^+ that is formed by Asp703. This site is missing in other Na^+-PPases, which have Asn at this location (161). Belogurov *et al.* suggested that Na^+ can regulate Tm-PPase, because the enzyme is not saturated at 50 mM Na^+ concentrations (161).

K^+-dependent H^+-PPase of *C. hydrogenoformans* and K^+-independent H^+-PPases of *R. rubrum* and *Pyrobaculum aerophilum* are active without Na^+ (161). It has also been shown that K^+-dependent H^+-PPases are inhibited at high Na^+ concentrations, especially at low K^+ (173, 174, 177). Li^+ can substitute Na^+ as the activator of Na^+-PPases although the activatory effect is less, and the activity is not increased in the presence of K^+ ions (86, 161). High Li^+ concentration inhibits some K^+-dependent H^+-PPases (174), but not the K^+-independent Rr-PPase (150).

1.4.5 Mechanism of action

The PP_i hydrolysis center of mPPases is located 20 Å above the membrane, whereas the gate residues important for ion transport specificity reside inside the membrane (Fig. 3). The estimated H^+/PP_i stoichiometries for PP_i hydrolysis and synthesis are 1 and >2, respectively (79, 178-180). The differences may be due to different assay conditions and/or different origins of the mPPases studied. PP_i synthesis and hydrolysis probably follow the same mechanism, but the reactions proceed in opposite directions. Catalysis is enabled by a conformational change induced by the binding of cations and/or the substrate (139). In the *C. tetani* mPPase, ligand-induced conformational changes have been detected by a single-molecule FRET -technique (181). Conformational changes occuring during the catalysis have been studied by monitoring changes in sensitivity to trypsin digestion and mersalyl inhibition and the reactivity of internal tryptophane residues (139, 182). In addition to above studies performed in solution, conformational dynamics is evident in mPPase crystal structures. Thus cytoplasmic part of the protein was seen in open or closed conformation in Na^+-PPase (Mg^{2+} and K^+ as bound ligands) (71) and H^+-PPase (Mg^{2+}, K^+ and competitive inhibitor as bound ligands) (72). The coupling mechanism of PP_i hydrolysis and H^+/Na^+ transport remains to be solved, but there are three competing models for this (Fig. 6).

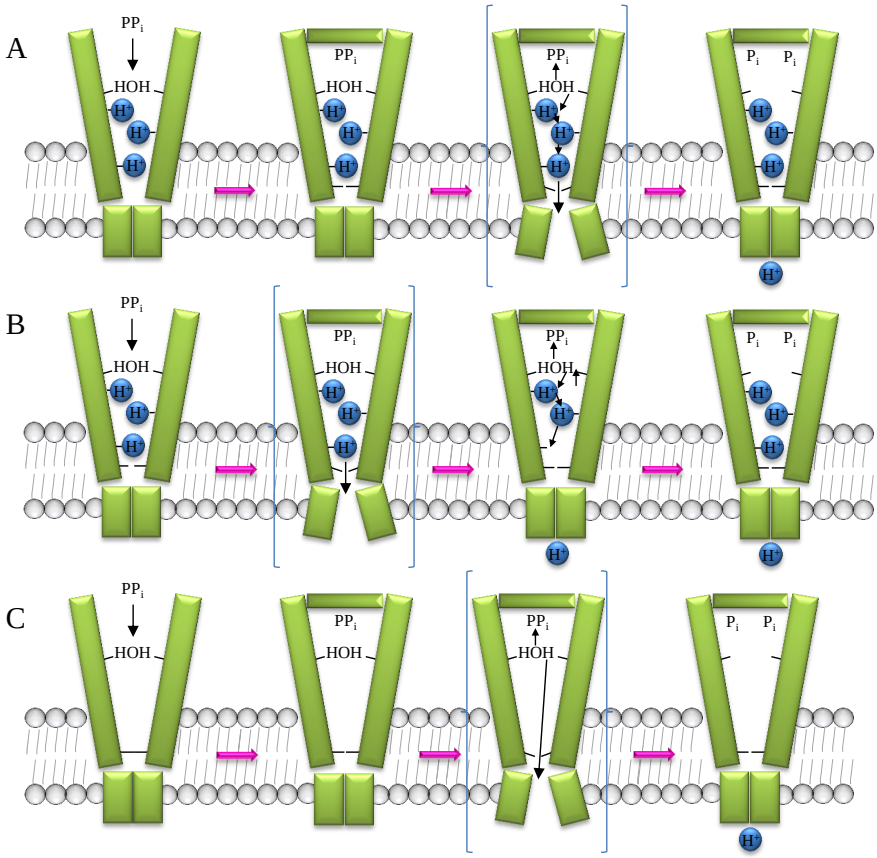

Figure 6. Three possible mechanisms for an H^+-PPase. A. PP_i hydrolysis induces a conformational change that leads to proton transport through the proton wire of the "Grotthuss mechanism". B. PP_i binding induces a conformational change and the proton is transported before PP_i is hydrolyzed. C. PP_i is hydrolyzed and the proton released from the water during PP_i hydrolysis is transported to the other side of the membrane. The figure was modified from Tsai *et al*. (30). (Reprinted and adapted from *Curr. Opin. Struct. Biol*, 27, Tsai, J. Y. *et al.*, Proton/sodium pumping pyrophosphatases: the last of the primary ion pumps, 38−47, Copyrigh (2014), with permission from Elsevier).

Lin *et al.* (72) predicted that H^+-PPases directly couple PP_i hydrolysis to H^+ transport, which occurs through a "Grotthuss mechanism" and involves three states called the resting, initation and transient states (Fig. 6A). During the resting state, the active site is opened into the cytoplasmic side. PP_i binding initiates hydrolysis, which induces a conformational change. As a result of PP_i hydrolysis, two phosphates are formed and the proton is transported by the gate residues in a chain reaction, the channel is transiently opened, and the proton is released into the vacuolar side of the membrane. After proton transport and P_i release, H^+-PPase will return back into the resting state (72). The second model, called the binding change mechanism, was proposed for Na^+-PPases by Kellosalo *et al.* (Fig. 6B) (71). They predict that PP_i binding causes conformational changes in two major regions between the loops of TM 5 and 6 and in the helices of 11 and 12 that drive the transport of Na^+. They indicate that helix 8 can bend by 5 Å, and this enables TM 12 to move 2 Å downwards, which breaks the Asp696-Lys499-Asp236 salt bridges and leads to gate opening. They further speculate that, following the conformational changes, Na^+ is transported from the high affinity binding site to the low affinity binding

site that may locate near the exit channel and enable Na^+ transport to the periplasm. After Na^+ release, the gate is closed and P_i is released. They suggest that Na^+ and H^+ are transported by the same mechanism (71). The third, billiards type direct coupling mechanism was proposed by Baykov *et al.* (Fig. 6C) (7). In this model, PP_i hydrolysis creates a H^+ from a nucleophilic water molecule that can displace Na^+ from its binding site. Thereafter, the proton is in turn replaced by Na^+, and the Na^+ is released into the extracellular space. H^+-PPases can function with the same mechanism, although they do not contain the transitional binding site for Na^+ and H^+ (7). It should be noted that in the third mechanism the proton that is transported is generated from the water molecule in the course of PP_i hydrolysis (30).

1.4.6 Inhibitors of mPPases

Many molecules including pyrophosphate analogs inhibit mPPases although the most specific inhibitors are low molecular weight 1,1-diphosphonates (150, 183-186). Aminomethylenediphosphonate, AMDP, is the strongest specific and competitive mPPase inhibitor (185, 187, 188), and is 6- and 38-fold more efficient than methylenediphosphonate and imidodiphosphate, respectively (184). In Na^+-PPases the inhibitory action of AMDP is increased at high Na^+ concentrations (139). However, AMDP has only been tested *in vitro* but not *in vivo* (184). Plant herbicides contain 1,1-diphosphonates (189), which inhibit H^+-PPases. A high H^+-PPase activity increases maize's tolerance towards mesotrione herbicides (190). Imidodiphosphate is a PP_i analog that inhibits H^+-PPases and H^+-ATPases (158, 186, 191, 192).

Soluble PPases are strongly inhibited by fluoride, but mPPases are only slightly inhibited because of structural differences between these enzymes (28, 72, 185). In mPPases, the binding of water, which is required for PP_i hydrolysis, is mediated by aspartates and in soluble PPases by Mg^{2+} ions. Fluoride has a negative charge and thus binds with higher affinity between positively charged Mg^{2+} ions than between the negatively charged carboxylate groups of Asp residues (24). Accordingly, in H^+-PPases fluoride cannot compete with the binding of nucleophilic water as effectively as in soluble PPases (72). Ca^{2+} inhibits mPPases non-competitively (188, 193). Buffer components have effects on mPPase activity in a K^+-concentration-dependent manner in the following order: Tris > BisTris-propane > Bicine > Tricine > imidazole (172). Furthermore, Tris analogs inhibit mPPases, but the zwitterionic buffers Mops and Hepes have no effects on the PP_i hydrolysis activity of H^+-PPases (143).

mPPases are inhibited unspecifically by *N*-ethylmaleimide (NEM), *N,N'*-dicyclohexylcarbodiimid (DCCD), 4-bromophenacyl bromide (BPB), fluorescein 5'- isothiocyanate and diethyl pyrocarbonate (DEPC), as was shown for Rr-PPase and *Streptomyces coelicolor* mPPase (Sc-PPase) (194). Acylspermidine derivatives inhibit plant and bacterial mPPases (194, 195). mPPase inhibition is dependent on pH (196), temperature (149, 186, 197), time, and concentration of the inhibitor (198). Mg_2PP_i protects H^+-PPases against inhibition (151, 199), and Mg^{2+} prevents DCCD binding

(200). H^+-ATPase specific inhibitors like vanadate, concanamycin A, oligomycin and fungal toxins do not or only slightly inhibit H^+-PPases (112, 186, 201-206). Many compounds including diethylstilbestrol, dihydroquercetin and anti-calmodulin drugs, triazole fungicides, cycloprodigiosin hydrochloride and Ca^{2+} antagonists inhibit both H^+-ATPases and H^+-PPases (207-211).

1.4.7 Conserved and functional residues in mPPases

The amino acid sequences of Na^+- and H^+-PPases are highly conserved. The importance of α-helices has been studied showing that TM6 particularly contains many essential residues for the structure and function of mPPases (212). However, it is not trivial to distinguish between direct and indirect functional roles of residues or helices as exemplified by the finding that several residues in TM3, which does not form part of the central ion transport funnel, are required for H^+ transport in H^+-PPases (213). The significance of conserved and non-conserved amino acid residues has been extensively studied by site-directed mutagenesis (Table 1) (Fig. 7) (214, 215) and random mutagenesis (216). The amino acid residues that have an effect on mPPase function are listed in Table 1.

Table 1. Amino acids residues shown to be important for mPPase function and/or structure based on site-directed mutagenesis studies (Vr-PPase numbering).

Amino acid residue	Residue important for function and/or structure of mPPase, Vr-PPase numbering
Ala	Ala137 (213, 216), Ala164 (213), Ala305 (212), Ala306 (212), Ala414 (216), Ala537 (170, 194)
Arg	Arg242 (147, 214, 216-218), Arg264 (216, 218), Arg272 (218), Arg523 (147, 218), Arg609 (147, 218) and Arg amino acids residue at position 207 (219)
Asn	Asn318 (212), Asn534 (220), Asn738 (161, 220)
Asp	Asp218 (220), Asp253 (216, 221), Asp257 (216), Asp269 (220), Asp270 (151), Asp279 (216, 221), Asp283 (151, 198, 214, 216, 221), Asp287 (216), Asp294 (72, 216), Asp500 (214, 222), Asp507 (220), Asp723 (221), Asp727 (221), Asp731 (221)
Cys	Cys304 (197, 221), Cys630 (170, 197), Cys at the position 288 (215, 223), Cys at the position 251 (223)
Glu	Glu263 (79, 221, 224), Glu268 (216, 224), Glu301 (212, 216, 222, 225), Glu423 (214, 222), Glu607 (224), Glu641 (214), Glu698 (224), Glu residues at the positions 228 and 297 in the K^+-independent H^+-PPases (216, 224)
Gly	Gly149 (213), Gly150 (213), Gly160 (213), Gly157 (213) Gly229 (216), Gly233 (216), Gly244 (214), Gly245 (216), Gly246 (216), Gly297 (224), Gly316 (220), Gly334 (216), Gly375 (216), Gly394 (216, 225), Gly411 (216), Gly451 (225)
His	His319 (220), His716 (151)
Ile	Ile163 (213), Ile277 (216), Ile418 (216), Ile545 (220)
Leu	Leu258 (216), Leu307 (212), Leu317 (212, 220), Leu555 (220), Leu749 (220)
Lys	Lys73 (215), Lys261 (79, 221), Lys541 (151), Lys742 (72), Lys457 (219)
Met	Met161(213), Met291 (216)
Phe	Phe240 (225), Phe296 (216, 225), Phe405 (216)
Pro	Pro573 (225)
Ser	Ser142 (72, 213), Ser153 (213), Ser298 (216), Ser368 (216, 225), Ser473 (213, 225), Ser634 (215)
Thr	Thr138 (72, 213), Thr165 (213), Thr228 (216), Thr249 (220), Thr426 (225), Thr446 (225)
Trp	Trp690 (182)
Tyr	Tyr166 (213), Tyr216 (220), Tyr230 (216), Tyr299 (212), Tyr425 (225)
Val	Val151 (213), Val259 (79, 221), Val433 (225), Val446 (225), Val746 (220)

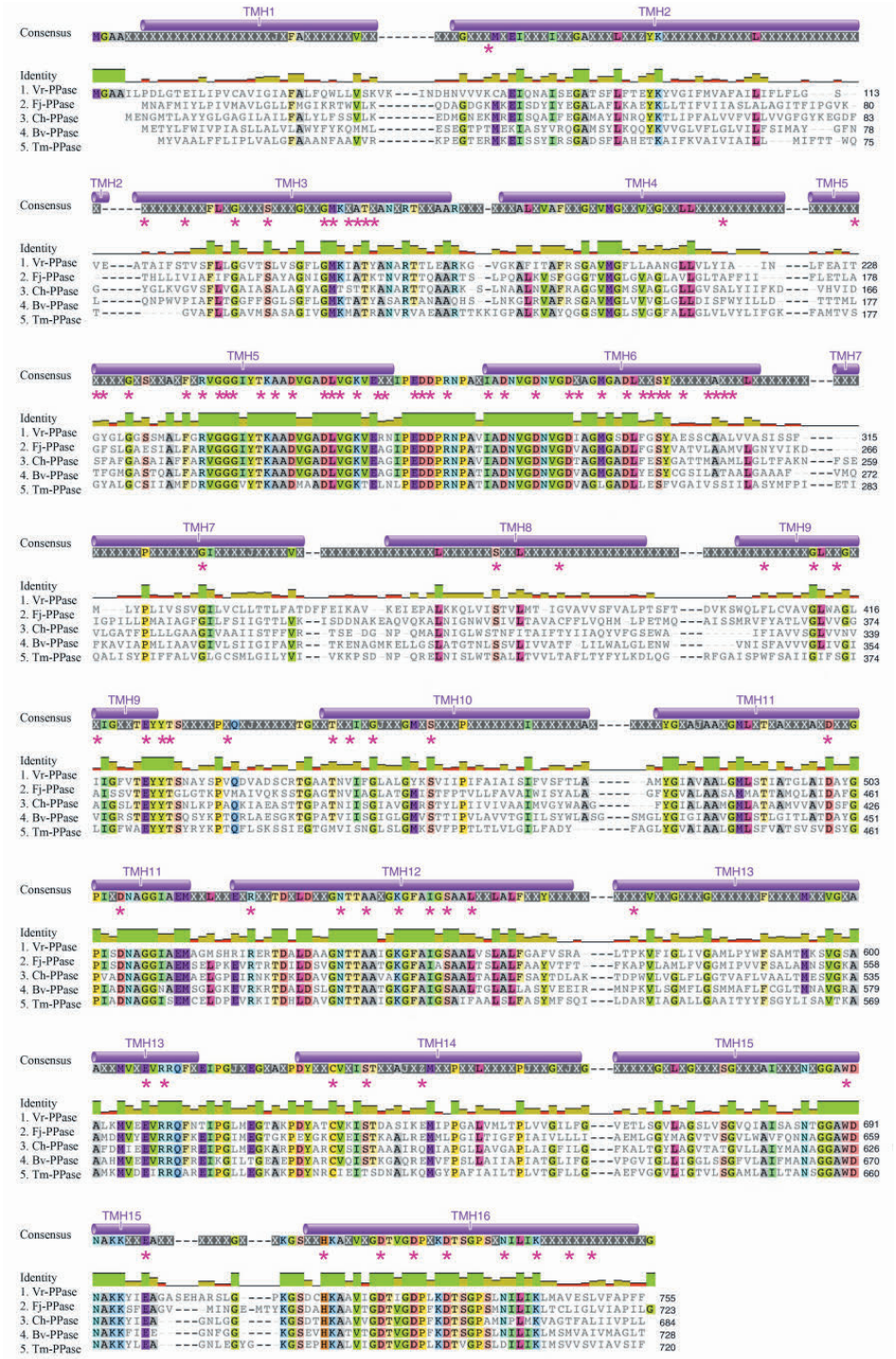

Figure 7. Amino acid residues (shown as pink stars) important for mPPase function and/or conformational stability according to the literature. The mPPases are from *V. radiata* (Vr-PPase), *Flavobacterium johnsoniae* (Fj-PPase), *C. hydrogenoformans* (Ch-PPase), *Bacteroides vulgatus* (Bv-PPase) and *T. maritima* (Tm-PPase). Both conserved and non-conserved residues were shown to be important for mPPase function. The figure was modified from Tsai *et al.* (30). (Reprinted and adapted from *Curr. Opin. Struct. Biol*, 27, Tsai, J. Y. *et al*., Proton/sodium pumping pyrophosphatases: the last of the primary ion pumps, 38−47, Copyrigh (2014), with permission from Elsevier).

mPPases contain many well conserved sequence motifs (Fig. 7), e.g. GGG, DVGADLVGK and DNVGDNVGD (120). All residues of the conserved GGG sequence are important for both PP_i hydrolysis and H^+ transport (214, 216). The **D**VGA**DL**V**G**K**VE** motif, which is part of the mPPase active site and locates in TM5, has been explored with amino acid substitution analyses (the substituted amino acid residues are shown in bold). Two Asp residues, Leu, Val, Lys and Glu of the sequence are important for PP_i hydrolysis and ion transport (79, 200, 216, 221, 224). The Asp residues of the sequence **D**NVG**D**NVG**D** in TM6 have been found to be important for PP_i hydrolysis activity (151, 198, 214, 216, 221). In addition, the bold-faced residues of the conserved **E**Y**Y**T sequence in the C-terminal end of TM9 are important for PP_i synthesis, PP_i hydrolysis and ion transport (167, 214, 222).

The conserved coupling funnel residues are **Asp253, Asp257**, **Glu268, Asp269, Asp279, Asp283, Asp287**, **Asp507**, Asp691, **Asp723, Asp727**, **Asp731, Asn534**, Lys250, Lys730 and Lys694 (30, 72). The residues in bold have been substituted by site-directed mutagenesis, and have been shown to be very important for PP_i hydrolysis and H^+ ion transport (151, 198, 214, 216, 220, 221, 224). **Arg242**, **Asp294, Lys742** and **Glu301** form the ion transport specificity determining gate residues in Vr-PPase. Arg242 (147, 214, 216-218), Asp294 and Lys742 are required for PP_i hydrolysis and H^+ transport (72, 216). Especially important is Glu301, which is required for coupling (212, 222), and determines the transporter specificity (72, 212, 216, 222, 225).

The amino acid residue at position 537 (Vr-PPase numbering) is Ala in K^+-dependent and Lys in K^+-independent mPPases. When the respective Ala was replaced with Lys, the K^+-dependence was lost (170). However, other residues are also involved in this as the K^+-independent H^+-PPase did not become K^+-dependent as a result of Lys to Ala substitution (194). Asparagines including Asn738 are linked to H^+ transport and provide a K^+-dependent Na^+ binding site (220). When the aspartate at the corresponding site in Tm-PPase was mutated to asparagine, Na^+ binding to the enzyme was altered (161).

1.4.8 Phylogenetics of mPPases

As was mentioned above, H^+-PPases are divided into K^+-independent/dependent families based on the evolutionary relationship and conserved Lys/Ala residue in the protein sequences (170). Both K^+-independent and K^+-dependent mPPases are found in plants, archaea, bacteria and protists (120). The mPPases of thermophilic bacteria can be either K^+-independent or K^+-dependent (226). Generally, plants and protists contain several kinds of mPPase genes in their genomes, whereas bacterial genomes have only one mPPase gene, even though there are exceptions to this rule (120). After the discovery of Na^+-PPases, a phylogenetic tree for mPPases was constructed. The K^+-independent clade of the tree has been characterized in detail, but there are many clades with unknown functions in the K^+-dependent H^+-PPase part of the tree (Fig. 8) (28).

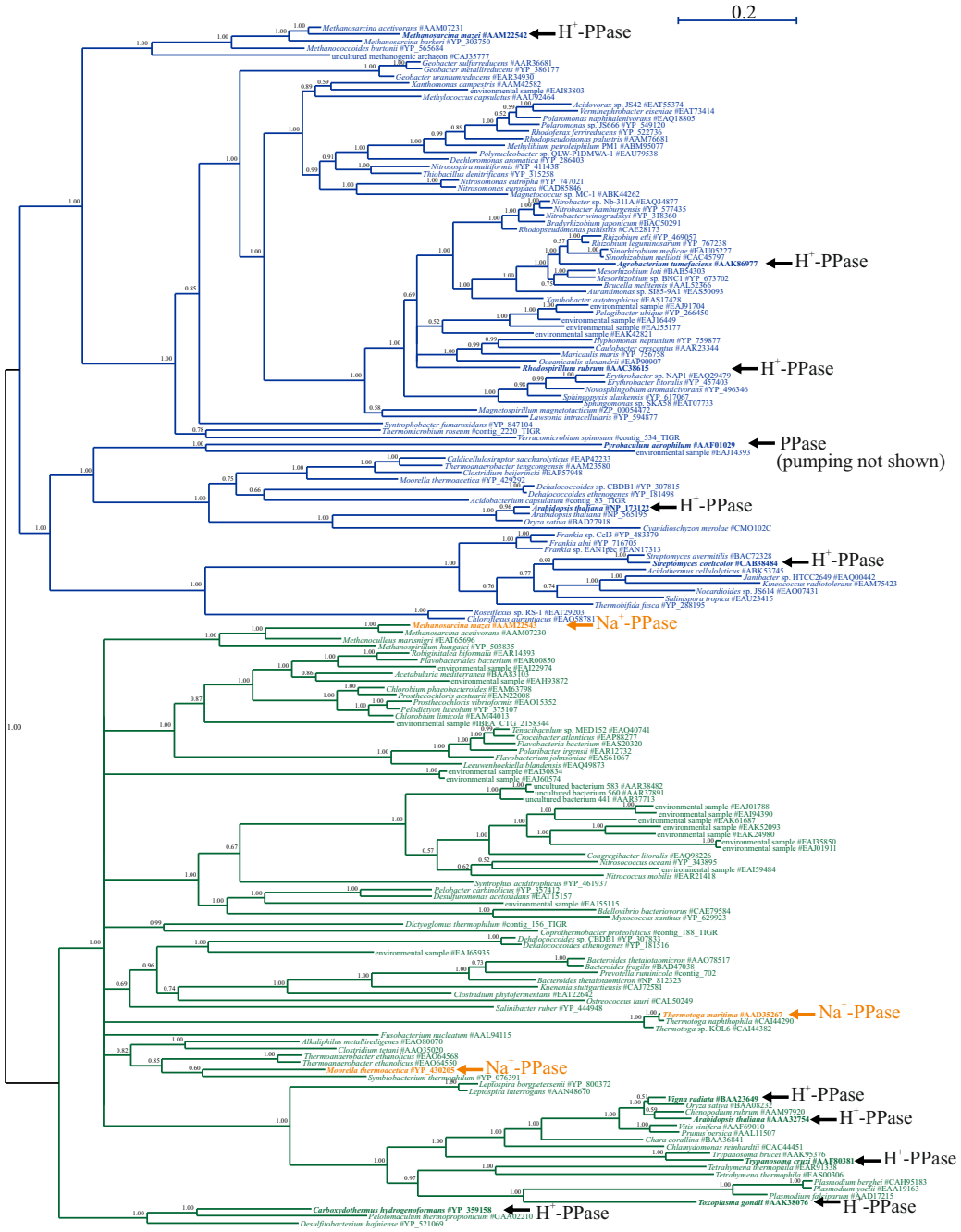

Figure 8. Phylogenetic tree of the mPPases according to Malinen *et al.* (28). Membrane-bound PPases are divided into K^+- independent (blue) and K^+-dependent subfamilies (green). The studied mPPases are showed in bold, Na^+-PPases are coloured in orange and H^+-PPases are shown in black. The creditability of the clades are shown in node numbers. The tree shows that there are many clades in the K^+-dependent side of the tree where ion transport specificity remains to be determined. The figure modified from Malinen *et al.* (28). (Reprinted and adapted with permission from *Biochemistry (N.Y.)* 46, 30, Malinen, A. M. *et al.*, Na^+-pyrophosphatase: A novel primary sodium pump 8872-8. Copyright (2007) American Chemical Society).

1.4.9 Expression of mPPases in *Escherichia coli* and *Saccharomyces cerevisiae*

Membrane-bound PPases of various origin have been successfully expressed in *E. coli* and *S. cerevisiae*, which are good hosts as they do not have any mPPases of their own and can be genetically manipulated (71, 161, 227). Bacterial mPPases are usually expressed in *E. coli* C43(DE3)ril or C41(DE3)ril cells (151, 161, 197, 214, 215, 223, 227), which have been designed for the production of membrane proteins (227). These strains contain a ril plasmid that provides tRNAs for codons that are rare in *E. coli*, but important for protein expression (28). mPPase genes have been cloned under the T7 isopropyl β-D-1-tiogalactopyranoside (IPTG) inducible promoter. mPPases have been expressed in rich culture medium, with a low amount of inducer (0.2 mM) and a long induction time (4−5 h), and have been isolated in inverted membrane vesicles (IMVs) (151, 161, 197, 214, 215, 223, 227). mPPases have also been expressed in *E. coli* BL21(DE3) cells (223) and BLR(DE3)pLysS (228), but the expression levels have been lower than in the C43 or C41 strains.

Yeast strains used for efficient bacterial and plant mPPase expression are BJ1991, BJ2168, and AACY1 under the PMA1- and GAL1 -promoters (71, 72, 134, 188, 229). The vacuolar protease-deficient yeast strain BJ5459 has also been used for mPPase production from the expression plasmids pYMD23-25, pYMD32, and pYES2-AVP1 (124, 230). In addition, a yeast strain lacking one of the V-ATPase subunits has been used for protein expression, and it was discovered that mPPase can complement the H^+-ATPase activity (231). A patch clamp analysis indicated that yeast giant vacuoles produced 4.2 x 10^6 molecules of H^+-PPases (79). In general, the mPPase yield has been low, about 1.5 mg of protein per 1 litre of yeast culture (132). Furthermore, the localization of an H^+-PPase can be changed by inserting a signal peptide sequence into the N-terminal part of the protein, as was shown by expression studies in yeast (232).

1.4.10 Purification and crystallization of mPPases

Purification and solving the structure of mPPases has been a demanding task, and versatile methods have been used for this. Bacterial and plant mPPases have been successfully purified and reconstituted into a lipid bilayer (71, 78, 132, 150, 168, 193, 229, 233-236). Kellosalo *et al*. (71) showed that a two-step purification process with an in-column detergent exchange was essential for mPPase purification and crystallization. High Mg^{2+} concentration is important for enzyme stabilization during solubilization and purification (71, 72, 193, 237). Various detergents have been used for mPPase purification (148, 177, 193, 229, 236, 238, 239). Solubilization and simultaneous enrichment of mPPase could be enhanced at a high temperature (75 °C), when the protein of interest was from a thermophilic organism (71, 132, 229). Membrane solubilization depends on the pH and is usually increased at high pH (240). Kellosalo *et al.* showed that detergents need to be optimized individually for different mPPases (229). The detergents in which Tm-PPase activity remained at least 85% of the non solubilized Tm-PPase activity were dodecyl-β-maltopyranoside (DDM), undecyl-β-maltopyranoside (UDM), undecyl-α-maltopyranoside (αUDM), decyl-α-maltopyranoside (αDM), decyl-β-

thiomaltopyranoside (D-thio-M), nonyl-β-maltopyranoside (NM), cyclohexylbutanoyl-N-hydroxyethylglucamide (C-HEGA-10), 6-cyclohexyl-1-hexyl-β-D-maltoside, 5-cyclohexyl-1-pentyl-β-D-maltoside and nonyl-β-glucoside (NG) (71, 229). The most widely used detergent for mPPase solubilization is DDM at a 3:1 (w/w) detergent to protein ratio. DDM does not interfere with the activity of mPPases (71, 72, 77, 132, 161, 229).

Purified mPPases have been His-tagged with six or eight residues and purified using Ni^{2+} affinity based chromatography (71, 72, 77, 132, 134, 229). The binding of a His-tagged Tm-PPase to the Ni^{2+} matrix increases with temperature (75 °C vs. 40 °C) (71, 229). After affinity chromatography the detergent has been removed with Bio-Beads SM-2 (239). mPPases have been reconstituted into a lipid environment created from soybean lecitin (229), asolectin (105, 236), soybean phospholipids (239), lysophosphatidylcholine (241), a phospholipid-cholesterol mixture (168) or phosphocholine and 1,2-dioleoyl-*sn*-glycero-3-phospho-choline (134). Liposomes have been created with freeze-thaw cycles (104) and the optimal lipid to protein ratio has been 100:1 for the H^+-PPase activity (236). Lipids reactivate PP_i hydrolysis (71, 105, 153, 193). Gel-filtration has been tested for the purification of mPPases (148, 161, 234, 236, 238, 242, 243). Furthermore, glycerol-density gradient centrifugation, dialysis (168) or ammonium sulphate fractionation and gel chromatography have been used for mPPase purification (153, 237). In order to retain a mPPase in its active form the solubilized enzyme requires detergents, Mg^{2+}, glycerol and phospholipids at different stages of the purification (78, 150, 233-235).

Tm-PPase crystals grew poorly with DDM as the detergent and so Kellosalo *et al*. (71, 138, 229) optimized the crystallization of Tm-PPase using octyl glucose neopentyl glycol (OGNPG) instead. DDM was replaced by 1% OGNPG during Ni^{2+} affinity purification with Bio-Spin® P-6 columns. The detergent exchange enabled reproducible crystal formation with a good diffraction quality, and high detergent concentrations facilitated the crystallization of Tm-PPase (138). Small molecular weight polyethyleneglycol (PEG-350) was used as a precipitant during crystal growth at 21 °C with the sitting-drop vapor diffusion method (71, 138). Vr-PPase was crystallized with DDM as the detergent and PEG-2000 as the precipitant using the hanging-drop vapor diffusion method (72).

1.5 Physiological importance of mPPases in different organisms

The first mPPase was discovered from the purple bacterium *R. rubrum* (29, 31). More mPPases were subsequently found in plants, algae, archaea and protists, but not in fungi and animals (Table 2) (169, 244). mPPases are a highly conserved superfamily of proteins that may have spread between species via lateral gene transfer (244). Prokaryotic mPPases are located usually in the photosynthetic, respiratory, acidocalcisome or volatin granule membranes (Fig. 9A) (150, 166, 245). mPPases exist also in the acidocalcisomal membranes of protists (Fig. 9B) (7) and they are used as marker proteins for acidocalcisomal location (14, 217, 246-248). In addition to acidocalcisomes, H^+-PPases may reside at the plasma membranes and Golgi complex of protists (192, 249-254).

In algae, mPPases are localized to the PMs, central, intracellular, lytic and contractile vacuole membranes of algae (Fig. 9B) (255, 256).

Table 2. Occurrence of mPPases in completely sequenced genomes of the KEGG (257, 258) database (February 2015) and based on Baykov *et al.* (7). Transport specificity was predicted by comparing unknown sequences with mPPase sequences with known functions.

Prokaryotes	**Transported ion**		**Eukaryotes**	**Transported ion**	
Bacteria	**H^+**	**Na^+**	**Protists**	**H^+**	**Na^+**
Acidobacteria	+	-	Alveolates	+	-
Actinobacteria	+	+	Amoebozoa	-	-
Alphaproteobacteria	+	+	Choanoflagellates	-	-
Aquificiae	-	-	Cryptomonads	+	-
Armatimonadetes	+	-	Diplomonads	-	-
Bacteroidetes	+	+	Euglenozoa	+	-
Betaproteobacteria	+	-	Haptyphyta	+	+
Caldiserica	-	+	Heterolobosea	+	-
Chlamydiae	+	+	Parabasalids	-	-
Chlorobi	+	+	Stramenophiles	+	+
Chloroflexi	+	+	**Fungi**		
Chrysiogenetes	+	-	Ascomycetes	-	-
Cyanobacteria	-	-	Basidiomycetes	-	-
Deferribacteres	-	+	Microsporidians	-	-
Deinococcus-Thermus	-	-	**Plants**		
Deltaproteobacteria	+	+	Basal Magnoliophyta	+	-
Dictyoglomi	-	+	Eudicots	+	-
Elusimicrobia	+	-	Ferns	+	-
Epsilonproteobacteria	-	-	Green algae	+	+
Fibrobacteres	-	-	Monocots	+	-
Firmicutes	+	+	Mosses	+	-
Fusobacteria	-	+	Red algae	+	-
Gammaproteobacteria	+	+	**Animals**		
Gemmatimonadetes	+	-	Anthropods	-	-
Nitrospirae	+	-	Ascidians	-	-
Planctomycetes	+	+	Cnidarians	-	-
Spirochaetes	+	+	Echinoderms	-	-
Synergistetes	-	+	Flatworms	-	-
Tenericutes	-	+	Lancelets	-	-
Thermodesulfobacteria	-	-	Nematodes	-	-
Thermotogae	+	+	Placozoans	-	-
Unclassified	+	-	Poriferans	-	-
Verrucomicrobia	+	+	Vertebrates	-	-
Archaea					
Crenarchaeota	+	-			
Euryarchaeota	+	+			
Korarchaeota	+	-			
Nanoarchaeota	-	-			
Thaumarchaeota	+	-			
Unclassified	-	-			

In plants mPPases are located at vacuolar and Golgi membranes (Fig. 9B) (7, 259). Tonoplast vesicles containing H^+-transporting mPPases, have been isolated from various plant sources (173, 260-263). The isolated tonoplast vesicles are oriented with their cytoplasmic side out as indicated by H^+ transport studies (263). H^+-PPase has been used as a vacuolar marker protein in various studies (264-269). Plant plasma membranes do not usually contain H^+-PPases (270), and so mPPases are used as control proteins to monitor if the isolated plant PMs are contaminated with tonoplast membranes (271). However, there are also results suggesting that plant mPPase reside at the PM (272). mPPases are found in organisms that are clinically, industrially or environmentally important (244). Furthermore, mPPases can provide a tool for engineering bacterial, protist and plant strains for the requirements of biotechnology (28). mPPases can complement soluble PPases as shown by yeast studies, in which viable cells were produced by replacing soluble PPase by H^+-PPase (9).

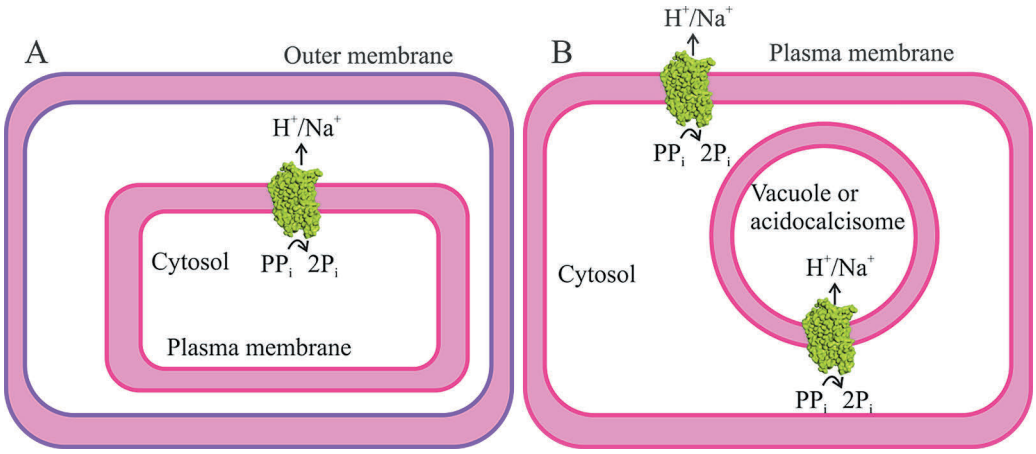

Figure 9. Localization of mPPases in bacteria, archaea, protists, plants and algae. A. Bacterial and archaeal mPPases reside at the plasma membranes and transport ions from the cytosol to the periplasmic space energized by PP_i hydrolysis. B. mPPases of plant, algae and protist are located in the vacuolar and plasma membrane and also in the plant Golgi apparatus (not shown here). The figure was modified from Baykov *et al.* (7). (Reprinted and adapted with the permission from Copyright © American Society for Microbiology, *Microbiol. Mol. Biol. Rev,* 77, 2, 2013, 267−76 DOI:10.1128/MMBR.00003-13).

1.5.1 mPPases in Prokaria

mPPases are found in all phyla of bacteria, except for Aquificiae, Cyanobacteria, Deinococcus-Thermus, Epsilonproteobacteria, Fibrobacteres and Thermodesulfobacteria, and in all phyla of archaea except Nanoarchaeota (Table 2) (7). mPPases have been detected mainly in organisms living in extreme conditions, e.g. the thermophilic archaeon *P. aerophilum* (124). Prokaryotic organisms contain K^+-independent and K^+-dependent H^+-PPases (7, 170) and Na^+-PPases (28, 86, 139).

H^+-PPases are coupled to versatile cellular bioenergetics processes in bacteria (82, 273). PP_i utilization in energy metabolism is vital also for anaerobic and fermentative bacteria (8, 274, 275). Prokaryotic mPPases contribute to the establishment of the transmembrane potential which is used for the transport and secretion of secondary

metabolites and waste products (194, 273). Furthermore, in bacterial acidocalcisomes, H^+-PPases and H^+-ATPases create a proton motive force that is utilized for secondary transport functions (276, 277). Proton gradients created by H^+-PPases are linked to nitrate respiration in sulfide oxidizing halophilic bacteria (278). H^+-PPases can also enable the synthrophic growth of *Syntrophomonas wolfei* with methanogens (279). Serrano *et* al. suggests that PP_i may have a central and ancient role in photosynthetic energy related processes in bacteria (169). Some prokaryotes can utilize Na^+-based bioenergetics in their cellular processes, and e.g. *A. woodii* creates Na^+-gradients by Na^+-PPases and uses them for the anaerobic caffeate respiration (86). Noteworthy, both soluble and membrane-bound PPases may enhance macromolecular biosynthesis by lowering the cytosolic PP_i concentration (1, 7).

Ion translocating mPPases and ATPases have similar functions (they both contribute to the establishment of ion gradients) and they work together in prokaryotic cells, but they can naturally be regulated in different ways. H^+-PPase and H^+-ATPase genes are located next to each other in e.g. *Thermoproteus tenax* (273). A mutational analysis suggested that the *R. rubrum* H^+-PPase provides an alternative energy source and H^+ gradient when the cellular H^+-ATPase activity is low e.g. under stressful conditions (280). Some prokaryotic genomes include more than one mPPase gene, e.g. *M. mazei* has two genes encoding mPPases, one for a Na^+-PPase and the other for a H^+-PPase (28, 281). These two adjacent genes are transcribed in opposite directions and may be regulated differently based on environmental conditions (281). The *M. mazei* H^+-ATPases and H^+-PPase are expressed when cells are grown in a methanol-containing medium (281, 282). Na^+-PPase possibly provides an essential Na^+ gradient for specific living conditions (28). The arrangement of adjacent H^+-PPase and Na^+-PPase genes in the *M. mazei* genome may be a relic of an ancient gene duplication event, which enabled the archaeon to alternatively use either Na^+- or H^+-coupled bioenergetics as a response to specific growth conditions (28).

Various prokaryotes contain both soluble and membrane-bound PPases and environmental conditions may regulate these enzymes differently (149, 283). For example, in *R. rubrum* the soluble PPase accounts for ~80% of the total cellular PPase activity and is expressed constitutively (284), whereas the H^+-PPase is expressed under anaerobic conditions and under aerobic conditions of high salinity (1M NaCl) but is not expressed under general aerobic conditions (283). When the soluble PPase was knocked-out in *R. rubrum*, the cells grew more slowly than usually, although their mPPase activity was unchanged (285). These results suggest that in *R. rubrum* the H^+-PPase is required for bacterial growth under challenging environmental conditions and the soluble PPase is needed for normal growth. This kind of regulation provides a competitive advantage for bacteria.

Prokaryotic mPPases can either hydrolyze or synthesize PP_i depending on the environmental conditions and cellular localization of the enzyme. For example, in *R. rubrum* the H^+-PPase generates a H^+ gradient with PP_i hydrolysis under conditions of

low energy in the dark, and utilizes a H^+ gradient for PP_i synthesis in light (107, 165, 283). Furthermore, when this enzyme is localized in chromatophore membranes it uses a H^+ gradient for PP_i synthesis and in acidocalcisomal membranes it hydrolyses PP_i and produces a H^+-gradient (150, 166, 167). Changes in the charge of the chromatophore surface had no effect on the PP_i hydrolysis catalyzed by the *R. rubrum* H^+-PPase (286), but the transmembrane electrical potential enhanced the activity of PP_i synthesis (106).

1.5.2 Plant mPPases and their physiological importance

Plant mPPases are found in all plant phyla (Table 2). The first plant H^+-translocating mPPase to be cloned and sequenced was from *A. thaliana* (287). Thus far, all plant mPPases seem to belong to the families of K^+-independent or K^+-dependent H^+-PPases (7). Plant H^+-PPases are important regulators of the cellular PP_i level (109, 163, 173, 288-290). H^+-PPase expression, usually together with H^+-ATPase expression, has been analyzed in various plants (145, 174, 206, 242, 291-293).

Active H^+ transport in plant cells is carried out by three transporters: 1. H^+-PPases and, 2. H^+-ATPases, which mediate H^+ transport into vacuoles and 3. plasma membrane ATPases that pumps protons out of the cell (294). Vacuoles are large organelles occupying as much as 90% of the space of mature plant cells. Their function is to serve as a storage organelle for nutrients, cations, anions, metabolites and toxic compounds (295-297). H^+-PPases are located together with H^+-ATPases at the vacuolar membranes (203, 296, 298, 299). It has been shown that H^+-PPases may be located anywhere in the vacuolar membrane, but H^+-ATPases are found at specific locations (300). When a plant cell grows and divides the vacuoles become enlarged and differentiated. Active H^+-transport is required for these processes (18, 296). H^+-PPases maintain the vacuoles large and regulate plant turgor pressure (18, 296, 301). Plants have also separate vacuolar organelles categorized as vegetative vacuoles and protein storage vacuoles (PSVs) (302-304). H^+-PPases are also present in the lytic vacuoles and PSVs of seeds during germination (302, 305-307). H^+-PPases are assembled at the endoplasmic reticulum (ER) (308) and transported to the vacuole with the possible targeting signal present in TM6 (212). However, protein transport inside the plant cell is not completely understood. In addition to Golgi related pathways H^+-PPases may be transported directly from the ER with provacuolar autophagosomes to vacuoles (309).

Vacuolar H^+-PPases together with H^+-ATPases are important generators of membrane H^+ gradients. The H^+ gradient can be utilized for the secondary transport of ions e.g. Na^+, K^+, Zn^{2+}, Ca^{2+}, Br^-, NO_3^-, Cl^-, malate, citrate and sucrose, amino acids, toxic compounds and nutrients (18, 310-321). H^+-transport has also been linked to photosynthesis (322). Mg^{2+}, K^+, Cl^-, H^+, Br^-, NO_3^-, acetate and malate stimulate plant H^+-PPase, although there are differences between species (154, 323-326). H^+-translocators regulate the pH balance of plant compartments including the cytosol or the vacuole (18, 299, 327-331). This has an effect on the colour of flower, for example (332, 333). In addition, H^+-PPases stabilize the pH of vesicles lacking a functional ATPase (334). Even though an H^+-PPase

is required for vacuolar pH regulation it is not responsible for the hyperacidification reactions which are mediated by H^+-ATPases (335, 336).

H^+-PPases are especially important for plant development. H^+-PPase usually dominate in young fruits whereas H^+-ATPase is the main H^+-transporter in mature cells (108). H^+-PPase expression and activity have been detected in growing and developing plant leaves and stems, seeds, coleoptiles, fruits and berries (109, 288, 289, 316, 337-353). An H^+-PPase activity is required for seed germination (109, 354), embryo and seedling development (355), ontogenesis (356), stomatal opening and closure (349) and callus formation (357). H^+-PPase is also important for the rolling of rice leaves (358) and the chalkiness of grains (359). H^+-PPase, H^+-ATPase and Na^+/H^+-antiporter activities and expression are enhanced towards the flower opening stage (360), even though the H^+-ATPase activity is usually quite unchanged during plant development (18, 322). The transcription of the genes encoding H^+-PPases is increased with fruit maturation, indicating *de novo* protein synthesis (241). During plant senescence, H^+-PPase activity is decreased before H^+-ATPase activity (361), but in the tomato the H^+-PPase activity is decreased and the H^+-ATPase activity is increased during fruit ripening (347). Based on the pH optima for H^+-ATPase and H^+-PPase activities, the two enzymes could in principle function under the same conditions (362). However, the results described above indicate that H^+-PPases and H^+-ATPases are differently regulated during different phases of plant growth and development (18, 109, 343, 363-365).

H^+-PPases usually maintain the proton-motive force under conditions where ATP levels are low or the H^+-ATPase is not functional (146, 175, 366, 367). Thus H^+-PPases provide a back-up system for H^+-ATPases (18, 146, 175, 180, 319, 367, 368). H^+-PPase activity regulates the cytoplasmic PP_i content (369) and the PP_i content controls H^+-PPase expression levels and activity (18). Furthermore, P_i regulates H^+-PPases (17, 370, 371), which help plants survive when P_i is scarce (180, 191, 372). Even though ATP does not directly regulate the activity or expression of H^+-PPases (373), H^+-PPase activity has been shown to be elevated at low ATP levels (146).

Plant genomes contain several genes encoding mPPases, e.g. *A. thaliana* has three (*AVP1−3*) (287, 374) *Oryza sativa* has five (*OVP1−5*) (375), tobacco (376) and *T. aestivum* have three (377), *C. rubrum* (378) and *B. vulgaris* have two mPPases (379). These genes usually encode different types of mPPases, e.g. in *A. thaliana* AVP1 is a K^+-dependent (188) and AVP2 is a K^+-independent H^+-PPase (374). The different mPPases are regulated individually (376) at the RNA (379) and protein levels (380), and their expression may be regulated differently based on environmental conditions, as has been shown in studies in wheat (377). There are also differences in the localization of different H^+-PPases in plants, for example the AVP1 encoding mPPase is highly expressed in the leaves, sieve element companion cell complexes and xylem vessels of *A. thaliana* (381), whereas the AVP2 encoding mPPase is present in trichome and stamen filaments (259). Furthermore, wheat mPPase 1 is usually expressed more in the roots than in the leaves (382). There are also differences in the subcellular localization of the *A. thaliana*

mPPases, e.g. AVP1 resides in the vacuolar membrane (383) and AVP2 in the Golgi complex (259).

1.5.2.1 Effects of various stresses on plant mPPases

Salinity induces two forms of stress in plants: water deficiency and an altered K^+/Na^+ ratio (384). During salinity stress, toxic Na^+ ions can be sequestered from the cytosol into vacuoles or pumped out of the cells with the proton gradient created by an H^+-ATPase and an H^+-PPase and a Na^+/H^+-antiporter (294, 367, 372, 384-393). Furthermore, the cytoplasmic pH is highly regulated during salinity stress (394, 395). A high cellular K^+/Na^+ ratio also alleviates salinity stress and it is maintained by creating a vacuolar ion gradient (367, 396) and by increasing K^+ uptake from the roots with the aid of a PM H^+-ATPase (397). Salinity induces changes in the composition of membrane lipids (393), which has an effect on H^+-PPase activity (301, 398). Polyamines or silicate can protect H^+-PPases during salinity and osmotic stress (396, 399, 400). Salinity also regulates Na^+/H^+-antiporter, H^+-ATPase and H^+-PPase activities (391, 401, 402). Furthermore, Katsuhara *et al.* suggested that during high salinity PP_i is not the limiting factor of the H^+-PPase activity (395). Salinity stress can also increase H^+-PPase expression at the mRNA and protein levels either transiently or constantly (301, 326, 388, 403-409), but there are differences in H^+-PPase expression levels between plant species (390, 410-413).

Halophytes are plants that grow in the presence of 200−300 mM NaCl (414). Also halophytic plants maintain their cytosolic Na^+ concentrations at low levels by compartmentalizing toxic Na^+ into vacuoles using a H^+ gradient as an energy source for transportation (384, 414-420). High Na^+ concentrations increase the activity of H^+-transporters, which enhance the uptake of Na^+, sugars, proline, and starch into vacuoles (414, 417) and leads to the formation of larger shoots compared to those of halophytes grown in non-stressful Na^+ concentrations (417). Also in halophytes the H^+-PPase activity supports the H^+-ATPase activity (418). Although plants have a universal mechanism for Na^+ sequestration, halophytes have also unique features (421), including salt responsive genes that are e.g. involved in ion binding, H^+ transport and photosynthesis (414).

In addition to salinity stress, H^+-PPases together with H^+-ATPases enhance stress tolerance under various conditions including drought (119), cold temperatures (422-424), hyper-osmotic conditions (425, 426), hypoxia (427), mineral deprivation (428) and toxic ion accumulation (429) as well as anaerobic conditions (330). H^+-PPases enhance a plant's drought stress tolerance and dominate over H^+-ATPases in this respect (119). Osmotic stress increases H^+-PPase activity (400). Nitric oxide (NO) alleviates salinity stress by increasing H^+-PPase activity (430). However, the redox state of the plant does not have an effect on H^+-PPase activity during osmotic stress (425, 431). During sucrose starvation and high osmotic pressure, both H^+-PPase and H^+-ATPase activities are decreased (426, 432). Ozone can also decrease H^+-PPase activity (433).

The activity of H^+-PPases is high under conditions of mineral deficiency (434). The accumulation of Cu^{2+} and Cd^{2+} upregulates H^+-PPase expression (410, 435, 436), and inhibits H^+-PPase activity (429, 437), but decreases the intracellular PP_i level (429). Furthermore, N and P_i deprivation resulting from salinity and/or drought stress can elevate the transcription of mPPases (428). Rice grown under conditions of nitrogen starvation can maintain root growth with the help of their H^+-PPase and H^+-ATPase activities (438). In addition, different fungi can either inhibit or activate H^+-PPase activity (439, 440).

1.5.2.2 Plant hormones and mPPases

Plant hormones can regulate the expression and activity of H^+-PPases (441). Auxin (indole-3-acetic acid) stimulates organogenesis and cell elongation. The secretion of protons into the plant cell wall is mediated by H^+-transporters and this enables cell growth (329, 442). Protonated auxin is imported and deprotonated exported from the cell (329). H^+-PPases may control auxin transport and hence auxin-regulated gene expression by regulating its protonation (329, 357, 428). The activity of H^+-PPases increases with high auxin transport rates and *vice versa* (357, 442). H^+-PPase expression is increased by auxin (321, 443) and it is more sensitive to auxin-based regulation than is the expression of H^+-ATPases (365, 444-446). Auxin homologues (indole-3-butyric acid, for example) also activate H^+-PPases (447). Abscisic acid (ABA) usually increases H^+-PPase activity (321, 445, 448, 449), but can also inhibit it, depending on the concentration (408). Increased H^+-PPase activity and enhanced salinity tolerance can result from ABA signaling (450). Furthermore, ABA can induce H^+-PPase expression (443, 451). 6-Benzyladenine (BA) (321) and gibberellic acid (GA) (321, 444, 445) can also modify the expression and activity of H^+-PPases. H^+-PPases are more sensitive to BA- and GA-based regulation than are H^+-ATPases (321, 365, 441, 446, 449). In addition, kinetin activates H^+-ATPases and H^+-PPases, the former being more sensitive to this kind of regulation (365, 445, 446). Brassinolide stimulates the activity and expression of both H^+-PPases and H^+-ATPases and the stimulatory effects are highest when red beet roots are treated with low brassinolide and high KCl concentration (441, 452). Jasmonic acids (JA) may regulate H^+-PPase gene expression at the transcriptional level (453).

1.5.2.3 mPPase overexpression in plants

H^+-PPase expression in plants can be modified with molecular biology techniques (454). The overexpression of plant and bacterial H^+-PPases in plants has enhanced their stress resistance towards salinity, drought/osmotic stress, cold temperatures, P_i and NO_3^- limitation, Cd and industrial waste phosphogypsum (PG) as is shown in Table 3 (359, 397, 451, 455-463). Furthermore, plants overexpressing mPPase are bigger in size (Fig. 10), have enlarged and better developed roots and shoots, more rosetta leaves (20/14 in *A. thaliana*), increased seed production and germination during stress and recover quicker after stress when compared to wild type plants (397, 428, 451, 455, 458-463).

Table 3. Plants overexpressing H^+-PPases have an enhaced tolerance towards various forms of abiotic stress.

Organisms constructed to overexpress H^+-PPase	H^+-PPase	Origin of overexpressed H^+-PPase	Stress tolerance	Reference
Arachis hypogaea	AVP1	*A. thaliana*	Salinity and drought	(455)
A. thaliana	AVP1	*A. thaliana*	Salinity	(397)
	AVP1	*A. thaliana*	Phosphorus limitation	(371)
	EVP1	*Eucalyptus globulus*	Salinity and drought	(451)
	SsVP	*Sueda salsa*	Salinity and drought	(415)
	MtVP1	*Medicago truncatula*	Cold	(464)
	TaVP1	*T. aestivum*	Cd and phophogypsum	(456)
Gossypium hirsutum	AVP1	*A. thaliana*	Salinity and drought	(465)
	AVP1	*A. thaliana*	Salinity and drought	(466)
	TsVP	*Thellungiella halophila*	Salinity	(460)
	TsVP	*T. halophila*	Drought	(459)
Lactuca sativa	AVP1	*A. thaliana*	NO_3^- limitation	(381)
Medicago sativa L.	AVP1	*A. thaliana*	Salinity and drought	(458)
Nicotiana tabacum	AVP1	*A. thaliana*	Salinity	(467)
	AVP1	*A. thaliana*	Salinity	(405)
	TsVP	*T. halophila*	Salinity	(467)
	TsVP	*T. halophila*	Salinity	(405)
	Rr-PPase	*R. rubrum*	Drought	(462)
	TaVP1	*T. aestivum*	Cd	(457)
Oryza sativa	OVP1	*Oryza sativa*	Cold	(468)
	AVP1	*A. thaliana*	Salinity and drought	(466)
	AVP1	*A. thaliana*	Phosphorus limitation	(371)
Solanum lycopersicum	AVP1	*A. thaliana*	Salinity and drought	(466)
	AVP1	*A. thaliana*	Phosphorus limitation	(371)
	AVP1	*A. thaliana*	Drought	(463)
Solanum tuberosum	MtVP1	*Medicago truncatula*	Cold	(464)
Zea mays	TsVP	*T. halophila*	Drought	(461)
Saccharomyces cerevisiae	TaVP1	*T. aestivum*	Decreased Na^+ sensitivity	(412)
(yeast, ena1 strain)	AVP1	*A. thaliana*	Decreased Na^+ sensitivity	(405)
	TsVP	*T. halophila*	Decreased Na^+ sensitivity	(405)

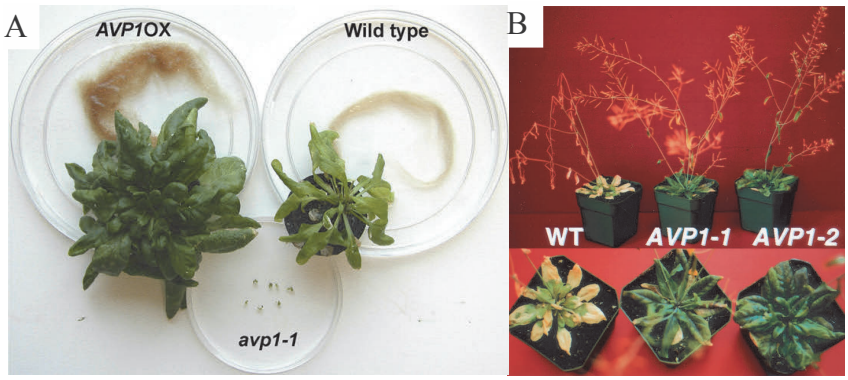

Figure 10. H^+-PPase is essential for plant viability and its overexpression increases the growth and stress resistance of versatile plants. A. *A. thaliana* overexpressing AVP1 (*AVP1OX*) has enlarged roots and shoots, whereas a plant having with a loss-of function mutation of AVP1 (*avp1-1*) is not viable (298). B. Plants, wild type and AVP1 overexpressing strains (*AVP1-1* and *AVP1-2*), ten days after being stressed with 250 mM NaCl reveal that mPPase expression enhances the salinity tolerance of the plants (298, 386). (Reprinted from *FEBS Lett.* 581, 12, Gaxiola R. A. *et al*., Plant proton pumps, 2204−14, Copyright (2007), with permission from Elsevier, and from *Proc. Natl. Acad. Sci. USA* 98, 20, Gaxiola R. A. *et al*., Drought- and salt-tolerant plants result from overexpression of the AVP1 H^+-pump, 11444−9, Copyright (2001) National Academy of Sciences, U.S.A.).

At the molecular level plants overexpressing H^+-PPases show higher solute, Na^+, K^+ and Ca^{2+} accumulation in leaves and shoots, elevated Na^+ and Cl^- sequestration in vacuoles, enhanced membrane integrity, decreased malonidialdehyde (MDA) accumulation, increased vacuolar acidification and cellular proline accumulation than wild type plants (405, 458-460, 463, 468, 469). Especially during salinity stress, H^+-PPase overexpression increases the formation of a vacuolar H^+-gradient, which can be used to increase the sequestration of Na^+, other ions and sugars into vacuoles to reduce the water potential of the cell and enhance water uptake from the roots (405, 458, 460, 463, 466, 467). H^+-PPase overexpression induces sucrose accumulation which promotes the biosynthesis of anthocyanins (464). In addition, photosynthetic activity is high in plants overexpressing H^+-PPases and is further increased during drought or salinity stress (455, 460). Especially under stressful conditions crop yields can be increased by the overexpression of H^+-PPases (386, 463, 466, 468). Cotton overexpressing an H^+-PPase, for example, produces a 20−51% higher yield than the corresponding wild type strains in dry field conditions (459, 466). Furthermore, H^+-PPase overexpressing plants grow better than wild type ones in P_i deficient soils (371). This property reduces the ulitization of phosphate as a fertilizer in agriculture and minimizes its polluting effects on aquatic environments (371).

There are many studies, in which a H^+-PPase has been overexpressed together with some other protein e.g. a Na^+/H^+-antiporter (428). The combined overexpression of an H^+-PPase and an Na^+/H^+-antiporter has led to a further enhancement in the saline and/or saline-alkaline stress tolerance of *N. tabacum* and *M. sativa* compared to both wild type plants and plants overexpressing only one of the proteins (470). Maize overexpressing both a *Thellungiella halophila* H^+-PPase and an *E. coli* beta choline dehydrogenase was more drougth tolerant and larger in size than plant lines that overexpressed one protein only (471). In addition, the overexpression of plant H^+-PPases in the *ena1* yeast strain, which is highly sensitive to Na^+, protected the strain from Na^+ toxicity (412). Furthermore, if the PM Na^+/H^+-antiporter is nonfunctional a H^+-PPase will not confer salinity tolerance to *A. thaliana* (397). H^+-PPases are essential for plant viability because e.g. a AVP1 loss-of-function mutant (*avp1-1*) was not able to grow as wild type plants as indicated in Fig. 10A (298).

1.5.3 mPPases in algae

Halotolerant, red and green algae (Table 2), including *Dunaliella viridis* (472), *Cyanidioschyzon merolae* (473), *Chlamydomonas reinhardtii* (255), *Acetabularia acetabulum* (474) and *Mesotaenium caldariorum* (475) have mPPases in their vacuolar membranes. Similarly to plants, algae control the size of their vacuoles based on environmental conditions, and compartmentalize toxic substances into vacuoles (476). The H^+-PPases in algae regulate primary and secondary vacuolar transport, vacuole size and pH, and enhance salinity tolerance (472, 475-477). H^+-transporters are also required for the maintenance of a constant cellular pH during salinity stress, which is important for the cell viability (395). In addition to H^+-transporters, other enzymes are required for salinity tolerance in algae, e.g. Na^+-ATPases (384), and there are differences in the salinity tolerance between algae species. *Chara corallina* tolerates only low Na^+ concentrations

(478) in contrast to *Chara longifolia* that can grow at high Na^+ concentrations. Notably, the vacuolar membranes of both algaea contain H^+-PPases and H^+-ATPases (477).

1.5.4 mPPases in protists

mPPases are widely distributed among protozoa (Table 2) and are found in all phyla, except Choanoflagellates, Amoebozoa, Parabasalids and Diplomonads. Protists may also contain multiple copies and isoforms of mPPase genes in their genomes (9, 142). Horizontal gene transfer may have occurred between phylogenetically diverse species (142). *Plasmodium falciparum*, the malaria parasite, has two types of H^+-PPases, a K^+-independent and a K^+-dependent one, that can be expressed and regulated based on growth conditions. The K^+-dependent enzyme is mainly involved in infectious phases and the K^+-independent enzyme in parasite reproduction (253, 479, 480). H^+-PPases exist also in other disease-causing protists e.g. *Trypanosoma cruzi* (Chagas' disease) (481), *Trypanosoma brucei* (African trypanosomiasis) (14), *L. donovani* (visceral leishmaniasis) (192), *Philasterides dicentrarchi* (infects turbot) (482) and *Plasmodium berghei* (infects murinae) (187). In these organisms the H^+-PPase activity alleviates the stress caused by the defence system of the host organism (9, 483, 484). Mammalian cells do not contain mPPases and thus these enzymes may provide good drug targets for treating malaria (9, 250, 253, 483). The most promising drugs are currently bisphosphonates e.g. AMDP that inhibits the mPPases of *Toxoplasma gondii* (230, 250) and *P. berghei* (187). However, the *in vivo* specificity of the inhibitors remains to be clarified (253). AMDP is a less efficient H^+-PPase inhibitor *in vivo* than in *vitro* (479). This may result from inefficient uptake of the inhibitor or because the inhibitor is a PP_i analogue and its effect depends on the concentration of PP_i (479). Related to this, protist cells can tolerate high PP_i concentrations (15, 485), their mPPases are inhibited if free PP_i concentrations are elevated in the cell (486).

Protist cells have multiple copies of acidocalcisomes (277, 487). Acidocalcisomes are organelles that have Ca^{2+}-ATPases, H^+-ATPases, H^+-PPases, Na^+/H^+- and Ca^{2+}/H^+-exchangers and aquaporins in their membranes. Polyphosphate, calcium and different cation concentrations are high inside these organelles (277, 485, 487-494). The chemical composition of acidocalcisomes varies, based on environmental conditions (495). Protists use acidocalcisomes for adaptation to environmental stress (158, 492, 496) and for special functions e.g. for the degradation of host hemoglobin (486). H^+-PPases together with H^+-ATPases and aquaporins are important for maintaining the cell's essential pH and ion gradients, and for osmoregulation (187, 479, 481, 486, 497-501). The protist *T. gondii* with a null mutated H^+-PPase was more sensitive to extracellular conditions, ion concentrations, hyper- and hypo-osmotic stress, than the wild type organism (498). Osmoregulation is important for host cell invasion suggesting that H^+-PPase activity is important for the lytic cycle of *T. gondii* (498). H^+-PPases are expressed during different developmental phases of protists (502), when the mPPase activity can dominate over the H^+-ATPase activity (192, 251). Also in protists the H^+-PPase can complement the functions of the H^+-ATPase (501, 503), especially in conditions of limited energy (479). The overexpression of different proteins in protists also changed the expression and activity of mPPases (246, 504).

2. AIMS OF THE STUDY

When I started my Ph.D. studies it was known that there were many different groups of H^+-translocating mPPases, but Na^+-transport had only just been described for three enzymes. We aimed to investigate whether Na^+-transport was a general function of mPPases or simply a peculiarity. Because the 3D-structures of mPPases were not available at the time, we started mapping the functional diversity of mPPases and elucidating the amino acid residues that determine transport specificity. We did this using a method that combined the phylogenetic mapping of sequence diversity in a protein family to the experimental characterization of the selected representative proteins. The predictions for the specificity determinants uncovered from this data were further tested using site-directed mutagenesis. My work comprised of four specific aims:

1. Unraveling the functional diversity and evolutionary history of membrane-bound PPases and identifying a general amino acid pattern that predicts the specificity of the transported ion.

2. Characterizing the detailed functional properties of the putative H^+ and Na^+-transporting mPPases which were discovered during the work towards aim 1.

3. Testing the hypothesis that at least some Na^+-transporting PPases may in specific conditions additionally transport H^+ ions.

4. Characterizing the functional properties of proteins ("divergent mPPases") that are distantly related to typical mPPases.

The results of my studies are presented in four international peer-reviewed articles (see page 6) and are summarized in Section 3 of this thesis.

3. SUMMARY OF THE MATERIALS AND METHODS

3.1 Construction of mPPase-expressing *Escherichia coli* lines

Mainly bacterial and archaeal mPPases were investigated in this research. The selected mPPases were those from *Anaerostipes caccae* (Ac-PPase), *Akkermansia muciniphila* (Am-PPase), *Bacteroides vulgatus* (Bv-PPase), *Cellulomonas fimi* (Cf-PPase), *Chlorobium limicola* [Cl-PPase, Cl-PPase(2)], *Clostridium leptum* (Clep-PPase), *Clostridium lentocellum* (Clen-PPase), *Clostridium tetani* E88 (Ctet-PPase), *Clostridium thermocellum* (Ct-PPase), *Clostridium sp.* 7_2_43FAA (Cs-PPase), *Desulfuromonas acetoxidans* (Da-PPase), *Flavobacterium johnsoniae* (Fj-PPase), *Leptospira biflexa* (Lb-PPase), *Prevotella oralis* (Po-PPase), *Verrucomicrobiae bacterium* (Vb-PPase). The mPPases were expressed under the T7 promoter in the pET36b(+) expression vector (Novagen) and the genes were typically cloned from the genomic DNA of the bacteria or archaea into the vectors using the NdeI, XhoI, HindIII, NotI and BamHI restriction sites. As controls we used mPPases with known functions from *C. hydrogenoformans* [Ch-PPase, K^+-dependent H^+-PPase (170)], *P. aerophilum* [Pa-PPase, K^+-independent H^+-PPase (124)], *S. coelicolor* [Sc-PPase, K^+-independent H^+-PPase (505)] *T. maritima* [Tm-PPase, Na^+-PPase (28, 161)]. Mutations were engineered into the mPPases with inverse PCR and both wild-type and mutated enzyme constructs were sequenced at Eurofinns-MWG (Germany).

3.2 Recombinant mPPase expression and IMV isolation

The proteins of interest were expressed in *E. coli*. The cells were broken with a French press at 14000 psi and the mPPases were isolated by sucrose gradient ultracentrifugation in inverted membrane vesicles (IMVs) using a method slightly modified from Belogurov *et al.* 2005 (161). The IMV storage buffer contained 10 mM MOPS-TMA hydroxide pH 7.2; 1 mM $MgCl_2$, 750−900 mM sucrose, 5 mM dithiotreitol (DTT) and 50 μM EGTA. Vesicles were frozen in liquid N_2 and stored at -85 °C. The Bradford assay was used to estimate the total protein content of the IMVs (506). mPPase expression in the IMVs was verified with Western blotting, 0.2−18 μg of the IMVs was loaded into the gel in 1xSDS loading buffer. The loading buffer consisted of 70 mM Tris-HCl, pH 6.8, 11% glycerol, 2% SDS, 2.5 mM DTT and 0.25 mg/mL bromophenol blue or OrangeG. Proteins were denatured at 50 °C 15 min to avoid precipitation and run on SDS-PAGE gels made up of a 4−20% acrylamide gradient (Thermo Fisher Scientific & Idgel). Proteins were transferred from the gel to a nitrocellulose membrane (0.45 μm pore size, Whatman) with a Mini Trans-Blot apparatus or a TE 77 PWR semi-dry electroblotting apparatus (Amersham Bioscience) in Towbin buffer (507) that contained 10−20% (v/v) methanol. The membrane was blocked by incubating it overnight in 20 mM Tris-HCl pH 7.6, 150 mM NaCl (TBS), 0.1% Tween-20 and 5% fat-free milk. A primary rabbit antiserum against the IYTKAADVGADLVGKVE peptide was used for the detection of mPPases (28), except for divergent mPPases, and the protein bands were visualized using an

anti-rabbit secondary antibody labeled with HRP or IRDye 800CW (Donkey anti-rabbit IgG (H+L) highly cross absorbed; Li-Cor). We used the Anti-6xHis Epitope Tag (Mouse) Mononclonal Antibody IRDYE® 800CW Conjugated (Rockland antibodies & assays, USA) for the detection of divergent mPPases with an 8xHis-tag. Membranes were washed with TBS and 0.05 % Tween-20 5 x 5 min and 1 x 10 min after each antibody treatment the last two washes after the incubation with the secondary antibody were carried out in TBS only to avoid Tween-20 interfering with the signal. When the HRP-labeled antibody was used the protein bands were detected with the ECL substrate (Amersham) and the chemiluminescent detecting Hyperfilm™ ECL (Amersham). The GelCode Blue Coomassie stain (Thermo Fisher Scientific) was used for staining the SDS gels. Images were analyzed with ImageJ (508). The molecular weights of proteins on the SDS gels were determined using the PageRuler Prestained Protein Ladder (Thermo Fisher Scientific) or the 6xHis Protein Ladder (Qiagen cat no. 34705).

3.3 PP_i hydrolysis measurements

We were able to measure the PP_i hydrolysis activity in IMVs because mPPases are absent from *E. coli* and any soluble PPase is washed away from the IMVs by the sequential sucrose gradient ultrasentifugations. PP_i hydrolysis was determined by continuous measurements detected with semi-automated phosphate analyzer (509). The measurements typically contained 0.1 M MOPS-TMA hydroxide pH 7.2, 5−40 μM EGTA, 5.3 mM $MgCl_2$, 0−200 mM NaCl, 0−200 mM KCl and 0.5−1000 μM Mg_2PP_i. Reactions were performed at 25 °C and initiated with the addition of the IMVs. The rate of PP_i hydrolysis was determined from the slopes of the curves for phosphate formation, which was measured for 2−3 min. The concurrent measurements differed less than 10% indicating that the results were reliable. 20 or 100 mM MOPS, MES, TAPS or CAPSO, TMA hydroxide buffers were used in the pH measurements. In addition, the Mg^{2+} and PP_i concentrations under different conditions were maintained comparable to measurements with 100 μM Mg_2PP_i at pH 7.2. We regularly used a MOPS buffer in our measurements because it does not inhibit mPPases (143).

3.4 Kinetic analysis

The PP_i hydrolysis activity of mPPases was measured at different Mg^{2+}, Na^+ and/or K^+ concentrations with saturated Mg_2PP_i concentrations. In each article the measured data was analyzed with the best fitting kinetic schemes, based on which the kinetic equations were developed. Kinetics analyses were also carried out as a function of substrate Mg_2PP_i concentration. Mg^{2+} and PP_i form two types of complexes, $MgPP_i$ and Mg_2PP_i (19, 143), and Na^+ and K^+ bind weakly to PP_i (21, 22). The apparent dissociation constants for the $MgPP_i$ complex are 0.859 (0 mM Na^+, 0 mM K^+), 0.161 (100 mM Na^+, 0 mM K^+), 0.140 mM (0 mM Na^+, 100 mM K^+). 2.84 mM was used as the dissociation constant for Mg_2PP_i under all conditions (19, 75). The SCIENTIST software (Micromath) was employed to fit the data and to determine the kinetic constants with standard errors (S.E.).

3.5 Na^+ transport

Na^+ transport into IMVs was determined with a radioactive $^{22}Na^+$ isotope and a membrane filtration procedure in an ice water bath (0 °C) or at room temperature (RT, 22−23 °C). The total protein content in the measurements was generally 1−2 mg/mL. The reactions were typically measured under conditions of 100 mM MOPS-TMA hydroxide pH 7.2, 0.1−10 mM Na^+, 50 mM K^+, 5 mM Mg^{2+}, 0/160 mM Cl^-. 0.3−14 µCi $^{22}NaCl$ (PerkinElmer Life Sciences) was added to the IMV dilutions and incubated ~0.5−1 h before the reactions were initiated with the addition of 1 mM TMA_4•PP_i. At the 15−90 s time points the reaction was stopped with the addition of 20 mM EDTA pH 7.2 and the IMVs were filtered through a 0.2 µm pore size nitrocellulose filter (Millipore) and washed with 1 ml of 5 mM MOPS-TMA hydroxide pH 7.2, 100 mM Na^+, 0.5 mM Mg^{2+}, 160 mM TMACl buffer. 1 ml of the Ultima Gold scintillation cocktail (Perkin Elmer Life Sciences) was added and the PP_i induced $^{22}Na^+$-accumulation inside the vesicles was measured with scintillation counting (Rackbeta 1215, LKB Wallac). Ionophores including, 20 µM ETH157 (a Na^+-ionophore), 5 µM CCCP (a H^+-ionophore), 2 µM valinomycin (a K^+-ionophore), were utilized into the transport measurement to determine the specificity and electrogenicity of the ion transport.

3.6 H^+ transport

9-Amino-6-chloro-2-methoxyacridine (ACMA) (Invitrogen), and acridine orange (AO), were employed as the pH dependent fluorescent dyes to detect H^+ transport (510). Reactions were performed at 25 °C and the excitation and emission wavelengths were 428/475 nm and 490/540 nm, depending of the probe used. H^+ transport measurements were typically performed at 25 °C in 20 mM MOPS-TMA hydroxide pH 7.2, 8 µM EGTA, 0−100 mM Na^+, 5.8 mM Mg^{2+}, 0−100 mM K^+, 2 µM AO or ACMA. The amount of Cl^- was kept constant at 150−160 mM with TMA chloride or measured only with SO_4^{2-} salts. The total protein content in the measurements was 0.2−0.6 mg and the reactions were initiated with the addition of 475 µM TMA_4•PP_i (300 µM Mg_2PP_i) after a 4 min incubation in the dark and a 2 min background level measurement. The reactions were terminated by adding 10 mM NH_4Cl. Ionophores were used similarly than as in Na^+ transport measurements.

3.7 Membrane potential measurements

Changes in membrane potential due to H^+-PPase function were recorded with the fluorescence probe $DiBAC_4(3)$ [(bis-(1,3-dibutylbarbituric acid)trimethine oxonol] (Life Technologies). IMVs with 0.3−0.6 mg/mL protein were preincubated for 2 h with the 25 nM $DiBAC_4(3)$ at 25 °C in a buffer of 0.1 M MOPS-TMAOH pH 7.2, 25 mM K_2SO_4, 5 mM $MgSO_4$. The ATPase activity of the *E. coli* IMVs was used as a control in these measurements and the ion transport was initiated with 0.5 mM ATP or 1 mM TMA_4•PP_i. These measurements were performed using 488 and 520 nm as the excitation and emission wavelengths, respectively.

3.8 Studies using *Bacteroides vulgatus* cells

B. vulgatus cells were grown anaerobically for 30 h at 37 °C in brain-heart infusion medium (Sigma) supplemented with 5 g/L yeast extract, 0.5 g/L cysteine-HCl, 1 µg/mL resazurin, 5 µg/mL hemin and 1 µg/mL menadione. Cells were harvested and the ions of the medium were washed away with 100 mM MOPS-TMA-hydroxide pH 7.2, 5 mM EDTA and 10% glycerol with three centrifugations at 6000 g, 15 min, +4 °C. Otherwise, the IMVs were isolated similarly to the *E. coli* IMVs.

3.9 Bioinformatics

mPPase sequences were collected from the KEGG Protein Sequence Database typically using the *R. rubrum* mPPase (Rru_A1818) as a query sequence in a BLAST search (511). Protein sequences were aligned with MUSCLE versions 3.6 and 3.8 (512). Sequence alignments were cured manually by removing the sequences with deletions or sequences that did not contain the amino acid residues that are essential for the mPPase-catalyzed PP_i hydrolysis and transport. Phylogenetic trees were constructed with the MrBayes program version 3.1.2. (513). Random trees were used as the basis for the four independent and weighted phylogenetic analyses that were run 2, 5 or 10 million generations with 0.15 as a temperature option on the CSC-IT Center for Science Ltd. (Espoo, Finland) computer cluster. The split frequence mean SD was lower than 0.01 after 2.5 million generations and represented the convergence of the analysis. The resulting trees were constucted using 25% of the samples as burn-in. The similar topologies were recovered using the maximum likelihood algorithm RAxML (514).

4. RESULTS AND DISCUSSION

4.1 Expression and PP_i hydrolysis activities of various types of mPPases (studies I–IV)

When I began my studies, our research group had identified and characterized just three Na^+-PPases (28). Malinen *et al.* had pointed out that while the K^+-independent clade of the phylogenetic tree of mPPases had been characterized in relative detail, the functions of many of the clades in the K^+-dependent H^+-PPase part of the tree were still unknown (Fig. 11). Furthermore, at that time it still remained to be shown how common Na^+ transport was among mPPases. Based on the phylogenetic analysis of ATPases it was predicted that Na^+ based bioenergetics could have preceded H^+ bioenergetics (126). We aimed to find out if the ion transport specificity of mPPases had evolved similarly. We also knew that there was a divergent group of mPPases, e.g. from *Chlorobium tepidum*, with uncharacterized functions (Fig. 11). These enzymes are, based on their amino acid sequence, evolutionarily less related to other mPPases (226). In addition, we wanted to identify the amino acid pattern that determines the ion transport specificity of mPPases. This would allow the prediction of the ion specificity for the large number of mPPases continuously unveiled by genome sequencing projects. I therefore picked up different bacterial and archaeal mPPases from the uncharacterized clades of the phylogenetic tree of mPPases (Fig. 11) and investigated their functional properties in detail.

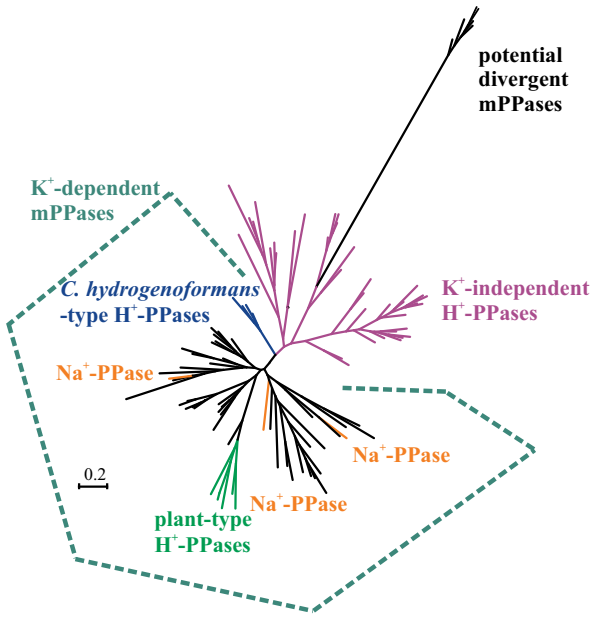

Figure 11. The phylogenetic tree of mPPases at the time I started my PhD studies. The tree was created with MrBayes 3.1.2. The K^+-independent clade (violet) and two K^+-dependent clades (green, blue) of H^+-PPases had been studied quite extensively, but many clades remained uncharacterized (shown in black) and we wished to analyze these in detail with special emphasis on their ion transport specificities.

In the first study (Article I) Ac-PPase, Cl-PPase, Ctet-PPase, Ct-PPase, Da-PPase, Fj-PPase, Lb-PPase mPPases were expressed in *E. coli* and isolated in IMVs. Ch-PPase (K^+-dependent H^+-PPase) (170), Pa-PPase (K^+-independent H^+-PPase) (124), Sc-PPase (K^+-independent H^+-PPase) (505), Tm-PPase (Na^+-PPase) (28, 161) were used as positive controls in this study, whereas IMVs isolated from a *E. coli* strain carrying only the cloning vector served as a negative control. Based on sequence and a phylogenetic analysis conserved amino acid residues were determined and compared. The conserved glutamate residues were site-directly mutated to clarify their role in ion transport specificity. Glu to Asp or Ser mutated enzymes were expressed in *E. coli* and their expression and PP_i hydrolysis activity were verified similarly to what was done for the wild type enzymes. The corresponding mutations were Lb-PPase E253D or E253S, Fj-PPase E185D or E185S, Cl-PPase E242D or E242S. All of the mutated enzymes were able to hydrolyze PP_i, except the Cl-PPase E242S variant. However, all mutated mPPases hydrolyzed PP_i at a lower rate than the wild type enzyme (Fig. 12A). In all four (I–IV) studies PP_i hydrolysis was analyzed with the known mPPase inhibitor AMDP and a soluble PPase inhibitor KF (184, 185), and as expected, our results showed that AMDP inhibited and KF did not inhibit the PP_i hydrolysis activity of mPPases.

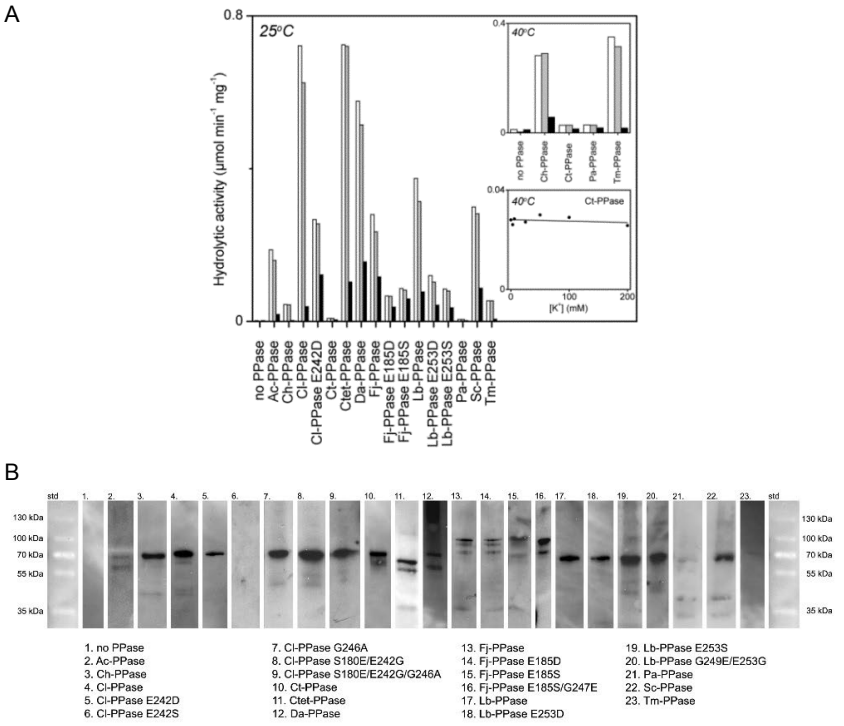

Figure 12. PP_i hydrolysis activities and expression of the mPPases studied in article I. A. PP_i hydrolysis was measured with 5 mM Mg^{2+}, 10 mM Na^+, 50 mM K^+, 100 μM Mg_2PP_i with – (white bars), 250 μM KF (grey bars) or 20 μM AMDP (black bars) at 25 °C. The PP_i hydrolysis activity of thermophilic mPPases (Ch-PPase, Ct-PPase, Pa-PPase, Tm-PPase) was measured also at 40 °C, because the activity of these enzymes is very low at 25 °C. Ct-PPase was shown to act as a K^+-independent mPPase at 40 °C when its activity was measured with 5 mM Mg^{2+}, 100 μM Mg_2PP_i and 0–200 mM KCl. B. Western blot of the wild type and site-directly modified mPPases of bacterial and archaeal origin. 0.2–2 μg of total protein was loaded onto the 4–20% SDS-PAGE gels and mPPases were detected with a primary rabbit antiserum specific for mPPases (IYTKAADVGADLVGKVE) and a HRP labeled secondary antibody.

In the second study (Article II) we expressed the following bacterial mPPases: Am-PPase, Bv-PPase, Clep-PPase, Clen-PPase, Cs-PPase and Vb-PPase. The archaeal Mm-PPase, (a Na^+-PPase) (28) was expressed as a positive control in these experiments. Protein expression in the vesicles was verified with Western blotting. All of the enzymes in studies I and II, both wild type and mutated ones, except Cl-PPase E242S were expressed in *E. coli* (Figs. 12B & 13A). The E242S substititution may induce big conformational changes to Cl-PPase and have a negative effect on the viability of *E. coli* cells. Some of the mPPases migrated differently in the SDS-PAGE gel although the sizes of the proteins do not differ markedly. Because mPPases are highly hydrophobic SDS may not be able to completely denaturate the proteins and this can result in differences in migration (253). Like in the study I, all of the enzymes expressed in study II were able to hydrolyze PP_i indicating that they are mPPases.

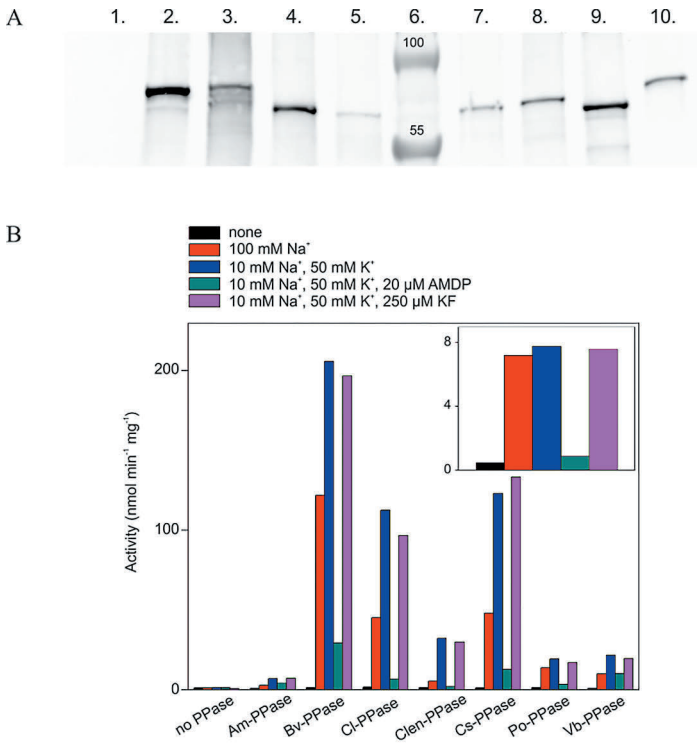

Figure 13. Western blot and PP_i hydrolysis activities of mPPases studied in article II. A. Proteins were loaded in the following order 1. no PPase, 2. Po-PPase, 3. Am-PPase, 4. Clep-PPase, 5. Clen-PPase, 6. protein ladder for size determination, 7. Cs-PPase, 8. Vb-PPase, 9. Mm-PPase, 10. Bv-PPase. B. PP_i hydrolysis activities of different bacterial mPPases were analyzed also in the presence of the inhibitors KF and AMDP. Furthermore, PP_i hydrolysis from the *B. vulgatus* IMVs (*inset*) showed similar behavior as the Bv-PPase expressed in *E. coli* IMVs.

In the third study (Article III) we described the functions of Na^+-PPases in detail and identified the amino acid residues that determine the Na^+-PPase ion transport specificity. The sequence and structure of Na^+-PPase monomers were analyzed and the gate amino acid residues (Lys681, Asn677, Ser243, Glu242, Asp239), which specify the transported ion in Cl-PPase, were modified with site-directed mutagenesis (Fig. 14).

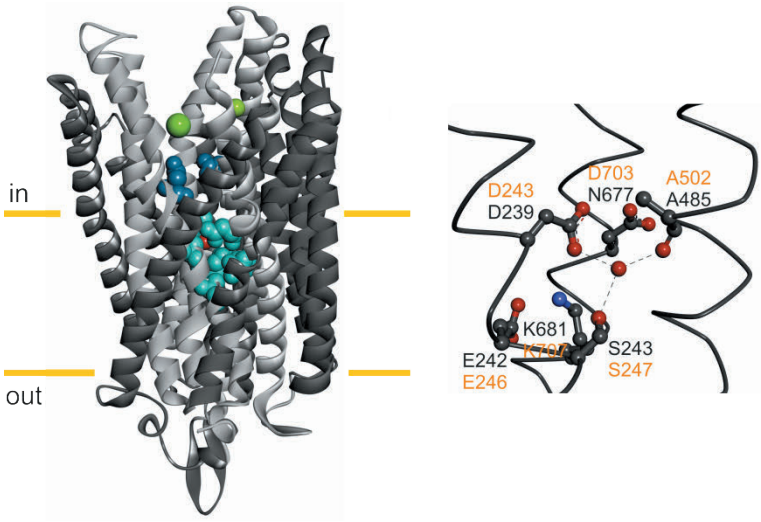

Figure 14. 3D-structure of the Tm-PPase monomer and the gate residues important for ion transport specificity. Mg^{2+} ions are shown in green and aspartate residues important for substrate binding are shown in blue. The gate amino acid residues are marked with cyan and water with red. The dark grey transmembrane helices (TMs) form the outer ring and the light grey TMs the inner ring of the mPPase monomer. The gate residues important for ion transport specificity were site-directly mutated and their residue numbers in Cl-PPase are coloured in black and in Tm-PPase in orange.

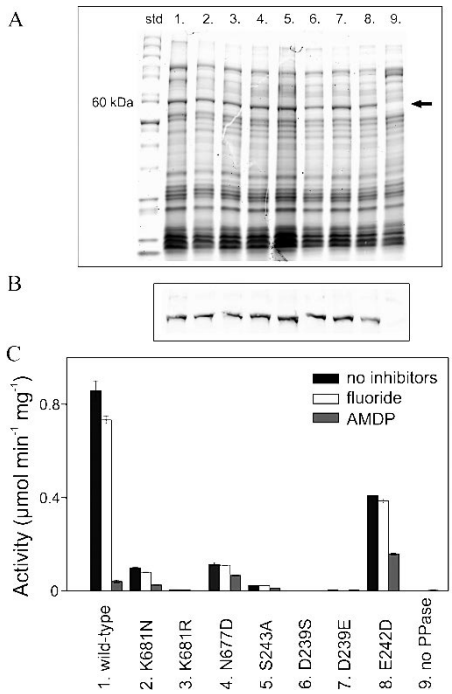

Figure 15. Expression and PP_i hydrolysis activities of the mPPases studied in article III. A. mPPase expression in *E. coli* IMVs was determined by SDS-PAGE (10−18 µg total protein loaded to 4−20 % acrylamide gradient gel) stained with Coomassie Blue. The protein expression was clearly demonstrated from the gel when compared to no-PPase containing IMVs. B. mPPase expression was also analyzed with Western blotting using a primary rabbit antibody that specifically binds to an mPPase sequence and an IR-labeled secondary anti-rabbit antibody. C. PP_i hydrolysis was determined in the presence of 10 mM Na^+, 50 mM K^+, 100 µM Mg_2PP_i, at pH 7.2, at 25 ºC. In addition, 250 µM KF, a soluble PPase inhibitor, or 20 µM AMDP, an mPPase inhibitor was added to the reaction.

The mutated Cl-PPases K681N, K681R, N677D, S243A, E242D, D239S, D239E were expressed in *E. coli* and isolated in IMVs. Their expression was verified both with Coomassie staining of the 4−20% polyacrylamide SDS gels (Fig. 15A) and with Western blotting (Fig. 15B). Site-directly modified enzyme activities and expression levels were compared to the activities of the Cl-PPase and no PPase IMVs. The Cl-PPase variants K681R, D239S and D239E were not able to hydrolyze PP_i although they were expressed in the IMVs (Fig. 15C).

Although mPPases form a conserved enzyme family based on their amino acid sequences, the phylogenetic tree includes sequences that are only distantly related (23−34% similarity) to other mPPases. These sequences have usually additional amino acid residues compared to the other prokaryotic mPPases, and they were long thought to be pseudogenes. In May 2014 there were 2828 completely sequenced prokaryotic genomes, of which about 25% (686) contained genes encoding mPPases, but only 46 bacterial strains and one archaeal strain had corresponding sequences to this divergent clade. In the fourth study (Article IV), we expressed and characterized two members of this clade of the tree. We named these enzymes divergent mPPases and the enzymes studied were those of *C. limicola* [Cl-PPase(2)] and *C. fimi* (Cf-PPase).

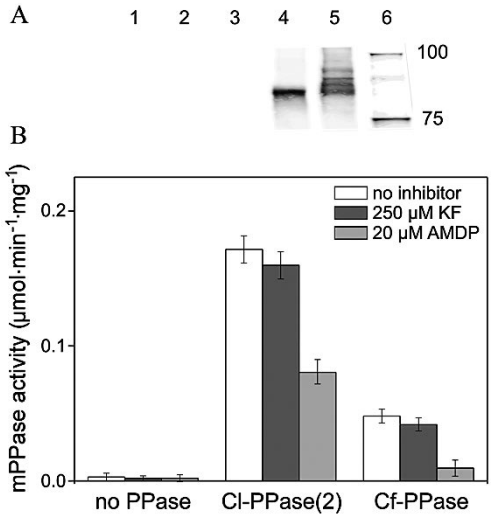

Figure 16. Expression and PP_i hydrolysis activities of the divergent mPPases studied in article IV. A. Expression was verified with Western blotting using an anti-His tag attaching antibody (Rockland Immunochemicals Inc.) and 10 µg of a total protein sample. The order on the gel was 1. no PPase, 2. Cl-PPase(2) without an 8xHis-tag, 3. Cf-PPase without an 8xHis-tag, 4 Cl-PPase(2) with an 8xHis-tag, 5. Cf-PPase with an 8xHis-tag. 6. 6xHisProtein ladder (Qiagen). B. PP_i hydrolytic activities were measured with 5 mM Mg^{2+} and 100 µM Mg_2PP_i with no addition, 250 µM KF or 20 µM AMDP to show that the enzymes are mPPases.

The protein expression of the Cl-PPase(2) and Cf-PPase proteins containing an uncleavable 8xHis-tag was analyzed with Western blotting and an anti-His-tag antibody (Fig. 16A). The amino acid sequence (I**F**TK**I**AD**IGS**DL**M-**K**IA)** of divergent mPPases

differs significantly from the peptide sequence against which the antibody specific for mPPases specific had been designed (IYTKAADVGADLVGKVE), therefore it does not recognize divergent mPPases. The PP_i hydrolysis activity of IMVs with no PPase, Cl-PPase(2) and Cf-PPase was analyzed at pH 7.2 with 5 mM Mg^{2+} and 100 µM Mg_2PP_i with 250 µM KF or 20 µM AMDP (Fig. 16B). It was also shown that the expression levels of divergent mPPases were 2−3% of the total *E. coli* IMV protein expression and that the PP_i hydrolysis activities of His-tagged versions of Cl-PPase(2) and Cf-PPase were the same as those of the wild type enzymes. We were not able to detect the expression of divergent mPPases in the Coomassie stained SDS-PAGE gels, because *E. coli* contains proteins of similar size and the mPPases are expressed at low levels. All the novel enzymes expressed and characterized in studies I-IV were able to hydrolyze PP_i, and this activity was inhibited by AMDP but not by KF, clearly indicating that the enzymes are mPPases.

4.2 Ion transport (studies I−IV)

Na^+ transport was detected using a radioactive $^{22}Na^+$ isotope in a membrane filtration assay at 25 ºC. The accumulation of $^{22}Na^+$ in IMVs was determined by scintillation counting. Four new Na^+-PPases were discovered (Ac-, Cl-, Da-, Ctet-PPases) suggesting that Na^+ transport is a general property, and not just a peculiarity among mPPases (Fig. 17). However, not all mPPases, for example Fj-, Lb- and Ct-PPases tested in study I, were able to transport Na^+. As a control in these measurements we used the previously characterized Na^+-PPase of *T. maritima*, K^+-dependent H^+-transporting Ch-PPase, and K^+-independent H^+-transporting Pa- and Sc-PPases. The accumulation of $^{22}Na^+$ as a function of time was also determined. E➔D/S modified enzymes were shown to follow the ion transport specificity of wild type mPPases (Fig. 17).

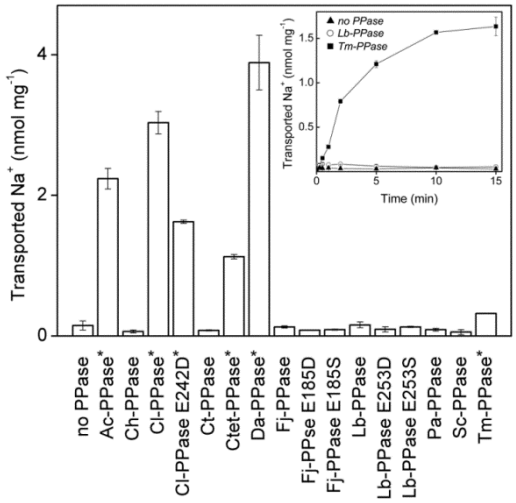

Figure 17. Na^+ transport activity of mPPases characterized in study I. Ac-, Cl-, Da-, Ctet-PPases and Cl-PPase E242D are Na^+-transporters, whereas Fj-, Lb-PPases and their mutants are not. To detect the limits of the assay Na^+ accumulation into the vesicles was determined as a function of time with IMVs containing Tm-PPase/Lb-PPase/no PPase (*inset*).

H^+ transport was detected in the mPPase-containing IMVs at 25 °C using ACMA as a pH dependent fluorescent dye. We found two new H^+-PPases, Lb- and Fj-PPase (Fig. 18A) and as a control in these measurements we used Ch-PPase. Na^+ transporting mPPases were not able to transport H^+ ions under the experimental conditions used (10 mM Na^+, 5 mM Mg^{2+}, 50 mM K^+, 100 μM Mg_2PP_i). The H^+ transport of Lb-PPase was detected at different PP_i hydrolysis rates adjusted by different Na^+ (and K^+) concentrations to determine the sensitivity of the assay (Fig. 18B). The effects of site-directed mutations on H^+ transport were also tested (Fig. 18C). Cl-PPase E242D behaved like the wild type Cl-PPase, i.e. it was not able to transport H^+. The mutant Lb-PPase E253D and Fj-PPase E185D were able to transport H^+. However, when the corresponding Glu residues were replaced with Ser residues the H^+ transport activity was completely abolished (Fig. 18C). All mutants retained PP_i hydrolysis activity in excess of the level required to support detectable H^+ transport activity (Fig. 12A). Accordingly, we concluded that the carboxylate group at position 253 in Lb-PPase and 185 in Fj-PPase is essential for H^+ transport function.

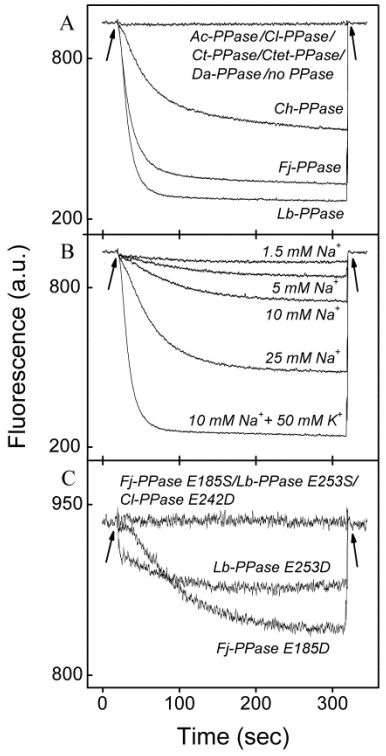

Figure 18. H^+ transport activity of mPPases characterized in study I. A. H^+ transport of wild type mPPases. Lb-, Ch- and Fj-PPases are H^+-transporters. Na^+-PPases do not transport H^+ when measured in 10 mM Na^+, 5 mM Mg^{2+}, 50 mM K^+, 300 μM Mg_2PP_i. B. Limits of our H^+ transport assay were determined by measuring the H^+ transport of Lb-PPase at different PP_i hydrolysis rates adjusted by Na^+ and K^+ concentrations. C. H^+ transport activity of mutated mPPases. A specific conserved Glu residue (E253 in Lb-PPase and E185 in Fj-PPase) is important for H^+ transport as shown by ES-substitutions which completely abolished H^+ transport but still had a high enough PP_i hydrolyzing activity to support H^+ transport. Mutating these glutamates to aspartates did not abolish proton pumping.

After Na^+-PPases were discovered in 2007 (28), ion pumping by mPPases was thought to be strictly specific for either Na^+ or H^+, i.e. H^+-PPases pump only protons and Na^+-PPases only sodium ions. However, in the second study, we characterized an mPPase of *B. vulgatus*, a bacterium of the human gastrointestinal tract, and showed that this mPPase transported both Na^+ and H^+ under physiological conditions (Fig. 19), and thus we named this enzyme a Na^+,H^+-PPase analogously to Na^+,H^+-ATPases (515). Based on Na^+ and H^+ transport measurements with and without ionophores, CCCP, ETH157, valinomycin and the mPPase inhibitor AMDP, we concluded that both the Na^+ and H^+ transport was due to an mPPase activity and not to secondary transport (Figs. 19A & B). Our results also indicated that transport of both Na^+ and H^+ was electrogenic. Na^+ and H^+ transport was measured with similar PP_i hydrolysis rates with the Na^+-translocating Ac-PPase and the H^+-translocating Lb-PPase to verify that the Na^+ and H^+ transport rates were proportional to those of the strictly Na^+- or H^+-transporting mPPases (Figs. 19 C & D).

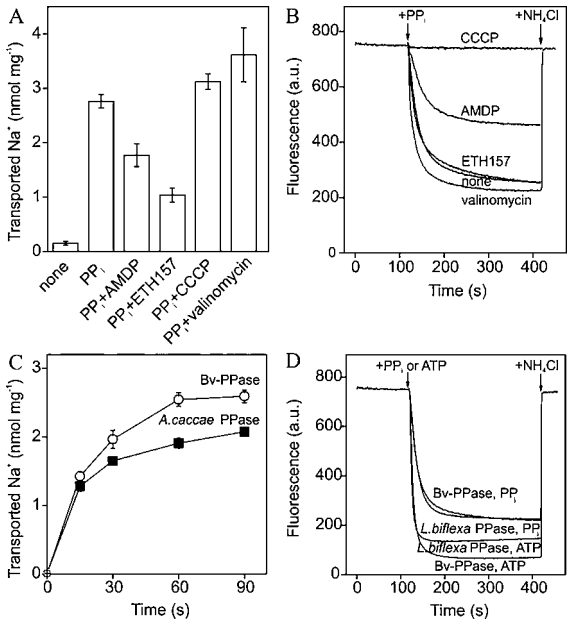

Figure 19. Na^+ and H^+ transport activities of the Bv-PPase characterized and measured in study II. A & B. Bv-PPase Na^+ and H^+ transport was measured with and without different ionophores and with AMDP. Based on these results we concluded that both Na^+ and H^+ transport is due to the mPPase and not caused by a secondary transport phenomenon. C & D. Na^+ and H^+ transport by Bv-PPase was measured together with the known Na^+-PPase of *A.caccae* and H^+-PPase of *L. biflexa*, to show that both of these ions were transported at rates comparable to those of monocation specific mPPase ion transporters.

To find out if Bv-PPase transports Na^+ and H^+ competitively we measured both ion transport activities at different pH and Na^+ concentrations (Fig. 20). Bv-PPase was able to transport protons in wide pH and [Na^+] ranges. These results indicated that high [Na^+] did not suppress H^+ transport under any conditions tested. Furthermore, Na^+ transport was highest at a low pH and a 10 mM Na^+ concentration (Fig. 20) and the Na^+-PPase transported Na^+ under all of the conditions tested. Accordingly, we concluded that Bv-PPase transports Na^+ and H^+ non-competitively.

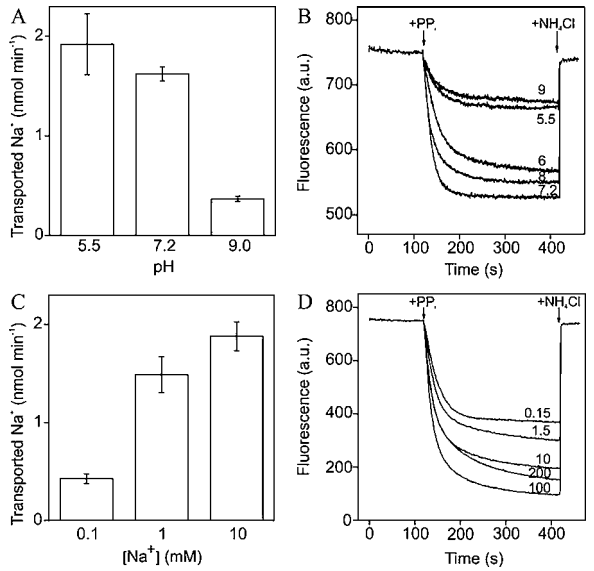

Figure 20. Bv-PPase catalyzed Na^+ and H^+ transport at pH 5.5 to 9.0 and at Na^+ concentrations of 0.1−200 mM (25 °C) (study II). A & B. Na^+ and H^+ transport was measured at different pH values to show that Na^+ and H^+ were not transported competitively. C & D. Na^+ and H^+ transport under different Na^+ concentrations.

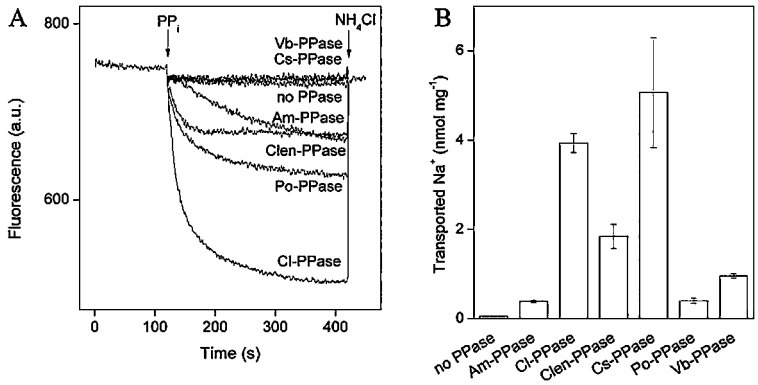

Figure 21. Ion transport studies of bacterial and archaeal mPPases that are evolutionary related to Bv-PPase (study II). A. H^+ transport with 5 mM Mg^{2+}, 10 mM Na^+, 50 mM K^+, 300 µM Mg_2PP_i and 2 µM ACMA revealed that all other new mPPases were able to transport H^+ except Vb- and Cs-PPase. B. All new mPPases tested were Na^+ transporters. *E. coli* IMVs with no PPase (transformed with the pET36b(+) vector only) were used as a control in these measurements.

When we showed that Bv-PPase was a Na^+,H^+-transporting enzyme, we did not know if there were also other bacterial mPPases that were able to transport both Na^+ and H^+. To address this question we constructed a new phylogenetic tree for mPPases and analyzed the Bv-PPase containing clade, from which we chose different bacterial mPPases for cloning, expression and characterization and showed that Po-PPase, Am-PPase, Clep-PPase and Clen-PPase were also Na^+,H^+-PPases, indicating that the double ion transport function was a common property for a specific group of mPPase (Fig. 21). However, we also discovered two mPPases, Vb-PPase and Cs-PPase, which did not transport H^+ and were strictly Na^+ transporters. When we

analyzed the amino acid sequence of these mPPases we discovered four conserved residues Thr90, Phe94, Asp146, Met176 (Bv-PPase numbering) that may act as a signature sequence for double ion transporters. This was further supported by the observation that strictly Na^+-transporting Cs-PPase and Vb-PPase did not contain all of these conserved residues.

The first Na^+-PPases discovered in 2007 (28) were characterized at nearly physiological conditions using 5−10 mM Na^+, a pH range of 5.5−9.0 and saturating PP_i concentrations. These were the conditions we also used in the first study of this thesis. However, as the Na^+-translocating ATPase of *Propiogenium modestum* had been shown to transport also H^+ at low Na^+ concentrations (516), in study III we tested whether this was true also for Na^+-PPases. Accordingly, by analyzing the ion transport of the *C. limicola* Na^+-PPase (Cl-PPase) at subphysiological Na^+ concentrations (below 5 mM), we found out that this enzyme transports also protons, but that its transport ability was abolished when the Na^+ concentration was increased to 5 mM or higher (Fig. 22A). The detection of the Na^+-PPase-mediated H^+ transport activity was facilitated by our efforts to increase the sensitivity of the H^+ transport assay during studies I and II. The H^+ ionophore CCCP abolished the H^+ transport signal, the Na^+ ionophore ETH157 had no effect and AMDP inhibited it. Furthermore, valinomycin enhanced H^+ transport indicating that this transport was electrogenic. These results (Fig. 22B) indicated that also in this case H^+ transport was catalyzed by a mPPase and was not due to secondary transport. The H^+ transport activity of Rr-PPase was measured at PP_i hydrolysis activity levels similar to those for Cl-PPase to find out if the H^+ transport signal of the *C. limicola* Na^+-PPase at subphysiological Na^+ concentrations was comparable to the proton transport signal of a "true" H^+-PPase. The Cl-PPase H^+ transport signal was lower than that of Rr-PPase, and this was not due to the leakiness of the membranes as indicated by a H^+-ATPase control (Fig. 22C). The results described above showed that a sodium pump, Cl-PPase, can transport both Na^+ and H^+ at low Na^+ concentrations (below 5 mM). Furthermore, this enzyme pumped protons at low Na^+ concentrations at all pH values tested (6.2−8.2). H^+ ions were not able to compete with Na^+ at high Na^+ concentrations even at pH 6.2 when there is 100-fold more protons than at pH 8.2 (Figs. 23A & 23B). All these results indicated that the ion transport specificity of Cl-PPase is complex and not based only on the competition between proton and sodium. We also observed that Cl^- ions stimulate H^+ and Na^+ transport. This is probably due to the fact that membranes e.g. vacuolar membranes are more permeable to Cl^- than to SO_4^{2-} and thus Cl^- can partially neutralize the inside positive charges of vesicles (291) leading to an increase in the signal.

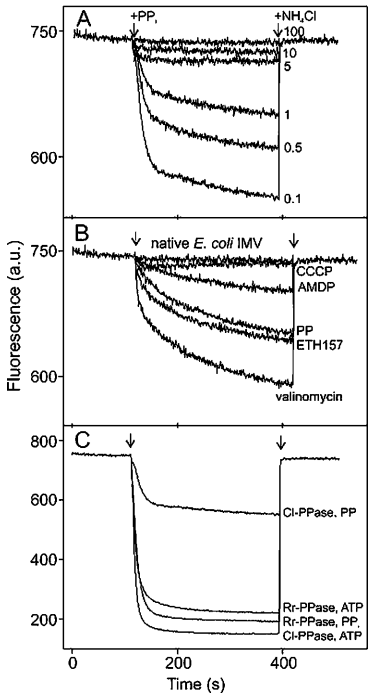

Figure 22. H^+ transport catalyzed by Cl-PPase was measured with ACMA at various Na^+ concentrations and with ionophores. Cl-PPase H^+ transport was compared to that of Rr-PPase which is known to transport H^+ (study III). Unless otherwise stated the reactions contained 300 μM Mg_2PP_i, 5 mM Mg^{2+}, 50 mM K^+ and were performed at pH 7.2 and 25 ºC. A. Cl-PPase H^+ transport was measured at a Na^+ range of 0.1−100 mM. B. The effects of ionophores and the inhibitor, AMDP, were determined at the following concentrations 5 μM CCCP, 20 μM ETH157, 2 μM valinomycin, 500 μM AMDP. C. H^+ transport of Cl-PPase was measured at a PP_i hydrolysis rates similar to that of Rr-PPase in the presence of 1 mM Na^+. In control reactions 250 μM ATP was used instead of 300 μM Mg_2PP_i to determine H^+ transport catalyzed by endogenous H^+-ATPase. These controls indicated that the vesicles were not leaking ions.

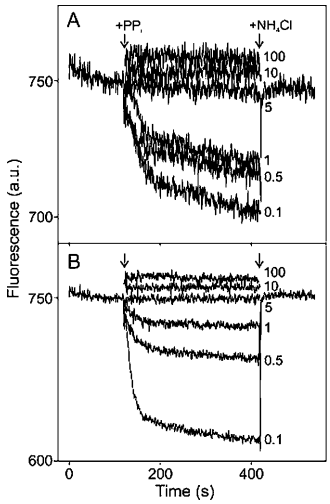

Figure 23. H^+-transport of Cl-PPase measured at pH 6.2 (A) and 8.2 (B) with 5 mM Mg^{2+}, 300 μM Mg_2PP_i, 50 mM K^+ (25 ºC) (study III). The enzyme transported protons at low Na^+ concentrations (below 5 mM) at all pH values (6.2, 7.2, 8.2) tested.

In addition, we measured Na^+ transport at different time points (0−90 s) at 0.05−10 mM Na^+ concentration (Fig. 24A). Na^+ transport (grey bars) and PP_i hydrolysis rates

(white bars) were analyzed under identical conditions and the results were converted to apparent Na^+/PP_i coupling ratios (Fig. 24B). Even though the coupling ratio was low due to the leakiness of *E. coli* IMVs, Cl-PPase transported Na^+ at a similar efficiency over the entire concentration range tested. Therefore, the emergence of a H^+ transport activity at a low Na^+ concentration did not lead to a decrease in the Na^+ transport activity as would have happened if H^+ simply competed with Na^+ as the transported ion (Fig. 24B).

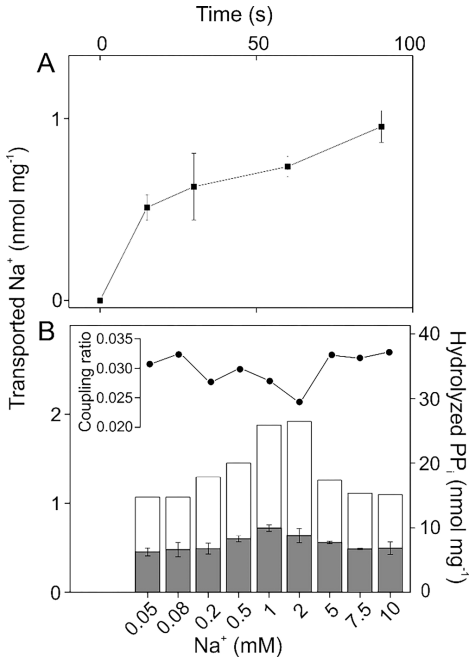

Figure 24. Na^+ transport catalyzed by Cl-PPase at different time points and Na^+ concentrations with corresponding PP_i hydrolysis activities (study III). A. Na^+ transport was detected at different time points at 0 ºC and pH 7.2 with 50 mM K^+. B. Cl-PPase Na^+ transport (grey bars) at 0.05−10 mM Na^+ and PP_i hydrolysis activities (white bars) measured under identical conditions. The coupling ratio indicates the ratio of Na^+ transported per PP_i hydrolyzed.

By analyzing the H^+ transport activity of several Na^+-PPases we showed that proton pumping at low (0.1−1 mM) but not at high (10 mM) Na^+ concentrations, is a general property of Na^+-PPases (Fig. 25). To analyze this unique property further, we mutated the gate amino acid residues of Cl-PPase (D239E, D239S, E242D, S243A, N677D, K681N and K681R) and studied the H^+ and Na^+ transport activities of the mutants. We showed that, in general, if the mutant was able to hydrolyze PP_i and its ion transporting properties were similar to those of the wild type enzyme (S243A, E242D and N677D variants), it transported both Na^+ (Fig. 26) and protons (Fig. 27) at low Na^+, whereas mutants which did not hydrolyze PP_i (K681R, D239E and D239S) pumped neither sodium ions nor protons. Interestingly, the K681N mutant behaved in a different way. It hydrolyzed PP_i and transported Na^+ but not H^+ at low [Na^+] (Fig. 27). Lys681 is one of the ion transport specificity determining gate residues of both Na^+- and H^+-PPases (71, 72). When this residue was replaced by alanine, arginine or asparagine the H^+ transport activity of the H^+-PPase was eliminated (72). Our results indicate that this conserved lysine residue is important also for the proton pumping by Na^+-PPases at low Na^+.

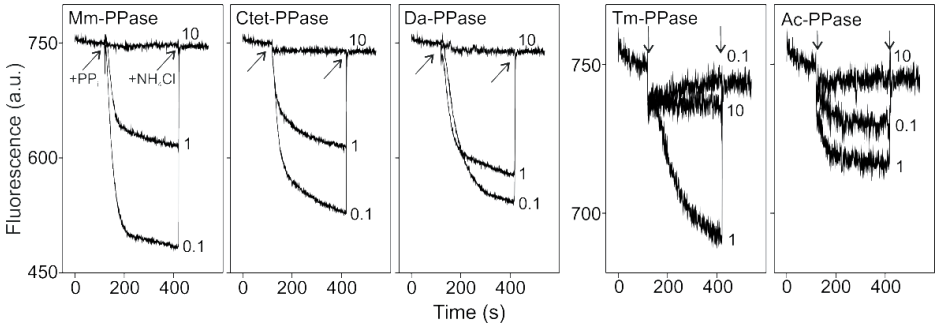

Figure 25. H^+ transport catalyzed by Na^+-PPases at different (0.1−10 mM) Na^+ concentrations. Reactions were carried out at 25 °C and the reaction mixtures included 300 μM Mg_2PP_i, 50 mM K^+ and 5 mM Mg^{2+} (25°C).

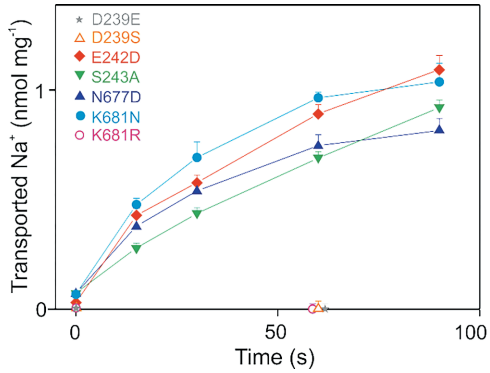

Figure 26. Na^+ transport catalyzed by a mutant Cl-PPases measured at 22 ºC and pH 7.2 with 1 mM Na^+, 5 mM Mg^{2+}, 50 mM K^+ and 1 mM TMA_4PP_i. Mutated mPPases which hydrolyzed PP_i also transported Na^+ but mutants having no PP_i hydrolysis activity did not transport Na^+.

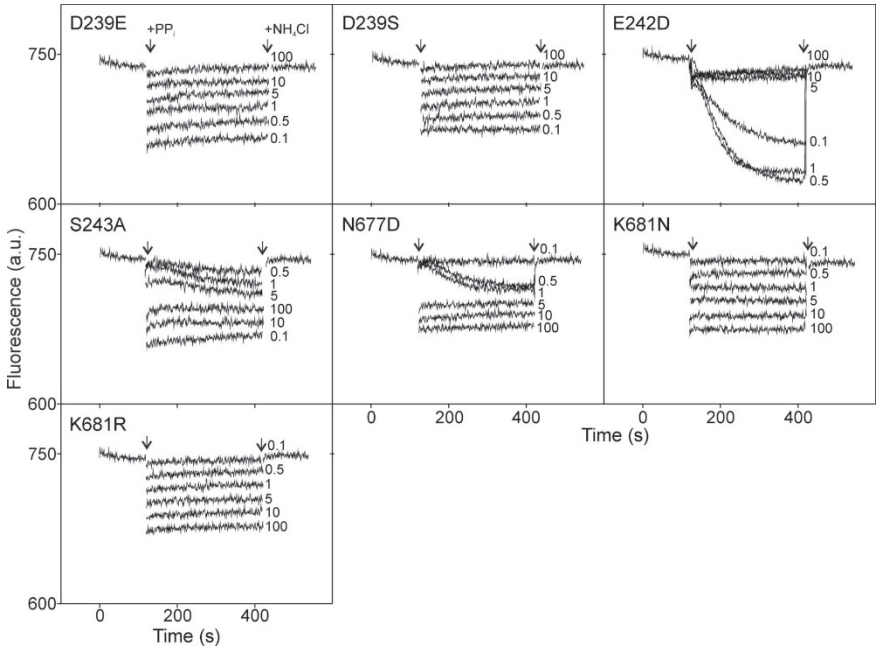

Figure 27. H^+ transport catalyzed by mutant Cl-PPases. Measurements were performed at 25 ºC with 50 mM K^+, 160 mM Cl^-, 300 μM Mg_2PP_i. All the mutants except K681N were able to hydrolyze PP_i transported H^+ at low Na^+, whereas mutants unable to hydrolyze PP_i did not transport H^+, indicating that Lys681 is important for the ion transport specificity.

In study IV we analyzed the ion transport specificity of divergent mPPases. H^+ transport was measured with 5 mM Mg^{2+} and 300 μM Mg_2PP_i in IMVs containing no PPase, Cf-PPase or Cl-PPase(2). Cl-PPase(2) H^+ transport was determined also in the presence of 500 μM AMDP, 100 mM Na^+, 150 mM K^+ or 5 μM CCCP and with various Mg_2PP_i concentrations (Fig. 28). A high K^+ concentration increased and high Na^+ and substrate concentrations decreased H^+ transport (Fig. 28). The membrane potential measured with bis-(1,3-dibutylbarbituric acid)trimethine oxonol [$DiBAC_4(3)$] showed that IMVs which did not have a mPPase created an ATP induced membrane potential, whereas a PP_i induced membrane potential was observed only with IMVs containing Cl-PPase(2). Valinomycin reversed the quenching of the fluorescence (Fig. 28C). Based on these results we concluded that H^+ transport is an electrogenic process also for divergent mPPases. Neither Cf-PPase nor Cl-PPase(2) transported Na^+. The Na^+-transporting Cl-PPase was used as a positive and IMVs with no PPase as a negative control in these measurements (Fig. 29).

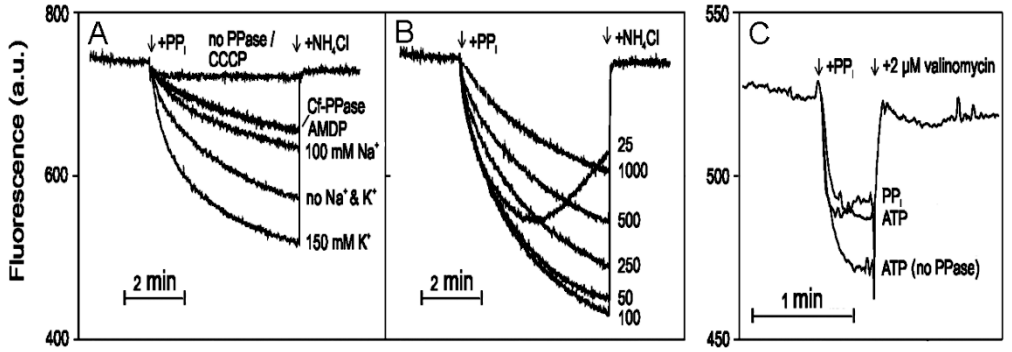

Figure 28. H^+ transport catalyzed by divergent mPPases (A, B) was determined with 2 μM ACMA and the electrogenic nature of the H^+ transport was analyzed with 25 nM $DiBAC_3(4)$ a fluorescent dye. A. Cl-PPase(2) and Cf-PPase transported H^+ ions in 5 mM Mg^{2+}, 300 μM Mg_2PP_i with and without 500 μM AMDP, 100 mM Na^+ or 150 mM K^+. Only the curve with Mg^{2+} and Mg_2PP_i is shown for Cf-PPase in the figure. The primary nature of H^+ transport was determined with 5 μM of the protonophore CCCP. B. Cl-PPase(2) H^+ transport measured with 25−1000 μM Mg_2PP_i indicated that transport was inhibited at high substrate concentrations. C. The electrogenic nature of H^+ transport was demonstrated by the Cl-PPase(2) containing vesicles. ATP mediated electrogenic transport was seen both with vesicles having no mPPase and with vesicles containing Cl-PPase(2).

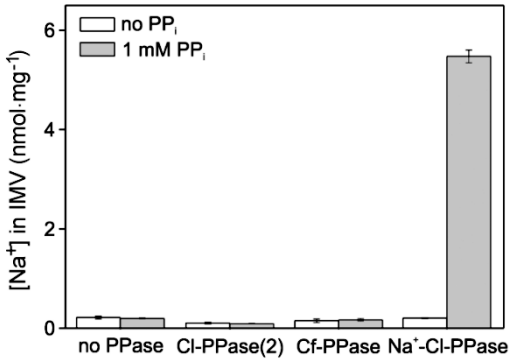

Figure 29. Na^+ transport measurements with divergent mPPases. IMVs with no mPPase (negative controls) gave similar signals as Cl-PPase(2) and Cf-PPase expressing vesicles, whereas the Na^+ transporting Cl-PPase (positive control) transported Na^+. These results indicated that divergent mPPases are strictly H^+ transporters.

4.3 Kinetic studies of ligand binding (studies I–IV)

The effects of ligands on hydrolysis kinetics of Na^+-PPases and K^+-dependent and -independent H^+-PPases are somewhat different (7, 28, 139, 149, 170). We carried out the steady state kinetics of PP_i hydrolysis with various types of mPPases at different Na^+, K^+, Mg^{2+}, and Mg_2PP_i concentrations (studies I–IV) to determine the number of ligand binding sites, ligand binding constants, and kinetic schemes for these enzymes. In the first study, several mPPases were cloned, expressed and isolated in IMVs and the Na^+ dependence of their PP_i hydrolysis activity was measured (25 °C) with or without 50 mM K^+ at a saturating substrate concentration (160 μM Mg_2PP_i) (Fig. 30). PP_i hydrolysis by all the Na^+-PPases studied were activated by Na^+ with or without 50 mM K^+, but K^+ enhanced their Na^+ binding. The E242D mutant of Cl-PPase required significantly more Na^+ than the wild type enzyme, indicating Glu242 to be important for Na^+-binding. In the absence of K^+, H^+-PPases (Fj- and Lb-PPase) were slightly activated by Na^+ but in the presence of 50 mM K^+ they were already fully active and Na^+ could not activate them further suggesting that H^+-PPases have an ion binding site, to which both Na^+ and K^+ can bind. Na^+-PPases seem to have one activating and one inhibiting Na^+ binding site. Similar results have been previously obtained with other Na^+-PPases (28, 139) and H^+-PPases (173, 174, 177). Fitting the data of Fig. 30 to Equation 1 derived for Scheme 1 gave the kinetic parameter values shown in Table 4.

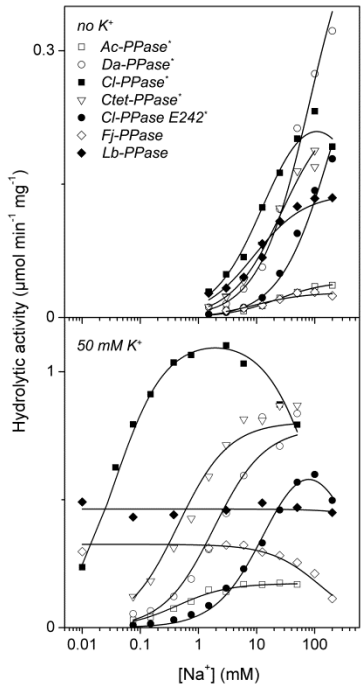

Figure 30. Na^+ dependence of PP_i hydrolysis catalyzed by mPPases studied in article I with or without 50 mM K^+. Na^+-PPases (shown by asterisk) were activated by Na^+ and K^+ enhanced their Na^+ binding. H^+-PPases were fully activated at 50 mM K^+ and Na^+ activated these enzymes in the absence of K^+.

$$\text{ES} \overset{K_a}{\leftrightarrow} \text{ESM} \overset{K_i}{\leftrightarrow} \text{ESM}_2 \quad \text{(Scheme 1)}$$

$$\downarrow V_1$$

$$v = \frac{V_1}{1 + K_a / [\text{M}] + [\text{M}] / \text{K}_i} \quad \text{(Equation 1)}$$

Scheme 1 and **Equation 1** describe the minimal model of Na^+ binding to the enzyme-substrate complexes (ES) of study I. M is the metal ion (Na^+), K_a and K_i are the binding constants for Na^+ and V_1 is the maximal velocity of PP_i hydrolysis catalyzed by the ESM complex. According to Scheme 1 the mPPase has one activating and one inhibiting binding site for Na^+ and maximum activity is achieved when one Na^+ is bound to the ES complex.

Table 4. Kinetic parameters describing Na^+ binding to the enzyme-substrate complex (ES) of selected mPPases in the presence and absence of 50 mM K^+ (study I)

	Parameter value				
	no K^{+a}		50 mM K^+		
Enzyme	V_1 *µmol·min^{-1}·mg^{-1}*	K_a *mM*	V_1 *µmol·min^{-1}·mg^{-1}*	K_a *mM*	K_i *mM*
Ac-PPase* [b]	0.04 ± 0.01	23 ± 5	0.17 ± 0.01	0.43 ± 0.04	NA [c]
Ctet-PPase*	0.24 ± 0.01	27 ± 2	0.80 ± 0.08	0.45 ± 0.08	NA
Da-PPase*	0.48 ± 0.08	80 ± 2	0.78 ± 0.09	1.9 ± 0.4	NA
Cl-PPase*	0.26 ± 0.04	14 ± 3	1.1 ± 0.1	0.036 ± 0.002	100 ± 20
Cl-PPase (E242D)*	0.38 ± 0.08	190 ± 50	0.81 ± 0.06	16 ± 2	400 ± 110
Fj-PPase	0.09 ± 0.01	9 ± 2	0.99 ± 0.04	NA	130 ± 20
Lb-PPase	0.14 ± 0.02	9 ± 2	0.46 ± 0.05	NA	NA

[a] K_i value was above 1000 mM in the absence of K^+.
[b] Na^+-PPases are marked by an asterisk
[c] NA = not applicable

Fig. 31 shows the K^+ dependence of PP_i hydrolysis catalyzed by mPPases characterized in study I in the presence of 50 mM Na^+ and 5 mM Mg^{2+}. All these Na^+- and H^+-PPases were activated by K^+ indicating that they are K^+-dependent enzymes. Interestingly, the E242D mutation of Cl-PPase had a significantly smaller effect on K^+ binding than it had on Na^+ binding (Figs. 30 & 31). The data shown in Fig. 31 was fitted to Equation 2 derived for Scheme 2 giving the parameter values listed in Table 5.

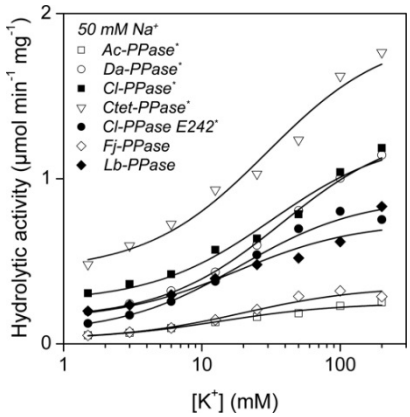

Figure 31. K^+ ion dependence of PP_i hydrolysis catalyzed by mPPases studied in article I in the presence of 50 mM Na^+. All these Na^+- and H^+-PPases are activated by K^+.

$$\begin{array}{ccc} & K_a & \\ \text{ES} & \leftrightarrow & \text{ESM} \\ \downarrow V_2 & & \downarrow V_1 \end{array} \qquad \text{(Scheme 2)}$$

$$v = \frac{V_1 + V_2 K_a / [\text{M}]}{1 + \text{K}_a / [\text{M}]} \qquad \text{(Equation 2)}$$

Scheme 2 and **Equation 2** describe the minimal model of K^+ binding to the ES complexes of study I. K_a is the K^+ binding constant and V_1 and V_2 are the maximal velocities of PP_i hydrolysis of the two ES complexes. K^+-dependent mPPases have one K^+ binding site and they are activated at high K^+.

Table 5. Kinetic parameter values describing K^+ activation of selected mPPases in the presence of 50 mM Na^+ (study I).

	Parameter value		
Enzyme	V_1 *μmol·min^{-1}·mg^{-1}*	V_2 *μmol·min^{-1}·mg^{-1}*	K_a *mM*
Ac-PPase* [b]	0.25 ± 0.01	0.03 ± 0.01	14 ± 2
Ctet-PPase*	1.9 ± 0.2	0.44 ± 0.04	30 ± 9
Da-PPase*	1.31 ± 0.04	0.15 ± 0.01	38 ± 2
Cl-PPase*	1.2 ± 0.1	0.25 ± 0.02	32 ± 8
Cl-PPase (E242D)*	0.89 ± 0.03	0.06 ± 0.01	19 ± 2
Fj-PPase	1.45 ± 0.08	0.11 ± 0.01	20 ± 2
Lb-PPase	0.74 ± 0.06	0.14 ± 0.01	18 ± 5

[b] Na^+-PPases are marked by asterisk

In study II we characterized the Na^+ and K^+ binding and measured the pH optimum for the Na^+,H^+ translocating Bv-PPase. The reaction mixture contained 160 μM PP_i and 5 mM free Mg^{2+} as in study I. Bv-PPase turned out to be similar to Na^+-PPases with respect to monovalent cation activation (28, 139), i.e., it has two Na^+ binding sites, one activatory and one inhibitory, and K^+ decreases the Na^+ concentration required for activity (Fig. 32A). The data was fitted to Equation 3 derived for Scheme 3 giving the parameter values shown in Table 6. Interestingly, K^+ enhances the Na^+ binding affinity to the activatory site 60-fold, but has no effect on Na^+ binding to the inhibitory site (Table 6). Furthermore, Na^+ is required for activity both at pH 7.2 and 5.5 suggesting that H^+ cannot replace Na^+ as an activator. Bv-PPase is a K^+-dependent enzyme (Fig. 32B). K^+ binding was fitted to Equation 3 by assuming that there is only one K^+ binding site and thus the K_i value for K^+ was fixed to ∞. Bv-PPase reached the half maximal activity in the presence of 11−12 mM K^+. The pH optimum of Bv-PPase is between 6.5−7.5 (Fig. 32C) which is similar to the pH optimum (6.5−8.0) previously observed with other mPPases (150, 152, 156-158). From the bell shaped pH dependence curve we estimated the pK_a values of the deprotonated and protonated groups to be 5.8 ± 0.1 or 7.9 ± 0.1, respectively (Fig. 32C). These are quite similar to the corresponding pK_a values 5.6 ± 0.1 or 9.3 ± 0.1 determined for Mm-PPase (28).

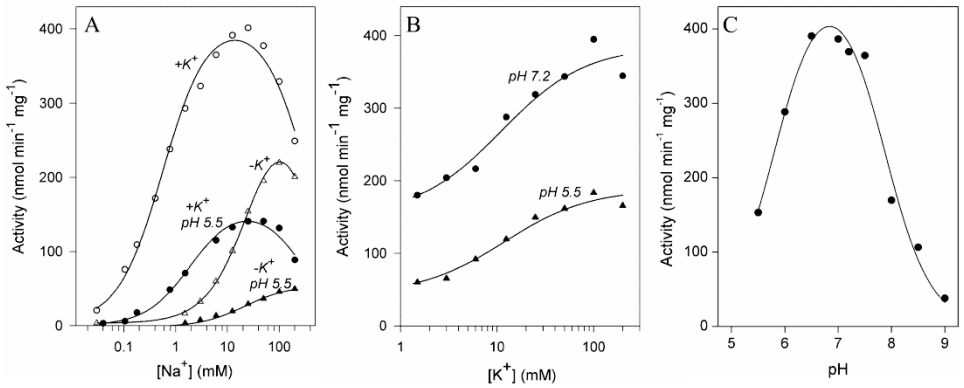

Figure 32. Na^+, K^+ and pH dependence of the hydrolytic activity of Bv-PPase. A. Na^+ dependence measured at pH 7.2 and 5.5 with and without 50 mM K^+. The curves show that K^+ had similar effects on the Na^+ dependence of the PP_i hydrolysis activity at both pH values tested. B. K^+ dependence with 50 mM Na^+ measured at pH 7.2 and 5.5. The K^+ dependence of the hydrolysis activity was similar at both pH values tested. C. pH dependence of the PP_i hydrolysis activity with 10 mM Na^+ and 50 mM K^+.

$$\begin{array}{ccccc} & & K_a & & K_i \\ \mathrm{ES} & \leftrightarrow & \mathrm{ESM} & \leftrightarrow & \mathrm{ESM_2} \\ \downarrow V_1 & & \downarrow V_2 & & \end{array} \qquad \text{(Scheme 3)}$$

$$v = \frac{V_1 K_a / [\mathrm{M}] + V_2}{1 + K_a / [\mathrm{M}] + [\mathrm{M}] / K_i} \qquad \text{(Equation 3)}$$

Scheme 3 and **Equation 3** describe the minimal model of Na^+ and K^+ binding to the Bv-PPase-substrate complexes (ES) of study II. K_a is a K^+ binding constant and both, K_a and K_i are Na^+ binding constansts. V_1 and V_2 are the maximal velocities of the PP_i hydrolysis of the two ES complexes.

Table 6. Kinetic parameter values describing Na^+ and K^+ binding to the Bv-PPase-substrate complex (study II).

Activator	pH	Parameter value			
		K_a *mM*	V_1 *nmol·min^{-1}·mg^{-1}*	V_2 *nmol·min^{-1}·mg^{-1}*	K_i *mM*
Na^+	7.2	0.57 ± 0.06/33 ± 3[a]	<3/<3	420 ± 20/360 ± 20	340 ± 60/320 ± 30
Na^+	5.5	2.0 ± 0.3/ 21 ± 2	<2/ <2	160 ± 10/56 ± 5	310 ± 70/n.d.[b]
K^+	7.2	11 ± 3	150 ± 10	390 ± 20	
K^+	5.5	12 ± 3	44 ± 4	170 ± 10	

[a] Parameter values left and right of the slashed line were measured in the presence and absence of 50 mM K^+, respectively. K^+ binding experiments were conducted in the presence of 50 mM Na^+.
[b] n.d., not determined.

In study I, the Na^+ dependence of the PP_i hydrolysis catalyzed by Cl-PPase was studied along with other Na^+-PPases (Figs. 30 & 31 and Tables 4 & 5). In study III Cl-PPase was analyzed further together with its mutants (Figs. 33 & 34 and Tables 7 & 8). These reactions were carried out at pH 7.2 and 25 ºC, and the reaction mixtures contained 5 mM Mg^{2+} (free) and 100 µM Mg_2PP_i. Consistent with previous observations with Na^+-PPases (28) K^+ increased Na^+ binding to the wild type Cl-PPase and as a Na^+-PPase this enzyme essentially requires Na^+ for its hydrolytic activity (Fig 33A). In addition to pH 7.2, the Na^+-dependence was measured also at pH 6.2 and 8.2 with 50 mM K^+. At pH 8.2

the K^+ induced Na^+-binding affinity was increased and at pH 6.2 decreased compared to pH 7.2 (Figs. 33A & B and Table 7). The K^+-dependence measured in the presence of 0.1−50 mM Na^+ indicated that Na^+ has only a minor effect on K^+ binding (Fig. 33C and Table 8).

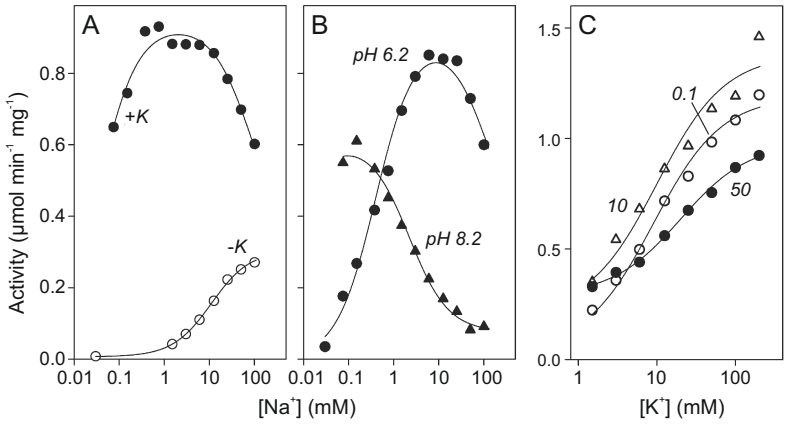

Figure 33. Na^+ and K^+ dependence of PP_i hydrolysis catalyzed by Cl-PPase (study III). A. Na^+ dependence at pH 7.2 with or without 50 mM K^+. B. Na^+ dependence at pH 6.2 and 8.2 with 50 mM K^+. C. K^+ dependence with 0.1, 10 and 50 mM Na^+.

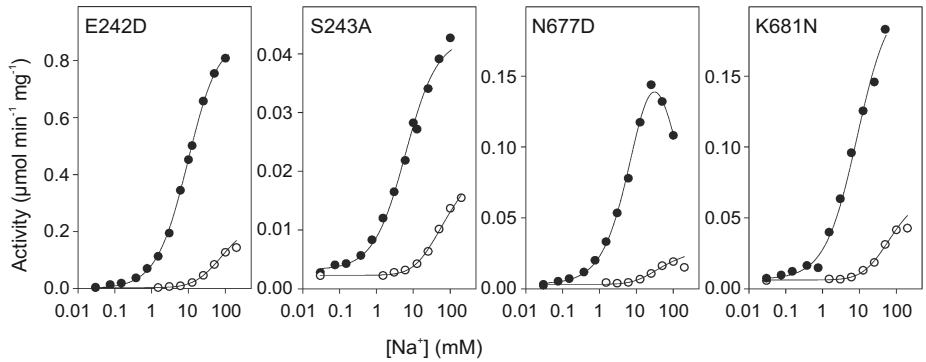

Figure 34. Na^+ dependence of PP_i hydrolysis catalyzed by Cl-PPase mutants PP_i with (black circles) or without (white circles) 50 mM K^+ (study III).

Like the wild type enzyme, the E242D, S243A, N677D and K681N variants of Cl-PPase absolutely required Na^+ for their activity (Fig. 34 and Table 7). K^+ further enhanced both Na^+ binding and maximal activity. However, there were drastic differences between the Na^+ dependence profiles of the wild type and mutants. All the variants required, both in the presence and absence of K^+, much more Na^+ to be active than did the wild type, indicating that all these residues are in close proximity to the Na^+ binding site. In addition, high Na^+ inhibited the wild type and the N677D variant, but not the E242D, S243A and K681N variants (Figs. 33A & 34).

Scheme 4A and 4B describe the Na^+ binding to the Cl-PPase-substrate complex in the absence and presence of K^+, respectively. Data presented in Figs. 33 and 34 was fitted

to Equations 4A and 4B giving the Na^+ binding constants (K_{a1}, K_{a2}, K_a, K_i) and maximal velocity values (V_N, V_K, V_1, V_2) shown in Table 7.

$$\mathrm{ES} \overset{K_{a1}}{\leftrightarrow} \mathrm{ESNa} \overset{K_{a2}}{\leftrightarrow} \mathrm{ESNa_2} \quad \text{(Scheme 4A)}$$
$$\downarrow V_N$$

$$\mathrm{ES} \overset{K_{a}}{\leftrightarrow} \mathrm{ESNa} \overset{K_{i}}{\leftrightarrow} \mathrm{ESNa_2} \quad \text{(Scheme 4B)}$$
$$\downarrow V_K \qquad \downarrow V_N$$

$$v = \frac{V_N}{1 + K_{a2}/[M] + K_{a1}K_{a2}/[M]^2} + a \quad \text{(Equation 4A)}$$

$$v = \frac{V_K + V_N[M]/K_i}{1 + K_a/[M] + [M]/K_i} + a \quad \text{(Equation 4B)}$$

Scheme 4 and **Equation 4** describe the minimal model of Na^+ binding to the Cl-PPase-substrate complexes in the absence (A) or presence (B) of K^+ in study III. K_{a1}, K_{a2}, K_a and K_i are Na^+ binding constansts. V_N, V_K V_1 and V_2 are the maximal velocities of the PP_i hydrolysis activities of the ES complexes. Parameter *a* refers to the Na^+ dependent background activity.

Table 7. Kinetic parameter values describing Na^+ binding to the Cl-PPase-substrate complex with or without 50 mM K^+ at pH 7.2 (study III).

		Parameter value					
		no K^{+a}			50 mM K^+		
Enzyme variant	pH	V_N $\mu mol \cdot min^{-1} \cdot mg^{-1}$	K_{a1} mM	K_{a2} mM	V_K $\mu mol \cdot min^{-1} \cdot mg^{-1}$	K_a mM	K_i mM
Wild-type	7.2	0.30 ± 0.01	<1	10 ± 1	0.94 ± 0.02	0.033 ± 0.004	85 ± 11
Wild-type	6.2	~0.3			0.91 ± 0.04	0.40 ± 0.05	120 ± 30
Wild-type	8.2	0.08 ± 0.01[b]			0.61 ± 0.05	< 0.05	2.2 ± 0.5
E242D	7.2	0.24 ± 0.04	9 ± 4	84 ± 30	0.91 ± 0.05	10 ± 1 (16 ± 2)[c]	NA[d]
S243A	7.2	0.014 ± 0.002	20 ± 16	32 ± 16	0.040 ± 0.001	6.2 ± 0.7	NA
N677D	7.2	0.016 ± 0.001	~10	31 ± 12	0.23 ± 0.02	11 ± 2	80 ± 20
K681N	7.2	0.042 ± 0.006	~10	60 ± 10	0.20 ± 0.02	9 ± 2	NA

[a] K_i value was greater than 1000 mM in the absence of K^+.
[b] Obtained from the curve measured in the presence of 50 mM K^+.
[c] From article I
[d] NA, not applicable.

Equation 5 derived for Scheme 5 describes K^+ binding to the Cl-PPase-substrate complex in the presence of 50 mM Na^+. The K^+ binding constant (K_a) and activities and maximal velocities (V_1, V_1) are shown in Table 8. An increase in the Na^+ concentration only slightly decreased K^+ binding (Table 8). All enzymes variants were K^+ dependent and the K^+ binding constant was not drastically changed by these mutations (Table 8).

$$\begin{array}{ccc} & K_a & \\ ES & \leftrightarrow & ESK \\ \downarrow V_1 & & \downarrow V_2 \end{array} \qquad \text{(Scheme 5)}$$

$$v = \frac{V_2 + V_1 K_a / [M]}{1 + K_a / [M]} \qquad \text{(Equation 5)}$$

Scheme 5 and **Equation 5** describe the minimal model of K^+ binding to the Cl-PPase-substrate complexes (ES) of study III. K_a is the K^+ binding constanst. V_1 and V_2 are the maximal velocities of the PP_i hydrolysis activity of the ES complexes.

Table 8. Kinetic parameter values describing K^+ binding to a Cl-PPase and its variants in the presence of varying amounts of Na^+ at pH 7.2 (study III).

		Parameter value		
Enzyme variant	[Na^+] *mM*	V_1 *μmol·min^{-1}·mg^{-1}*	V_2 *μmol·min^{-1}·mg^{-1}*	K_a *mM*
Wild-type	50	0.29 ± 0.01	0.98 ± 0.02	20 ± 2 (32 ± 8)[a]
Wild-type	10	0.21 ± 0.07	1.38 ± 0.07	10 ± 3
Wild-type	2	0.10 ± 0.03	1.34 ± 0.03	7 ± 1[b]
Wild-type	0.5	0.06 ± 0.03	1.41 ± 0.03	7 ± 1[b]
Wild-type	0.1	0.04 ± 0.03	1.19 ± 0.03	9 ± 1
E242D	50	0.068 ± 0.004	0.75 ± 0.03	21 ± 2 (19 ± 2)[a]
S243A	50	0.008 ± 0.001	0.046 ± 0.002	8 ± 2
N677D	50	0.017 ± 0.007	0.23 ± 0.01	36 ± 3
K681N	50	0.028 ± 0.002	0.25 ± 0.02	38 ± 8

[a] From article I
[b] Data is not shown in Fig. 33C for clarity.

The PP_i hydrolysis activity of divergent mPPases was explored as a function Na^+, K^+, Mg^{2+} and Mg_2PP_i in study IV. Divergent mPPases hydrolyzed PP_i without added K^+ and were thus first classified as K^+-independent PPases. However, a high K^+ concentration at 20 μM Mg_2PP_i inhibited Cl-PPase(2) (Fig. 35A). The data shown in Fig. 35A was fitted to Equation 6 derived for Scheme 6 giving an apparent dissociation constant of 210 mM for K^+ binding (Table 9). Na^+ inhibited Cl-PPase(2) hydrolysis with or without 50 mM K^+ (Fig. 35A). K^+ increased Na^+ binding ~1.5-fold (Table 9). Similarly to Cl-PPase(2), Cf-PPase was inhibited at high Na^+ (Table 9). Cl-PPase(2) inhibition at high Na^+ or K^+ was not due to the high ionic strength as is shown by measurements performed with TMA chloride (Fig. 35A). The Hill coefficient (h=1.9 ± 0.1) obtained from the Hill plot of Na^+ binding to Cl-PPase(2) indicated that the ligand binds to the enzyme in a positively cooperative manner (Fig. 35B).

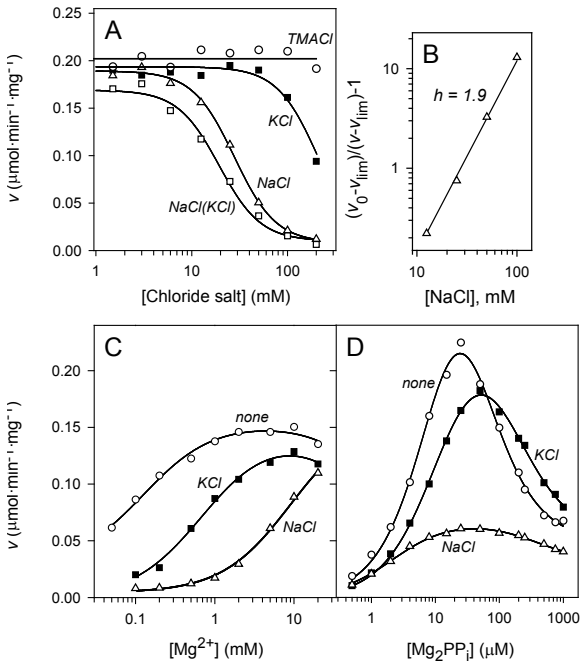

Figure 35. PP_i hydrolysis kinetics of Cl-PPase(2) (study IV). A. Activity measured at 20 μM Mg_2PP_i and 1 mM Mg^{2+} as a function of K^+, TMACl, and Na^+ with or without 50 mM K^+. This data was fitted to Equation 6 derived from Scheme 6. B. Hill plot presentation of the Na^+ dependence data to demonstrate coperativity in ligand binding. C. Activity measured at 20 μM Mg_2PP_i as a function of Mg^{2+} with and without 100 mM Na^+ or K^+. The curves were fitted to Equation 7 derived for Scheme 7. D. Activity measured at 5 mM Mg^{2+} as a function of Mg_2PP_i with and without 100 mM Na^+ or 150 mM K^+. The curves were fitted to Equation 8 derived for Scheme 8.

$$\begin{array}{ccc} & K_N & \\ ES & \leftrightarrow & ESN \\ \downarrow v_0 & & \downarrow v_N \end{array} \qquad \text{(Scheme 6)}$$

$$v = v_0 - (v_0 - v_N) / \{1 + (K_N / [N])^2\} \quad \text{(Equation 6)}$$

Scheme 6 and **Equation 6** describe the minimal model of K^+ and Na^+ binding to divergent mPPases of study IV. v_0 and v_N are activity values observed at zero and infinite effector (N) concentrations, respectively, and $K_{N,}$ is the apparent dissociation constanst.

Table 9. Kinetic parameter values describing Na^+ and K^+ inhibition of divergent mPPases (study IV).

Enzyme	Modulating cation	v_0	v_N	K_N [a]
		μmol·min⁻¹·mg⁻¹	*μmol·min⁻¹·mg⁻¹*	*mM*
Cl-PPase(2)	Na^+	0.19 ± 0.01	0.008 ± 0.003	28 ± 2
Cl-PPase(2)	K^+	0.19 ± 0.01	ND[b]	210 ± 15
Cl-PPase(2)	Na^+ (K^+)[c]	0.17 ± 0.01	0.010 ± 0.005	19 ± 2
Cf-PPase	Na^+	0.062 ± 0.002	< 0.005	81 ± 8

[a] Binding constant calculated assuming highly cooperative binding of two alkali metal ions.
[b] ND, not determined.
[c] Effect of Na^+ measured in the presence of 50 mM K^+.

When the activity of Cl-PPase(2) was measured as a function of free Mg^{2+} at 20 µM Mg_2PP_i with 100 mM Na^+ or K^+ it was shown that both cations decreased the PP_i hydrolysis activity compared to that observed in their absence (Fig. 35C). When either of the two cations were present Cl-PPase(2) required significantly more Mg^{2+} to be activated. The data in Fig. 35C was fitted to Equation 7 derived for Scheme 7 giving the kinetic parameter values listed in Table 10 which shows, for example, that 100 mM K^+ and Na^+ decreased Mg^{2+} binding to Cl-PPase(2) by 6.3 and 113-fold, respectively.

$$E \overset{K_{M,app}}{\leftrightarrow} EMg \leftrightarrow EMg_a \quad \text{(Scheme 7)}$$
$$\downarrow v_{max}$$

$$v = v_{max} / (1 + K_{M,app}/[Mg]) + a[Mg]) \quad \text{(Equation 7)}$$

Scheme 7 and **Equation 7** describe the minimal model of Mg^{2+} binding to Cl-PPase(2) of study IV. v_{max} is the maximal rate of the PP_i hydrolysis activity, $K_{M,app}$ is the apparent Mg^{2+} binding constant and the term a[Mg] takes into account the small decrease in the activity observed at high Mg^{2+} concentrations.

Table 10. Kinetic parameter values describing the effects of Na^+ and K^+ on the Mg^{2+}-dependent activation of Cl-PPase(2) (study IV).

	v_{max}	$K_{M,app}$
Modulating cation	*µmol·min⁻¹·mg⁻¹*	*mM*
None	0.147 ± 0.002	0.08 ± 0.01
Na^+	0.156 ± 0.007	9 ± 1
K^+	0.16 ± 0.02	0.5 ± 0.2

Cl-PPase(2) activity measured as a function of substrate at 5 mM free Mg^{2+} and pH 7.2 in the presence or absence of 100 mM Na^+ or 150 mM K^+ revealed a substrate inhibition that is dependent on monovalent cations. K^+ somewhat protects the enzyme against substrate inhibition at high Mg_2PP_i (Fig. 35D). The data shown in Fig. 35D was fitted to Equation 8 derived for Scheme 8 giving specific activities (A_1, A_2), and Michaelis constants (K_{m1}, K_{m2}) for different enzyme substrate complexes (Table 11). Interestingly even though Na^+ inhibits the enzyme it increases the binding of the activatory Mg_2PP_i (K_{m1}) by 3-fold. Both K^+ and Na^+ slightly protect Cl-PPase(2) from the substrate inhibition as shown by the K_{m2} values. Cf-PPase was also inhibited at high substrate concentrations (Table 11).

$$E \overset{K_{m1}}{\leftrightarrow} ES \overset{K_{m2}}{\leftrightarrow} ES_2 \quad \text{(Scheme 8)}$$
$$\downarrow A_1 \qquad \downarrow A_2$$

$$v = [E]_t(A_1 + A_2[S] / K_{m2}) / (1 + [S] / K_{m2} + K_{m1} / [S]) \quad \text{(Equation 8)}$$

Scheme 8 and **Equation 8** describe the minimal model of Mg_2PP_i binding to divergent mPPases at fixed a Mg^{2+} concentration. A_1 and A_2 are the specific activities and K_{m1} and K_{m2} the binding constants of the different enzyme substrate complexes (study IV).

Table 11. Kinetic parameter values describing the effects of Na^+ and K^+ on the substrate saturation curve for Cl-PPase(2) (study IV).

Enzyme	A_1 *μmol·min^{-1}·mg^{-1}*	A_2 *μmol·min^{-1}·mg^{-1}*	K_{m1} μM	K_{m2} μM
Cl-PPase(2)	0.44 ± 0.04	0.049 ± 0.004	13 ± 2	85 ± 15
Cl-PPase(2)[b]	0.067 ± 0.01	0.040 ± 0.008	4.2 ± 0.5	290 ± 70
Cl-PPase(2)[c]	0.26 ± 0.01	0.053 ± 0.004	12 ± 1	260 ± 100
Cf-PPase	0.093 ± 0.04	0.016 ± 0.005	8 ± 1	240 ± 70

[a] The original dependencies for Cl-PPase(2) are shown in Fig. 35D.
[b] Measured in the presence of 100 mM NaCl.
[c] Measured in the presence of 100 mM KCl.

The results showed that divergent mPPases require Mg^{2+} for their hydrolysis activity, but that also Na^+ and K^+ are able regulate this activity. A more detailed description of the kinetic analysis of divergent mPPases is presented in article IV.

4.4 Phylogenetics and the evolution of membrane-bound PPases (studies I–IV)

We have constructed phylogenetic trees of mPPases to decipher their evolutionary relationships. Our results clarified the ion transport specificities of mPPases (Fig. 36) and revealed that Na^+ transport is a common function of mPPases. All Na^+-PPases can be traced to the same ancestral node. Na^+-PPases require Na^+ for their activity and are further activated by K^+ (study I). Results obtained from the phylogenetic and functional analysis suggest that Na^+-PPases have appeared only once during the evolution of the mPPase protein family. We also discovered a novel group of mPPases able to simultaneously transport both Na^+ and H^+. This group is located in a specific clade in the middle of the Na^+-PPases (study II). H^+-PPases, in contrast, are a versatile group of mPPases. They form multiple branches in the phylogenetic tree and are divided into K^+-dependent and K^+-independent groups (study IV). The phylogenetics and functional properties of these enzymes suggest that different types of H^+-PPases are a result of independent evolutionary pathways that changed the transport specificity from Na^+ to H^+. Furthermore, we discovered an evolutionary distantly related mPPase group of enzymes which we named divergent mPPases. These enzymes are H^+-PPases that are active in the absence of K^+ even though they are regulated by Na^+ and K^+ ions.

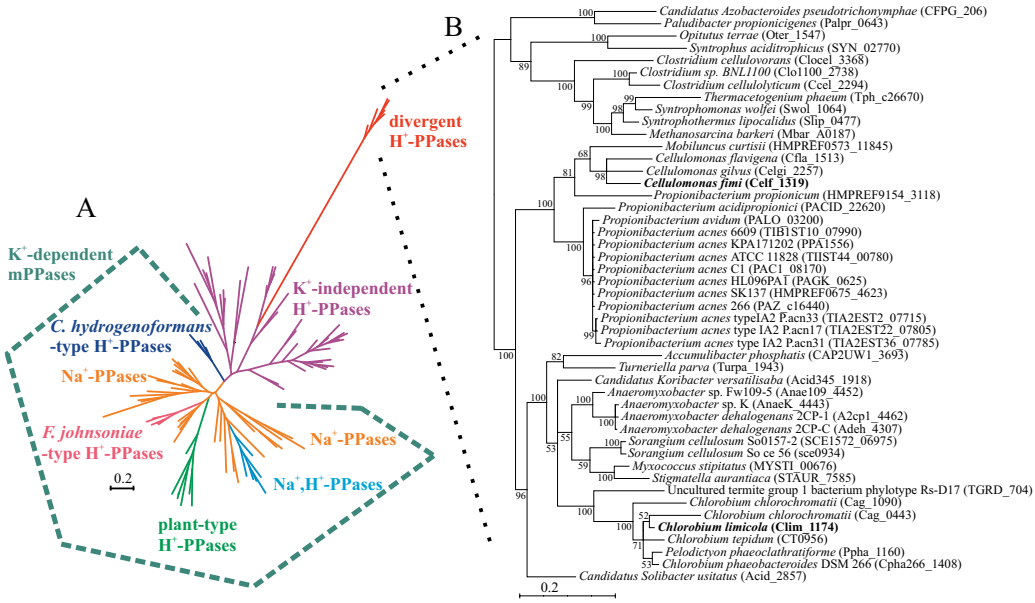

Figure 36. Evolution and occurrence of mPPase families with different functions. A.Phylogenetic tree of mPPases and B. clade of the divergent mPPase subfamily (study IV). Phylogenetic analysis of mPPase sequences (130 taxa, 398 amino acid residues) retrieved from the KEGG databank revealed a novel evolutionary divergent mPPase family. The divergent mPPase clade (47 taxa, 450 amino acid residues) included the *C. limicola,* Cl-PPase(2) and the *C. fimi*, Cf-PPase that were characterized in this research.

Based on our results, we created a model for the mPPase mechanism (Fig. 37). The model suggests that Na^+-PPases transport Na^+ with the energy released from PP_i. PP_i hydrolysis occurs when PP_i reacts with a nucleophilic water molecule (Fig. 37A). In the reaction a proton is released and a conformational change in the enzyme drives Na^+ transport across the membrane (Fig. 37B). At low Na^+, a proton binds to the Na^+ binding site and is transported to the other side of the membrane when the next PP_i hydrolysis occurs (Fig. 37C). At high Na^+, Na^+ binds to its binding site and only Na^+ is transported. Furthermore, we showed that H^+-PPases do not transport Na^+ under any of the conditions tested. Accordingly, H^+-PPases, which transport protons only, are more specific than Na^+-PPases. In our model, this difference in specificity is explained so that H^+-PPases do not have a binding site to which Na^+ and H^+ can transiently bind (Fig. 37D).

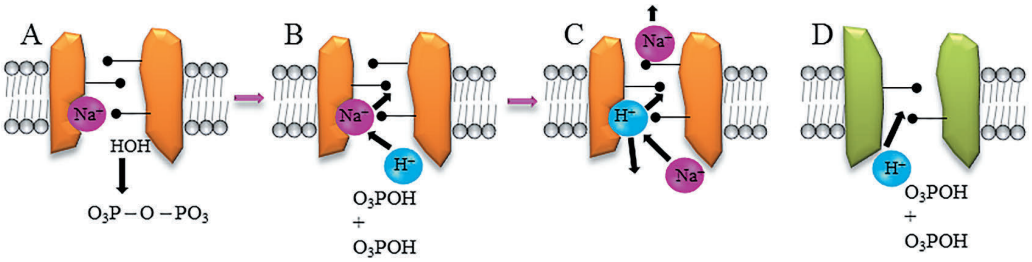

Figure 37. Our model for the mechanisms of mPPases activity, which was created based on the results presented in article III. The detailed description of the figure is shown in the main text above. Figure modified from Baykov *et al.* (7). (Adapted with the permission from Copyright © American Society for Microbiology, *Microbiol. Mol. Biol. Rev*, 77, 2, 2013, 267–276 DOI:10.1128/MMBR.00003-13).

Na^+-PPases are mainly found in anaerobic organisms and organisms living under extreme conditions, whereas H^+-PPases are present in plants, protists and aerobic bacteria. Novel double ion transporters are predominantly found in anaerobic bacteria and bacteria of the gastrointestinal tract and may provide one way for how these bacteria survive under the stressful conditions of the host. In studies I and III we characterized the *C. limicola* Na^+-PPase (Cl-PPase) and in study IV, the divergent H^+-PPase [Cl-PPase(2)] of the same bacterium. Interestingly the genes encoding these two enzymes are located next to each other in the genome. Perhaps this is a remnant of an ancient gene duplication event that eventually led to the evolution of divergent H^+-PPases. Because Cl-PPase is activated and Cl-PPase(2) is inhibited by Na^+, the enzymes can be differentialy regulated *in vivo*. 47 Divergent mPPases are found in bacteria, including the phyla Acidobacteria, Bacteroidetes, Chlorobi, Elusimicrobia, Firmicutes, Proteobacteria, Spirochaetes and Verrucomicrobia and one archaea of Euryarchaeota (Fig. 36B). These organisms live under aerobic/anaerobic and mesophilic/thermophilic conditions and are isolated mainly from environmental or human samples (Table 12). 20% of the organisms containing divergent H^+-PPase, also contain K^+-independent H^+-PPases or Na^+-PPases but not K^+-dependent H^+-PPases or Na^+,H^+-PPases (Table 12). A soluble PPase, either family I or a CBS-PPase, is found almost always in an organism together with a divergent H^+-PPase (Table 12), suggesting that soluble and membrane-bound PPases are strictly regulated within the cell. However, the regulatory mechanisms and the division of labour between the different types of PPases remain to be explored.

Based on our results we proposed that Na^+-PPases were the ancestral form of mPPases and H^+-PPases evolved from Na^+-PPases on different occasions (Fig. 38). Based on site-directed mutagenesis analysis the conserved glutamate residues that form the ion transport funnel gate were shown to be important for ion transport specificity. Relying on our observations the ion transport specificity of mPPases can now be predicted using a sequence alignment in combination with a phylogenetic analysis. Furthermore, our results support theories predicting that Na^+-based bioenergetics would have preceded a H^+-based system (88, 126).

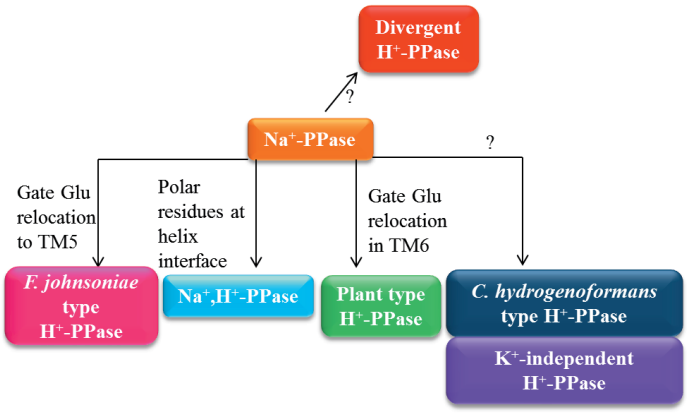

Figure 38. Evolution of mPPase families. We propose that a Na^+-PPase was the ancient form of the mPPase enzyme family and the ion transport specificities have evolved from it via multiple amino acid replacements. There are still some questions concerning the evolution of mPPases that remain to be answered. Figure modified from Baykov *et al.* (7). (Adapted with the permission from Copyright © American Society for Microbiology, *Microbiol. Mol. Biol. Rev*, 77, 2, 2013, 267–276 DOI:10.1128/MMBR.00003-13).

Table 12. Organisms containing divergent H^+-PPases and alternative PPases.

Phylum	Species	Temperature / oxygen preference	Isolation environment	Accompanying alternative PPases	
				H^+- / Na^+-PPase	Family I / CBS-PPase
Euryarchaeota	*Methanosarcina barkeri*	Mesophilic/Anaerobic	Sewage, mud, cattle rumen	+/-	++/-
Acidobacteria	*Cand. Solibacter usitatus*	Mesophilic/Aerobic	Soil	-/-	+++/-
Acidobacteria	*Cand. Koribacter versatilis*	Mesophilic/Aerobic	Soil	-/-	+/-
Actinobacteria	*Cellulomonas flavigena*	Mesophilic/Facultative	Soil	+/-	+/-
Actinobacteria	*Cellulomonas fimi*	Mesophilic/Aerobic	Soil	+/-	+/-
Actinobacteria	*Cellulomonas gilvus*	Mesophilic/Anaerobic	Bovine feces	+/-	+/-
Actinobacteria	*Mobiluncus curtisii*	Mesophilic/Anaerobic	Human vaginal secretions	-/-	+/-
Actinobacteria	*Propionibacterium acidipropionici*	Mesophilic/Anaerobic	Cheese	-/-	+/-
Actinobacteria	*Propionibacterium acnes* 6609	Mesophilic/Anaerobic	Human skin	-/-	+/-
Actinobacteria	*Propionibacterium acnes* KPA171202	Mesophilic/Anaerobic	Human skin	-/-	+/-
Actinobacteria	*Propionibacterium acnes* ATCC 11828	Mesophilic/Anaerobic	Human skin	-/-	+/-
Actinobacteria	*Propionibacterium acnes* HL096PA1	Mesophilic/Anaerobic	Human skin	-/-	+/-
Actinobacteria	*Propionibacterium acnes* SK137	Mesophilic/Anaerobic	Human skin	-/-	+/-
Actinobacteria	*Propionibacterium acnes* C1	Mesophilic/Anaerobic	Human skin	-/-	+/-
Actinobacteria	*Propionibacterium acnes*266	Mesophilic/Anaerobic	Human pleuropulmonary	-/-	+/-
Actinobacteria	*Propionibacterium acnes* TypeIA2 P.acn33	Mesophilic/Anaerobic	Human skin	-/-	+/-
Actinobacteria	*Propionibacterium acnes* TypeIA2 P.acn17	Mesophilic/Anaerobic	Human skin	-/-	+/-
Actinobacteria	*Propionibacterium acnes* TypeIA2 P.acn31	Mesophilic/Anaerobic	Human skin	-/-	+/-
Actinobacteria	*Propionibacterium avidum* 44067	Mesophilic/Anaerobic	Human nose, axilla, perineum	-/-	+/-
Actinobacteria	*Propionibacterium propionicum* F0230a	Mesophilic/Anaerobic	Human oral cavity	-/-	+/-
Bacteroidetes	*Cand. Azobacteroides pseudotrichonymphae genomovar*	Mesophilic/NA[d]	*Pseudotrichonympha grassii*	-/-	-/-
Bacteroidetes	*Paludibacter propionicigenes*	Mesophilic/Anaerobic	Soil	-/-	+/-
Chlorobi	*Chlorobium chlorochromatii*	Mesophilic/Anaerobic	Lake water	-/-	+/-
Chlorobi	*Chlorobium limicola*	Mesophilic/Anaerobic	Hot spring	-/+	+/-
Chlorobi	*Chlorobium phaeobacteroides*	Mesophilic/Facultative	Lake water	-/-	+/-
Chlorobi	*Pelodictyon phaeoclathratiforme*	Mesophilic/Anaerobic	Lake water	-/-	+/-
Chlorobi	*Chlorobaculum tepidum*	Thermophilic/Anaerobic	Hot spring	-/-	+/-
Elusimicrobia	Uncultured Termite group 1 bacterium phylotype Rs-D17	NA/NA	Termite gut	-/-	-/-
Firmicutes	*Clostridium cellulolyticum*	Mesophilic/Anaerobic	Soil	-/-	-/+
Firmicutes	*Clostridium cellulovorans*	Mesophilic/Anaerobic	Cellulose digester	-/+	+/+
Firmicutes	*Clostridium* sp. BNL1100	Mesophilic/NA	Corn stover	-/-	-/+
Firmicutes	*Syntrophothermus lipocalidus*	Thermophilic/Anaerobic	Granular sludge	+/-	-/+
Firmicutes	*Syntrophomonas wolfei*	NA/Anaerobic	Digester sludge	-/-	-/+
Firmicutes	*Thermacetogenium phaeum*	Thermophilic/Anaerobic	Digester sludge	-/+	-/-
Proteobacteria	*Anaeromyxobacter dehalogenans* 2CP-1	Mesophilic/Facultative	Soil	-/-	++/-
Proteobacteria	*Anaeromyxobacter dehalogenans* 2CP-C	Mesophilic/Facultative	Soil	-/-	++/-
Proteobacteria	*Anaeromyxobacter* sp. K	Mesophilic/Anaerobic	Soil	-/-	++/-
Proteobacteria	*Anaeromyxobacter* sp. Fw109-5	Mesophilic/Anaerobic	Subsurface sediments	-/-	++/-
Proteobacteria	*Accumulibacter phosphatis*	Mesophilic/Facultative	Sludge and sediments	-/-	++/-
Proteobacteria	*Myxococcus stipitatus*	Mesophilic/Aerobic	Soil	-/-	+++/-
Proteobacteria	*Sorangium cellulosum* So0157-2	Mesophilic/Aerobic	Soil	-/-	+/-
Proteobacteria	*Sorangium cellulosum* So ce 56	Mesophilic/Aerobic	Soil	+/+	+/-
Proteobacteria	*Stigmatella aurantiaca*	Mesophilic/Aerobic	Rotting wood and bark	-/-	+++/-
Proteobacteria	*Syntrophus aciditrophicus*	Mesophilic/Anaerobic	Sewage treatment plant	-/-	-/-
Spirochaetes	*Turneriella parva*	Mesophilic/Aerobic	Culture medium	-/-	+/-
Verrucomicrobia	*Opitutus terrae*	Mesophilic/Anaerobic	Soil	-/-	-/+

5. CONCLUDING REMARKS AND FUTURE PROSPECTS

PP_i is a molecule produced as a byproduct in biologically important reactions, and enzymes able to hydrolyze and synthesize it are important for the viability of the cell. Membrane-bound PPases are simple ion transporters that can act as model proteins and provide answers to questions on bioenergetics and its early evolution. These enzymes pump ions across membranes and are crucial for the survival of the cell. Furthermore, mPPases are especially important for stress regulation in bacteria, plants and protists. Accordingly, mPPases may be potential drug targets against malaria and Chagas' disease, for example, and provide means of creating more stress resistant plants with bigger sizes and crop yields for the production of food and energy. Because mPPases are also found in the bacteria of the human gastrointestinal tract, these enzymes probably influence the well-being of the human gut. The studies I did were basic research on the function and evolution of mPPases. I showed that mPPases are functionally versatile enzymes and I delineated the evolutionary pathways which led to this divergence. The novel types of mPPases discovered during this study may have multiple applications in the future particularly for engineering stress-tolerant organisms. Still several important questions remain to be answered. Firstly, for example, what is the detailed mechanism of mPPase catalysis and, especially how are PP_i hydrolysis and ion transport coupled to each other. Secondly, how did mPPases evolve in detailed molecular level to select different coupling ions. And thirdly, how are the soluble and membrane bound PPases of an organism regulated and how are the various tasks divided between them.

ACKNOWLEDGEMENTS

The research belonging to this thesis was done during 2009−2015 at the Department of Biochemistry, the University of Turku. I thank the Department of Biochemistry and professor Jyrki Heino for providing excellent facilities to do the research and professor Eeva-Mari Aro for providing the opportunity to work at the facilities of Molecular Plant Biology. I thank professor Mark Johnson for directing the fantastic The National Doctoral Programme in Informational and Structural Biology (ISB) graduate school. I am thankful for ISB, Turun Yliopistosäätiö and Emil Aaltonen Foundation which provided funding for my studies. I thank ISB and Turku Centre for Systems Biology for the travel funds.

I greatly thank professor Volker Müller for acting as the opponent in the public defence for the dissertation. I am grateful to the reviewers Associate Professor, Ph.D. Blanca Barquera and Head of laboratory Ph.D. Manuela M. Pereira for pre-examining my thesis.

I owe my success to my supervisors, professor Reijo Lahti, professor Alexander Baykov and Ph.D. Anssi Malinen. I have learned great things from them and I will always remember and be grateful about that. I am thankful for their support and guidance during my studies. I especially and significantly thank Anssi for his daily support, encouragement, friendship and happy memories. I thank Docent, Ph.D. Saijaliisa Kangasjärvi for teaching me to make experiments with plants.

I had the privilege to work with extremely gifted people during my Ph.D. studies. I warmly thank the old and new POP members Anu Salminen, Marko Tammenkoski, Annamari Paino, Heidi Tuominen, Matti Lahti and Joonas Jämsen. I am very happy to know that the mPPase research is continuing by a fantastic young Ph.D. student Erika Nordbo. I thank talented students Tiina Pettersson, Edita Jetullahi, Fred Saarinen, Laura Laaksonen and Venla Kumpulainen for their wonderful work. I thank all the other students who were working in our laboratory during my studies. I am very grateful for Professor Herrick Baltcheffsky who was an excellent academic mentor for me and supported me during my Ph.D. studies. I greatly thank Satu Jasu, Teija Luotovaara, Venla Tyystjärvi, Anu Hirvensalo, Jani Sointusalo, Tiina Heinonen and Fredrik Karlsson for their wonderful work!

I am extremely happy that I have met fantastic people during my Ph.D. studies. I thank my colleagues working at the Biochemistry, Food Chemistry and Molecular Plant Biology, my ISB colleagues and the MBA4PhD students for their friendship. I especially thank Annamari Paino, for the daily support and being a great friend for me. I thank Mona Rahikainen for helping me with plant experiments. I am very grateful that I had the opportunity to meet the fantastic scientists of bioenergetics in multiple international scientific conferences.

I thank my fantastic, wonderful, amazing best friends who bring joy and happiness to my life, especially Anna, Annamari, Anni, Anniina, Henna, Irma, Katrina, Leeni, Merja, Tiia, Venla and Timo, and all of the others! I thank Olli for supporting me when I did great part of the laboratory work related to my Ph.D. studies. I also thank my hairdresser Sinikka for helping me to relax after a stressful day. I thank all the people that I have shared hobbies with and who have encouraged me to do this.

I thank my family and friends for believing in me and supporting me all the way through. My mother Anne and my father Matti have always encouraged me to try different things, try my best and not to give up. They have believed in me and supported me during my whole life. They both have very good leading skills and I have learned very much from them. I thank them for that they understood and encouraged me when I was little and collected stones, cooked perfumes from the wild flowers, read a lot and wished to go to school at the age of four. I want to thank my wonderful little brother, Henri, for growing up together with me. He has really taught me very much about cars, traffic and football and everything not related to biochemistry. I thank all of my grandparents for always believing in me and supporting me. I thank my great godmother Helena, my dear cousin Aija and my uncles Jarkko and Jouni, and their wives and children for their support during my life. I thank Helena and Risto for their great support.

I thank all of our family dogs and especially Rolle, for giving me an example of how I should also relax.

During my Ph.D. studies, I have learned that life never goes as expected, things change and novel information creates new perspectives and motivations in life. Change is the only thing that is constant. Now I have to change from Ph.D. student to something else. *The End is the New Beginning.*

Turku, May 2015

Heidi

REFERENCES

1. Heinonen., J. (2001) *Biological role of Inorganic Pyrophosphatase*, Kluwer Academic Publisher, USA

2. Holm, N.G., and Baltscheffsky, H. (2011) Links between hydrothermal environments, pyrophosphate, Na^+, and early evolution. *Orig.Life Evol. Biosph.* **41,** 483-93

3. Barge, L.M., Doloboff, I.J., Russell, M.J., VanderVelde, D., White, L.M., Galen, G.D., Baumd, M.M., Zeytounian, J., Kidd, R., and Kanik, I. (2014) Pyrophosphate synthesis in iron mineral films and membranes simulating prebiotic submarine hydrothermal precipitates. *Geochim. Cosmochim.Acta.* **128,** 1-12

4. Kulaev, I., and Kulakovskaya, T. (2000) Polyphosphate and phosphate pump. *Annu.Rev.Microbiol.* **54,** 709-34

5. Ferjani, A., Segami, S., Asaoka, M., and Maeshima, M. (2014) Regulation of PP_i Levels Through the Vacuolar Membrane H^+-Pyrophosphatase. *Prog.Bot.* **75,** 145-65

6. Netting, A.G. (2002) pH, abscisic acid and the integration of metabolism in plants under stressed and non-stressed conditions. II. Modifications in modes of metabolism induced by variation in the tension on the water column and by stress. *J.Exp.Bot.* **53,** 151-73

7. Baykov, A.A., Malinen, A.M., Luoto, H.H., and Lahti, R. (2013) Pyrophosphate-fueled Na^+ and H^+ transport in prokaryotes. *Microbiol. Mol.Biol.Rev.* **77,** 267-76

8. Bielen, A.A., Willquist, K., Engman, J., van der Oost, J., van Niel, E.W., and Kengen, S.W. (2010) Pyrophosphate as a central energy carrier in the hydrogen-producing extremely thermophilic *Caldicellulosiruptor saccharolyticus*. *FEMS Microbiol.Lett.* **307,** 48-54

9. Perez-Castineira, J.R., Lopez-Marques, R.L., Villalba, J.M., Losada, M., and Serrano, A. (2002) Functional complementation of yeast cytosolic pyrophosphatase by bacterial and plant H^+-translocating pyrophosphatases. *Proc.Natl.Acad.Sci.U.S.A.* **99,** 15914-9

10. Eberl, D., Preissler, M., Steingraber, M., and Hampp, R. (1992) Subcellular compartmentation of pyrophosphate and dark/light kinetics in comparison to fructose 2,6-bisphosphate. *Physiol.Plantarum.* **84,** 13-20

11. Hemalatha, K.P., and Prasad, D.S. (2002) Purification, physicochemical properties, and subcellular location of alkaline inorganic pyrophosphatase from sesame (*Sesamum indicum* L.) cotyledons. *Biochem Cell Biol.* **80,** 215-24

12. Terkeltaub, R.A. (2001) Inorganic pyrophosphate generation and disposition in pathophysiology. *Am.J.Physiol.Cell.Physiol.* **281,** C1-C11

13. Nociti, F.H.J., Berry, J.E., Foster, B.L., Gurley, K.A., Kingsley, D.M., Takata, T., Miyauchi, M., and Somerman, M.J. (2002) Cementum: a phosphate-sensitive tissue. *J.Dent.Res.* **81,** 817-21

14. Luo, S., Rohloff, P., Cox, J., Uyemura, S.A., and Docampo, R. (2004) *Trypanosoma brucei* plasma membrane-type Ca^{2+}-ATPase 1 (TbPMC1) and 2 (TbPMC2) genes encode functional Ca^{2+}-ATPases localized to the acidocalcisomes and plasma membrane, and essential for Ca^{2+} homeostasis and growth. *J.Biol.Chem.* **279,** 14427-39

15. Acosta, H., Dubourdieu, M., Quiñones, W., Cáceres, A., Bringaud, F., and Concepción, J.L. (2004) Pyruvate phosphate dikinase and pyrophosphate metabolism in the glycosome of *Trypanosoma cruzi* epimastigotes. *Comp Biochem Physiol B Biochem Mol Biol.* **138,** 347-56

16. Casolo, V., Micolini, S., Macri, F., and Vianello, A. (2002) Pyrophosphate import and synthesis by plant mitochondria. *Physiol.Plant.* **114,** 516-23

17. Costa dos Santos, A., Seixas da-Silva, W., de Meis, L., and Galina, A. (2003) Proton transport in maize tonoplasts supported by fructose-1,6-bisphosphate cleavage. Pyrophosphate-dependent phosphofructokinase as a pyrophosphate-regenerating system. *Plant Physiol.* **133,** 885-92

18. Nakanishi, Y., and Maeshima, M. (1998) Molecular cloning of vacuolar H^+-pyrophosphatase and its developmental expression in growing hypocotyl of mung bean. *Plant Physiol.* **116,** 589-97

19. Volk, S.E., Baykov, A.A., Duzhenko, V.S., and Avaeva, S.M. (1982) Kinetic studies on the interactions of two forms of inorganic pyrophosphatase of heart mitochondria with physiological ligands. *Eur J Biochem.* **125,** 215-20

20. Baykov, A.A., Bakuleva, N.P., and Rea, P.A. (1993) Steady-state kinetics of substrate hydrolysis by vacuolar H^+-pyrophosphatase. A simple three-state model. *Eur J Biochem.* **217,** 755-62

21. McCarthy, W.J., Smith, D.M.A., Adamowicz, L., Saint Martin, H., and Ortega-Blake, I. (1998) An ab initio study of the isomerization of Mg- and Ca-pyrophosphates. *J.Am.Chem.Soc.* **120,** 6113-20

22. Wang, J.H. (1970) Possible role of pyrophosphate linkage in the active transport of sodium ions. *Proc.Natl.Acad.Sci.U.S.A.* **67,** 59-61

23. Baykov, A.A., Cooperman, B.S., Goldman, A., and Lahti, R. (1999) Cytoplasmic inorganic pyrophosphatase. *Prog.Mol.Subcell.Biol.* **23,** 127-50

24. Kajander, T., Kellosalo, J., and Goldman, A. (2013) Inorganic pyrophosphatases: One substrate, three mechanisms. *FEBS Lett.* **587,** 1863-9

25. Aravind, L., and Koonin, E.V. (1998) A novel family of predicted phosphoesterases includes Drosophila prune protein and bacterial recJ exonuclease. *Trends Biochem.Sci.* **23,** 17-9

26. Jämsen, J., Tuominen, H., Salminen, A., Belogurov, G.A., Magretova, N.N., Baykov, A.A., and Lahti, R. (2007) A CBS domain-containing pyrophosphatase of *Moorella thermoacetica* is regulated by adenine nucleotides. *Biochem.J.* **408,** 327-33

27. Lee, H.S., Cho, Y., Kim, Y.J., Lho, T.O., Cha, S.S., Lee, J.H., and Kang, S.G. (2009) A novel inorganic pyrophosphatase in *Thermococcus onnurineus* NA1. *FEMS Microbiol.Lett.* **300,** 68-74

28. Malinen, A.M., Belogurov, G.A., Baykov, A.A., and Lahti, R. (2007) Na^+-pyrophosphatase: A novel primary sodium pump. *Biochemistry (N.Y.).* **46,** 8872-8

29. Baltscheffsky, M. (1967) Inorganic pyrophosphate and ATP as energy donors in chromatophores from *Rhodospirillum rubrum*. *Nature.* **216,** 241-3

30. Tsai, J.Y., Kellosalo, J., Sun, Y.J., and Goldman, A. (2014) Proton/sodium pumping pyrophosphatases: the last of the primary ion pumps. *Curr.Opin.Struct.Biol.* **27,** 38-47

31. Baltscheffsky, H., Von Stedingk, L.V., Heldt, H.W., and Klingenberg, M. (1966) Inorganic pyrophosphate: formation in bacterial photophosphorylation. *Science.* **153,** 1120-2

32. Baykov, A.A., Hyytia, T., Volk, S.E., Kasho, V.N., Vener, A.V., Goldman, A., Lahti, R., and Cooperman, B.S. (1996) Catalysis by *Escherichia coli* inorganic pyrophosphatase: pH and Mg^{2+} dependence. *Biochemistry.* **35,** 4655-61

33. Behrens, M.I., and De Meis, L. (1985) Synthesis of pyrophosphate by chromatophores of *Rhodospirillum rubrum* in the light and by soluble yeast inorganic pyrophosphatase in water-organic solvent mixtures. *Eur J Biochem.* **152,** 221-7

34. Smirnova, I.N., Kasho, V.N., Volk, S.E., Ivanov, A.H., and Baykov, A.A. (1995) Rates of elementary steps catalyzed by rat liver cytosolic and mitochondrial inorganic pyrophosphatases in both directions. *Arch. Biochem.Biophys.* **318,** 340-8

35. Baykov, A.A., Kasho, V.N., Bakuleva, N.P., and Rea, P.A. (1994) Oxygen exchange reactions catalyzed by vacuolar H^+-translocating pyrophosphatase. Evidence for reversible formation of enzyme-bound pyrophosphate. *FEBS Lett.* **350,** 323-7

36. Kay, H.D. (1928) The phosphatases of mammalian tissues: Pyrophosphatase. *Biochem.J.* **22,** 1446-8

37. Harutyunyan, E., Terzyan, S.S., Voronova, A.A., Kuranova, I., Smirnova, E.A., Vainshtein, B.K., Höfne, W., and Hansen, G. (1981) An X-ray study of yeast inorganic pyrophosphatase at 3 Å resolution. *Dokl Akad Nauk SSSR.* **258,** 1481-5

38. Salminen, A., Parfenyev, A.N., Salli, K., Efimova, I.S., Magretova, N.N., Goldman, A., Baykov, A.A., and Lahti, R. (2002) Modulation of dimer stability in yeast pyrophosphatase by mutations at the subunit interface and ligand binding to the active site. *J.Biol.Chem.* **277,** 15465-71

39. Salminen, A., Efimova, I.S., Parfenyev, A.N., Magretova, N.N., Mikalahti, K., Goldman, A., Baykov, A.A., and Lahti, R. (1999) Reciprocal effects of substitutions at the subunit interfaces in hexameric

pyrophosphatase of *Escherichia coli*. Dimeric and monomeric forms of the enzyme. *J.Biol.Chem.* **274,** 33898-904

40. Efimova, I.S., Salminen, A., Pohjanjoki, P., Lapinniemi, J., Magretova, N.N., Cooperman, B.S., Goldman, A., Lahti, R., and Baykov, A.A. (1999) Directed mutagenesis studies of the metal binding site at the subunit interface of *Escherichia coli* inorganic pyrophosphatase. *J.Biol. Chem.* **274,** 3294-9

41. Velichko, I.S., Mikalahti, K., Kasho, V.N., Dudarenkov, V.Y., Hyytia, T., Goldman, A., Cooperman, B.S., Lahti, R., and Baykov, A.A. (1998) Trimeric inorganic pyrophosphatase of *Escherichia coli* obtained by directed mutagenesis. *Biochemistry.* **37,** 734-40

42. Heikinheimo, P., Lehtonen, J., Baykov, A., Lahti, R., Cooperman, B.S., and Goldman, A. (1996) The structural basis for pyrophosphatase catalysis. *Structure.* **4,** 1491-508

43. Kankare, J., Neal, G.S., Salminen, T., Glumoff, T., Cooperman, B.S., Lahti, R., and Goldman, A. (1994) The structure of *E. coli* soluble inorganic pyrophosphatase at 2.7 Å resolution. *Protein Eng.* **7,** 823-30

44. Oganessyan, V.Y., Kurilova, S.A., Vorobyeva, N.N., Nazarova, T.I., Popov, A.N., Lebedev, A.A., Avaeva, S.M., and Harutyunyan, E.H. (1994) X-ray crystallographic studies of recombinant inorganic pyrophosphatase from *Escherichia coli. FEBS Lett.* **348,** 301-4

45. Salminen, T., Käpylä, J., Heikinheimo, P., Kankare, J., Goldman, A., Heinonen, J., Baykov, A.A., Cooperman, B.S., and Lahti, R. (1995) Structure and function analysis of *Escherichia coli* inorganic pyrophosphatase: is a hydroxide ion the key to catalysis?. *Biochemistry.* **34,** 782-91

46. Heikinheimo, P., Pohjanjoki, P., Helminen, A., Tasanen, M., Cooperman, B.S., Goldman, A., Baykov, A., and Lahti, R. (1996) A site-directed mutagenesis study of *Saccharomyces cerevisiae* pyrophosphatase. Functional conservation of the active site of soluble inorganic pyrophosphatases. *Eur.J.Biochem.* **239,** 138-43

47. Heikinheimo, P., Tuominen, V., Ahonen, A.K., Teplyakov, A., Cooperman, B.S., Baykov, A.A., Lahti, R., and Goldman, A. (2001) Toward a quantum-mechanical description of metal-assisted phosphoryl transfer in pyrophosphatase. *Proc.Natl.Acad.Sci.U.S.A.* **98,** 3121-6

48. Oksanen, E., Ahonen, A., Tuominen, H., Tuominen, V., Lahti, R., Goldman, A., and Heikinheimo, P. (2007) A complete structural description of the catalytic cycle of yeast pyrophosphatase. *Biochemistry (N.Y.).* **46,** 1228-39

49. Pohjanjoki, P., Fabrichniy, I.P., Kasho, V.N., Cooperman, B.S., Goldman, A., Baykov, A.A., and Lahti, R. (2001) Probing essential water in yeast pyrophosphatase by directed mutagenesis and fluoride inhibition measurements. *J.Biol.Chem.* **276,** 434-41

50. Halonen, P., Baykov, A.A., Goldman, A., Lahti, R., and Cooperman, B.S. (2002) Single-turnover kinetics of *Saccharomyces cerevisiae* inorganic pyrophosphatase. *Biochemistry (N.Y.).* **41,** 12025-31

51. Zyryanov, A.B., Pohjanjoki, P., Kasho, V.N., Shestakov, A.S., Goldman, A., Lahti, R., and Baykov, A.A. (2001) The electrophilic and leaving group phosphates in the catalytic mechanism of yeast pyrophosphatase. *J.Biol.Chem.* **276,** 17629-34

52. Pohjanjoki, P., Lahti, R., Goldman, A., and Cooperman, B.S. (1998) Evolutionary conservation of enzymatic catalysis: quantitative comparison of the effects of mutation of aligned residues in *Saccharomyces cerevisiae* and *Escherichia coli* inorganic pyrophosphatases on enzymatic activity. *Biochemistry.* **37,** 1754-61

53. Hyytiä, T., Halonen, P., Salminen, A., Goldman, A., Lahti, R., and Cooperman, B.S. (2001) Ligand binding sites in *Escherichia coli* inorganic pyrophosphatase: effects of active site mutations. *Biochemistry.* **40,** 4645-53

54. Belogurov, G.A., Fabrichniy, I.P., Pohjanjoki, P., Kasho, V.N., Lehtihuhta, E., Turkina, M.V., Cooperman, B.S., Goldman, A., Baykov, A.A., and Lahti, R. (2000) Catalytically important ionizations along the reaction pathway of yeast pyrophosphatase. *Biochemistry.* **39,** 13931-8

55. Baykov, A.A., Fabrichniy, I.P., Pohjanjoki, P., Zyryanov, A.B., and Lahti, R. (2000) Fluoride effects along the reaction pathway of pyrophosphatase: evidence for a second enzyme pyrophosphate intermediate. *Biochemistry.* **39,** 11939-47

56. Shintani, T., Uchiumi, T., Yonezawa, T., Salminen, A., Baykov, A.A., Lahti, R., and Hachimori, A. (1998) Cloning and expression of a unique inorganic pyrophosphatase from *Bacillus subtilis*: evidence for a new family of enzymes. *FEBS Lett.* **439,** 263-6

57. Young, T.W., Kuhn, N.J., Wadeson, A., Ward, S., Burges, D., and Cooke, G.D. (1998) Bacillus subtilis ORF yybQ encodes a manganese-dependent inorganic pyrophosphatase with distinctive properties: the first of a new class of soluble pyrophosphatase?. *Microbiology.* **144,** 2563-71

58. Ahn, S., Milner, A.J., Fütterer, K., Konopka, M., Ilias, M., Young, T.W., and White, S.A. (2001) The "open" and "closed" structures of the type-C inorganic pyrophosphatases from *Bacillus subtilis* and *Streptococcus gordonii*. *J.Mol.Biol.* **313,** 797-811

59. Merckel, M.C., Fabrichniy, I.P., Salminen, A., Kalkkinen, N., Baykov, A.A., Lahti, R., and Goldman, A. (2001) Crystal structure of *Streptococcus mutans* pyrophosphatase: a new fold for an old mechanism. *Structure.* **9,** 289-97

60. Celis, H., Franco, B., Escobedo, S., and Romero, I. (2003) *Rhodobacter sphaeroides* has a family II pyrophosphatase: comparison with other species of photosynthetic bacteria. *Arch.Microbiol.* **179,** 368-76

61. Parfenyev, A.N., Salminen, A., Halonen, P., Hachimori, A., Baykov, A.A., and Lahti, R. (2001) Quaternary structure and metal ion requirement of family II pyrophosphatases from *Bacillus subtilis*, *Streptococcus gordonii*, and *Streptococcus mutans. J.Biol.Chem.* **276,** 24511-8

62. Jämsen, J., Tuominen, H., Baykov, A.A., and Lahti, R. (2011) Mutational analysis of residues in the regulatory CBS domains of *Moorella thermoacetica* pyrophosphatase corresponding to disease-related residues of human proteins. *Biochem.J.* **433,** 497-504

63. Chao, T.C., Huang, H., Tsai, J.Y., Huang, C.Y., and Sun, Y.J. (2006) Kinetic and structural properties of inorganic pyrophosphatase from the pathogenic bacterium *Helicobacter pylori*. *Proteins.* **65,** 670-80

64. Rajagopal, L., Clancy, A., and Rubens, C.E. (2003) A eukaryotic type serine/threonine kinase and phosphatase in *Streptococcus agalactiae* reversibly phosphorylate an inorganic pyrophosphatase and affect growth, cell segregation, and virulence. *J.Biol.Chem.* **278,** 14429-41

65. Nováková, L., Bezousková, S., Pompach, P., Spidlová, P., Sasková, L., Weiser, J., and Branny, P. (2010) Identification of multiple substrates of the StkP Ser/Thr protein kinase in *Streptococcus pneumoniae. J.Bacteriol.* **192,** 3629-38

66. Salminen, A., Anashkin, V.A., Lahti, M., Tuominen, H.K., Lahti, R., and Baykov, A.A. (2014) Cystathionine ß-Synthase (CBS) Domains Confer Multiple Forms of Mg^{2+}-dependent Cooperativity to Family II Pyrophosphatases. *J.Biol.Chem.* **289,** 22865-76

67. Baykov, A.A., Tuominen, H.K., and Lahti, R. (2011) The CBS domain: a protein module with an emerging prominent role in regulation. *ACS Chem.Biol.* **6,** 1156-63

68. Ignoul, S., and Eggermont, J. (2005) CBS domains: structure, function, and pathology in human proteins. *Am.J.Physiol.Cell.Physiol.* **289,** C1369-78

69. Tuominen, H., Salminen, A., Oksanen, E., Jämsen, J., Heikkilä, O., Lehtiö, L., Magretova, N.N., Goldman, A., Baykov, A.A., and Lahti, R. (2010) Crystal structures of the CBS and DRTGG domains of the regulatory region of *Clostridium perfringens* pyrophosphatase complexed with the inhibitor, AMP, and activator, diadenosine tetraphosphate. *J.Mol.Biol.* **398,** 400-13

70. Huang, H., Patskovsky, Y., Toro, R., Farelli, J.D., Pandya, C., Almo, S.C., Allen, K.N., and Dunaway-Mariano, D. (2011) Divergence of structure and function in the haloacid dehalogenase enzyme superfamily: *Bacteroides thetaiotaomicron* BT2127 is an inorganic pyrophosphatase. *Biochemistry.* **50,** 8937-49

71. Kellosalo, J., Kajander, T., Kogan, K., Pokharel, K., and Goldman, A. (2012) The structure and catalytic cycle of a sodium-pumping pyrophosphatase. *Science.* **337,** 473-6

72. Lin, S.M., Tsai, J.Y., Hsiao, C.D., Huang, Y.T., Chiu, C.L., Liu, M.H., Tung, J.Y., Liu, T.H., Pan, R.L., and Sun, Y.J. (2012) Crystal structure of a membrane-embedded H^+-translocating pyrophosphatase. *Nature.* **484,** 399-403

73. Fabrichniy, I.P., Lehtiö, L., Tammenkoski, M., Zyryanov, A.B., Oksanen, E., Baykov, A.A., Lahti, R., and Goldman, A. (2007) A trimetal site and substrate distortion in a family II inorganic pyrophosphatase. *J.Biol. Chem.* **282,** 1422-31

74. Zyryanov, A.B., Vener, A.V., Salminen, A., Goldman, A., Lahti, R., and Baykov, A.A. (2004) Rates of elementary catalytic steps for different metal forms of the family II pyrophosphatase from *Streptococcus gordonii. Biochemistry.* **43,** 1065-74

75. Gordon-Weeks, R., Steele, S.H., and Leigh, R.A. (1996) The role of magnesium, pyrophosphate, and their complexes as substrates and activators of the vacuolar H^+-pumping inorganic pyrophosphatase -

Studies using ligand protection from covalent inhibitors. *Plant Physiol.* **111,** 195-202

76. Avaeva, S.M. (2000) Active site interactions in oligomeric structures of inorganic pyrophosphatases. *Biochemistry (Mosc).* **65,** 361-72

77. Hsu, S.H., Hsiao, Y.Y., Liu, P., F., Lin, S.M., Luo, Y.Y., and Pan, R.L. (2009) Purification, characterization, and spectral analyses of histidine-tagged vacuolar H^+-pyrophosphatase expressed in yeast. *Botanical Studies.* **50,** 291-301

78. Sarafian, V., and Poole, R.J. (1989) Purification of an H-translocating inorganic pyrophosphatase from vacuole membranes of red beet. *Plant Physiol.* **91,** 34-8

79. Nakanishi, Y., Yabe, I., and Maeshima, M. (2003) Patch clamp analysis of a H^+ pump heterologously expressed in giant yeast vacuoles. *J.Biochem.* **134,** 615-23

80. Yang, L., Liao, R.Z., Yu, J.G., and Liu, R.Z. (2009) DFT study on the mechanism of *Escherichia coli* inorganic pyrophosphatase. *J Phys Chem B.* **113,** 6505-10

81. Fabrichniy, I.P., Lehtiö, L., Salminen, A., Zyryanov, A.B., Baykov, A.A., Lahti, R., and Goldman, A. (2004) Structural studies of metal ions in family II pyrophosphatases: the requirement for a Janus ion. *Biochemistry.* **43,** 14403-11

82. Skulachev, V., Bogachev, A., and Kasparinsky, F. (2013) *Principles of Bioenergetics*, Springer, Berlin Heidelberg

83. Nord, F.F., and Werkman, C.H. (1941) *Advances in Enzymology and Related Areas of Molecular Biology*, John Wiley & Sons, Inc., Hoboken, NJ, USA

84. Mulkidjanian, A.Y., Galperin, M.Y., and Koonin, E.V. (2009) Co-evolution of primordial membranes and membrane proteins. *Trends Biochem.Sci.* **34,** 206-15

85. Skulachev, V.P. (1989) The sodium cycle: a novel type of bacterial energetics. *J.Bioenerg.Biomembr.* **21,** 635-47

86. Biegel, E., and Müller, V. (2010) A Na^+-translocating pyrophosphatase in the acetogenic bacterium *Acetobacterium woodii*. *J.Biol.Chem.* **286,** 6080-4

87. Kogure, K. (1998) Bioenergetics of marine bacteria. *Curr.Opin. Biotechnol.* **9,** 278-82

88. Mulkidjanian, A.Y., Dibrov, P., and Galperin, M.Y. (2008) The past and present of sodium energetics: may the sodium-motive force be with you. *Biochim.Biophys.Acta.* **1777,** 985-92

89. Bruggemann, H., Baumer, S., Fricke, W.F., Wiezer, A., Liesegang, H., Decker, I., Herzberg, C., Martinez-Arias, R., Merkl, R., Henne, A., and Gottschalk, G. (2003) The genome sequence of *Clostridium tetani*, the causative agent of tetanus disease. *Proc.Natl.Acad.Sci.U.S.A.* **100,** 1316-21

90. Häse, C.C., Fedorova, N.D., Galperin, M.Y., and Dibrov, P.A. (2001) Sodium ion cycle in bacterial pathogens: evidence from cross-genome comparisons. *Microbiol Mol Biol Rev.* **65,** 353-70

91. Mayer, F., and Müller. V. (2014) Adaptations of anaerobic archaea to life under extreme energy limitation. *FEMS Microbiol.Rev.* **38,** 449-72

92. Schlegel, K., and Müller V. (2013) Evolution of Na^+ and H^+ bioenergetics in methanogenic archaea. *Biochem.Soc.Trans.* **41,** 421-6

93. Grüber, G., Manimekalai, M.S., Mayer, F., and Müller, V. (2014) ATP synthases from archaea: the beauty of a molecular motor. *Biochim. Biophys.Acta.* **1837,** 940-52

94. Mayer, F., Lim, J.K., Langer, J.D., Kang, S.G., and Müller.V. (2015) Na^+ transport by the A_1A_O ATP synthase purified from *Thermococcus onnurineu*s and reconstituted into liposomes. *J.Biol.Chem.* **290,** 6994-7002

95. McMillan, D.G.G., Ferguson, S.A., Dey, D., Schröder, K., Aung, H.L., Carbone, V., Attwood, G., Ronimus, R.S., Meier, T., Janssen, P.H., and Cook, G.M. (2011) A_1A_o-ATP synthase of *Methanobrevibacter ruminantium* couples sodium ions for ATP synthesis under physiological conditions. *J.Biol.Chem.* **286,** 39882-92

96. Krulwich, T.A. (1995) Alkaliphiles: 'basic' molecular problems of pH tolerance and bioenergetics. *Mol.Microbiol.* **15,** 403-10

97. Batista, A.P., Marreiros, B.C., and Pereira, M.M. (2012) The role of proton and sodium ions in energy transduction by respiratory complex I. *IUBMB Life.* **64,** 492-8

98. Beliakova, T.N., Glagolev, A.N., and Skulachev, V.P. (1976) [Electrochemical gradient of H^+ ions as an immediate source of energy during bacteria movement]. *Biokhimiia.* **41,** 1478-83

99. Blair, D.F. (2003) Flagellar movement driven by proton translocation. *FEBS Lett.* **545,** 86-95

100. Seidel, T., Siek, M., Marg, B., and Dietz, K.J. (2013) Energization of vacuolar transport in plant cells and its significance under stress. *Int.Rev. Cell.Mol.Biol.* **304,** 57-131

101. Juárez, O., and Barquera, B. (2012) Insights into the mechanism of electron transfer and sodium translocation of the Na^+-pumping NADH:quinone oxidoreductase. *Biochim.Biophys.Acta.* **1817,** 1823-32

102. Nore, B.F., Sakai, Y., and Baltscheffsky, M. (1990) Comparison of the contribution from different energy-linked reactions to the function of a membrane potential in photosynthetic bacteria. *Biochim.Biophys.Acta.* **1015,** 189-94

103. Baltscheffsky, M., and Baltscheffsky, H. (1995) Alternative photophosphorylation, inorganic pyrophosphate synthase and inorganic pyrophosphate. *Photosynthesis Res.* **46,** 87-91

104. Nyrén, P., and Baltscheffsky, M. (1983) Inorganic pyrophosphate-driven ATP-synthesis in liposomes containing membrane-bound inorganic pyrophosphatase and F_0-F_1 complex from *Rhodospirillum rubrum*. *FEBS Lett.* **155,** 125-30

105. Kondrashin, A.A., Remennikov, V.G., Samuilov, V.D., and Skulachev, V.P. (1980) Reconstitution of biological molecular generators of electric current. Inorganic pyrophosphatase. *Eur J Biochem.* **113,** 219-22

106. Strid, Å, Nyrén, P., Boork, J., and Baltscheffsky, M. (1986) Kinetics of the membrane-bound inorganic pyrophosphatase from *Rhodospirillum rubrum* chromatophores: Effect of the transmembrane electrical potential on the rate constants. *FEBS Lett.* **196,** 337-40

107. Nyrén, P., and Strid, Å (1991) Hypothesis: the physiological role of the membrane-bound proton-translocating pyrophosphatase in some phototrophic bacteria. *FEMS Microbiol.Lett.* **77,** 265-9

108. Shiratake, K., Kanayama, Y., Maeshima, M., and Yamaki, S. (1997) Changes in H^+-pumps and a tonoplast intrinsic protein of vacuolar membranes during the development of pear fruit. *Plant Cell Physiol.* **38,** 1039-45

109. Rocha Facanha, A., and de Meis, L. (1998) Reversibility of H^+-ATPase and H^+-pyrophosphatase in tonoplast vesicles from maize coleoptiles and seeds. *Plant Physiol.* **116,** 1487-95

110. Vila-Costa, M., Sharma, S., Moran, M.A., and Casamayor, E.O. (2013) Diel gene expression profiles of a phosphorus limited mountain lake using metatranscriptomics. *Environ.Microbiol.* **15,** 1190-203

111. Harvey, G.W., and Keister, D.L. (1981) Energy-linked reactions in photosynthetic bacteria: P_i in equilibrium with HOH oxygen exchange catalyzed by the membrane-bound inorganic pyrophosphatase of *Rhodospirillum rubrum*. *Arch.Biochem.Biophys.* **208,** 426-30

112. Guillory, R.J., and Fisher, R.R. (1972) Studies on the light-dependent synthesis of inorganic pyrophosphate by *Rhodospirillum rubrum* chromatophores. *Biochem.J.* **129,** 571-81

113. Martin, W.F., Sousa, F.L., and Lane, N. (2014) Evolution. Energy at life's origin. *Science.* **344,** 1092-3

114. Lane, N., and Martin, W.F. (2012) The origin of membrane bioenergetics. *Cell.* **151,** 1406-16

115. Mulkidjanian, A.Y., Bychkov, A.Y., Dibrova, D.V., Galperin, M.Y., and Koonin, E.V. (2012) Origin of first cells at terrestrial, anoxic geothermal fields. *Proc.Natl.Acad.Sci.U.S.A.* **109,** E821-30

116. Baltscheffsky, M., Schultz, A., and Baltscheffsky, H. (1999) H+ -PPases: a tightly membrane-bound family. *FEBS Lett.* **457,** 527-33

117. Russell, M.J., Nitschke, W., and Branscomb, E. (2013) The inevitable journey to being. *Philos Trans R Soc Lond B Biol Sci.* **368,** 20120254

118. Baltscheffsky, H., and Persson, B. (2014) On an Early Gene for Membrane-Integral Inorganic Pyrophosphatase in the Genome of an Apparently Pre-LUCA Extremophile, the Archaeon *Candidatus Korarchaeum cryptofilum*. *J.Mol.Evol.* **78,** 140-7

119. Venancio, J.B., Catunda, M.G., Ogliari, J., Rima, J.A., Okorokova-Facanha, A.L., Okorokov, L.A., and Facanha, A.R. (2014) A vacuolar H^+-pyrophosphatase differential activation and energy coupling integrate the responses of weeds and crops to drought stress. *Biochim.Biophys. Acta.* **1840,** 1987-92

120. Hedlund, J., Cantoni, R., Baltscheffsky, M., Baltscheffsky, H., and Persson, B. (2006) Analysis of ancient sequence motifs in the H^+-PPase family. *FEBS J.* **273,** 5183-93

121. Rea, P.A., Kim, Y., Sarafian, V., Poole, R.J., Davies, J.M., and Sanders, D. (1992) Vacuolar H^+-translocating pyrophosphatases: a new category of ion translocase. *Trends Biochem.Sci.* **17,** 348-53

122. Seufferheld, M.J., Kim, K.M., Whitfield, J., Valerio, A., and Caetano-Anollés, G. (2011) Evolution of vacuolar proton pyrophosphatase domains and volutin granules: clues into the early evolutionary origin of the acidocalcisome. *Biol Direct.* **6,** 50

123. Seufferheld, M.J., and Caetano-Anollés, G. (2013) Phylogenomics supports a cellularly structured urancestor. *J.Mol.Microbiol.Biotechnol.* **23,** 178-91

124. Drozdowicz, Y.M., Lu, Y.P., Patel, V., Fitz-Gibbon, S., Miller, J.H., and Rea, P.A. (1999) A thermostable vacuolar-type membrane pyrophosphatase from the archaeon *Pyrobaculum aerophilum*: implications for the origins of pyrophosphate-energized pumps. *FEBS Lett.* **460,** 505-12

125. Nitschke, W., and Russell, M.J. (2009) Hydrothermal focusing of chemical and chemiosmotic energy, supported by delivery of catalytic Fe, Ni, Mo/W, Co, S and Se, forced life to emerge. *J.Mol.Evol.* **69,** 481-96

126. Mulkidjanian, A.Y., Galperin, M.Y., Makarova, K.S., Wolf, Y.I., and Koonin, E.V. (2008) Evolutionary primacy of sodium bioenergetics. *Biol Direct.* **3,** 13

127. van de Vossenberg, J.L.C.M., Ubbink-Kok, T., Elferink, M.G.L., Driessen, A.J.M., and Konings, W.N. (1995) Ion permeability of the cytoplasmic membrane limits the maximum growth temperature of bacteria and archaea. *Mol.Microbiol.* **18,** 925-32

128. Wilson, M.A., Wei, C., and Pohorille, A. (2015) Towards Co-Evolution of Membrane Proteins and Metabolism. *Orig.Life Evol.Biosph.* in press

129. Sojo, V., Pomiankowski, A., and Lane, N. (2014) A bioenergetic basis for membrane divergence in archaea and bacteria. *PLoS Biol.* **12,** e1001926

130. Huang, Y.T., Liu, T.H., Chen, Y.W., Lee, C.H., Chen, H.H., Huang, T.W., Hsu, S.H., Lin, S.M., Pan, Y.J., Lee, C.H., Hsu, I.C., Tseng, F.G., Fu, C.C., and Pan, R.L. (2010) Distance variations between active sites of H^+-pyrophosphatase determined by fluorescence resonance energy transfer. *J.Biol.Chem.* **285,** 23655-64

131. Liu, T.H., Hsu, S.H., Huang, Y.T., Lin, S.M., Huang, T.W., Chuang, T.H., Fan, S.K., Fu, C.C., Tseng, F.G., and Pan, R.L. (2009) The proximity between C-termini of dimeric vacuolar H^+-pyrophosphatase determined using atomic force microscopy and a gold nanoparticle technique. *FEBS J.* **276,** 4381-94

132. López-Marqués, R.L., Pérez-Castiñeira, J.R., Buch-Pedersen, M.J., Marco, S., Rigaud, J.L., Palmgren, M.G., and Serrano, A. (2005) Large-scale purification of the proton pumping pyrophosphatase from *Thermotoga maritima*: A "Hot-Solve" method for isolation of recombinant thermophilic membrane proteins. *Biochim Biophys Acta.* **1716,** 69-76

133. Mimura, H., Nakanishi, Y., and Maeshima, M. (2005) Oligomerization of H^+-pyrophosphatase and its structural and functional consequences. *Biochimica et Biophysica Acta (BBA) - Bioenergetics.* **1708,** 393-403

134. Hsu, S.H., Lo, Y.Y., Liu, T.H., Pan, Y.J., Huang, Y.T., Sun, Y.J., Hung, C.C., Tseng, F.G., Yang, C.W., and Pan, R.L. (2014) Substrate Induced Changes in Domains Interaction of Vacuolar H^+-Pyrophosphatase. *J.Biol.Chem.* **290,** 1197-209

135. Maeshima, M. (1990) Oligomeric structure of H^+-translocating inorganic pyrophosphatase of plant vacuoles. *Biochem.Biophys.Res.Commun.* **168,** 1157-62

136. Sato, M.H., Maeshima, M., Ohsumi, Y., and Yoshida, M. (1991) Dimeric structure of H^+-translocating pyrophosphatase from pumpkin vacuolar membranes. *FEBS Lett.* **290,** 177-80

137. Yang, S.J., Ko, S.J., Tsai, Y.R., Jiang, S.S., Kuo, S.Y., Hung, S.H., and Pan, R.L. (1998) Subunit interaction of vacuolar H^+-pyrophosphatase as determined by high hydrostatic pressure. *Biochem.J.* **331,** 395-402

138. Kellosalo, J., Kajander, T., Honkanen, R., and Goldman, A. (2013) Crystallization and preliminary X-ray analysis of membrane-bound pyrophosphatases. *Mol.Membr.Biol.* **30,** 64-74

139. Malinen, A.A., Baykov, A.A., and Lahti, R. (2008) Mutual effects of cationic ligands and substrate on activity of the Na^+-transporting pyrophosphatase of *Methanosarcina mazei*. *Biochemistry (N.Y.).* **47,** 13447-54

140. Rea, P.A., Britten, C.J., Jennings, I.R., Calvert, C.M., Skiera, L.A., Leigh, R.A., and Sanders, D. (1992) Regulation of vacuolar H-pyrophosphatase by free calcium : a reaction kinetic analysis. *Plant Physiol.* **100,** 1706-15

141. Rea, P.A., Britten, C.J., and Sarafian, V. (1992) Common identity of substrate binding subunit of vacuolar H-translocating inorganic pyrophosphatase of higher plant cells. *Plant Physiol.* **100,** 723-32

142. Pérez-Castiñeira, J.R., López-Marqués, R.L., Losada, M., and Serrano, A. (2001) A thermostable K(+)-stimulated vacuolar-type pyrophosphatase from the hyperthermophilic bacterium *Thermotoga maritima*.. *FEBS Lett.* **496,** 6

143. Baykov, A.A., Sergina, N.V., Evtushenko, O.A., and Dubnova, E.B. (1996) Kinetic characterization of the hydrolytic activity of the H^+-pyrophosphatase of *Rhodospirillum rubrum* in membrane-bound and isolated states. *Eur J Biochem.* **236,** 121-7

144. Leigh, R.A., Gordon-Weeks, R., Steele, S.H., and Koren'kov, V.D. (1994) The H^+-pumping inorganic pyrophosphatase of the vacuolar membrane of higher plants. *Symp.Soc.Exp.Biol.* **48,** 61-75

145. Leigh, R.A., Pope, A.J., Jennings, I.R., and Sanders, D. (1992) Kinetics of the Vacuolar H^+-Pyrophosphatase : The Roles of Magnesium, Pyrophosphate, and their Complexes as Substrates, Activators, and Inhibitors. *Plant Physiol.* **100,** 1698-705

146. White, P.J., Marshall, J., and Smith, J.A. (1990) Substrate kinetics of the tonoplast H-translocating inorganic pyrophosphatase and its activation by free Mg. *Plant Physiol.* **93,** 1063-70

147. Kuo, S.Y., and Pan, R.L. (1990) An essential arginyl residue in the tonoplast pyrophosphatase from etiolated mung bean seedlings. *Plant Physiol.* **93,** 1128-33

148. Maeshima, M., and Yoshida, S. (1989) Purification and properties of vacuolar membrane proton-translocating inorganic pyrophosphatase from mung bean. *J.Biol.Chem.* **264,** 20068-73

149. Randahl, H. (1979) Characterization of the membrane-bound inorganic pyrophosphatase in *Rhodospirillum rubrum*. *Eur J Biochem.* **102,** 251-6

150. Romero, I., Gómez-Priego, A., and Celis, H. (1991) A membrane-bound pyrophosphatase from respiratory membranes of *Rhodospirillum rubrum*. *J.Gen.Microbiol.* **137,** 2611-16

151. Schultz, A., and Baltscheffsky, M. (2004) Inhibition studies on *Rhodospirillum rubrum* H^+-pyrophosphatase expressed in *Escherichia coli*. *Biochim.Biophys.Acta.* **1656,** 156-65

152. Celis, H., and Romero, I. (1987) The phosphate-pyrophosphate exchange and hydrolytic reactions of the membrane-bound pyrophosphatase of *Rhodospirillum rubrum*: effects of pH and divalent cations. *J.Bioenerg. Biomembr.* **19,** 255-72

153. Jiang, S.S., Fan, L.L., Yang, S.J., Kuo, S.Y., and Pan, R.L. (1997) Purification and characterization of thylakoid membrane-bound inorganic pyrophosphatase from *Spinacia oleracia* L. *Arch.Biochem. Biophys.* **346,** 105-12

154. Fraichard, A., Trossat, C., Perotti, E., and Pugin, A. (1996) Allosteric regulation by Mg^{2+} of the vacuolar H^+-PPase from *Acer pseudoplatanus* cells. Ca^{2+}/Mg^{2+} interactions. *Biochimie.* **78,** 259-66

155. Ordaz, H., Sosa, A., Romero, I., and Celis, H. (1992) Thermostability and activation by divalent cations of the membrane-bound inorganic pyrophosphatase of *Rhodospirillum rubrum*. *Int.J.Biochem.* **24,** 1633-8

156. Pugliarello, M.C., Rasi-Caldogno, F., De Michelis, M.I., and Olivari, C. (1991) The tonoplast H^+-pyrophosphatase of radish seedlings: biochemical characteristics. *Physiol.Plantarum.* **83,** 339-45

157. Takeshige, K., Tazawa, M., and Hager, A. (1988) Characterization of the H Translocating Adenosine Triphosphatase and Pyrophosphatase of Vacuolar Membranes Isolated by Means of a Perfusion Technique from *Chara corallina*.. *Plant Physiol.* **86,** 1168-73

158. Moraes Moreira, B.L., Soares Medeiros, L.C., Miranda, K., de Souza, W., Hentschel, J., Plattner, H., and Barrabin, H. (2005) Kinetics of pyrophosphate-driven proton uptake by acidocalcisomes of *Leptomonas wallacei*. *Biochem.Biophys.Res.Commun.* **334,** 1206-13

159. Keister, D.L., and Raveed, N.J. (1974) Energy-linked reactions in photosynthetic bacteria. IX. P_i-PP_i exchange in *Rhodospirillum rubrum*. *J.Biol.Chem.* **249,** 6454-8

160. Hackney, D.D. (1980) Theoretical analysis of distribution of $[^{18}O]P_i$ species during exchange with water. Application to exchanges catalyzed by yeast inorganic pyrophosphatase. *J.Biol.Chem.* **255,** 5320-8

161. Belogurov, G.A., Malinen, A.M., Turkina, M.V., Jalonen, U., Rytkönen, K., Baykov, A.A., and Lahti, R. (2005) Membrane-bound pyrophosphatase of *Thermotoga maritima* requires sodium for activity. *Biochemistry (N.Y.).* **44,** 2088-96

162. Baykov, A.A., Shestakov, A.S., Kasho, V.N., Vener, A.V., and Ivanov, A.H. (1990) Kinetics and thermodynamics of catalysis by the inorganic pyrophosphatase of *Escherichia coli* in both directions. *Eur J Biochem.* **194,** 879-87

163. Obermeyer, G., Sommer, A., and Bentrup, F.W. (1996) Potassium and voltage dependence of the inorganic pyrophosphatase of intact vacuoles from *Chenopodium rubrum. Biochim.Biophys.Acta.* **1284,** 203-12

164. Celis, H., Romero, I., and Gómez-Puyou, A. (1985) The phosphate-pyrophosphate exchange and hydrolytic reactions of the membrane-bound pyrophosphatase of *Rhodospirillum rubrum*: effects of Mg^{2+}, phosphate, and pyrophosphate. *Arch.Biochem.Biophys.* **236,** 766-74

165. de Meis, L. (1985) Role of water in processes of energy transduction: Ca^{2+}-transport ATPase and inorganic pyrophosphatase. *Biochem Soc Symp.* **50,** 97-125

166. Seufferheld, M., Lea, C.R., Vieira, M., Oldfield, E., and Docampo, R. (2004) The H^+-pyrophosphatase of *Rhodospirillum rubrum* is predominantly located in polyphosphate-rich acidocalcisomes. *J.Biol. Chem.* **279,** 51193-202

167. Baltscheffsky, M., Nadanaciva, S., and Schultz, A. (1998) A pyrophosphate synthase gene: molecular cloning and sequencing of the cDNA encoding the inorganic pyrophosphate synthase from *Rhodospirillum rubrum. Biochim.Biophys.Acta.* **1364,** 301-6

168. Britten, C.J., Zhen, R.G., Kim, E.J., and Rea, P.A. (1992) Reconstitution of transport function of vacuolar H^+-translocating inorganic pyrophosphatase. *J.Biol.Chem.* **267,** 21850-5

169. Serrano, A., Pérez-Castiñeira, J.R., Baltscheffsky, M., and Baltscheffsky, H. (2007) H^+-PPases: yesterday, today and tomorrow. *IUBMB Life.* **59,** 76-83

170. Belogurov, G., A., and Lahti, R. (2002) A lysine substitute for K^+. A460K mutation eliminates K^+ dependence in H^+-pyrophosphatase of *Carboxydothermus hydrogenoformans. J.Biol.Chem.* **277,** 49651-4

171. Davies, J.M., Rea, P.A., and Sanders, D. (1991) Vacuolar proton-pumping pyrophosphatase in *Beta vulgaris* shows vectorial activation by potassium. *FEBS Lett.* **278,** 66-8

172. GordonWeeks, R., Korenkov, V.D., Steele, S.H., and Leigh, R.A. (1997) Tris is a competitive inhibitor of K^+ activation of the vacuolar H^+-pumping pyrophosphatase. *Plant Physiol.* **114,** 901-5

173. Wang, Y., Leigh, R.A., Kaestner, K.H., and Sze, H. (1986) Electrogenic H-pumping pyrophosphatase in tonoplast vesicles of oat roots. *Plant Physiol.* **81,** 497-502

174. Karlsson, J. (1975) Membrane-bound potassium and magnesium ion-stimulated inorganic pyrophosphatase from roots and cotyledons of sugar beet (*Beta vulgaris* L). *Biochim.Biophys.Acta.* **399,** 356-63

175. Taiz, L. (1992) The plant vacuole. *J.Exp.Biol.* **172,** 113-22

176. Ros, R., Romieu, C., Gibrat, R., and Grignon, C. (1995) The plant inorganic pyrophosphatase does not transport K^+ in vacuole membrane vesicles multilabeled with fluorescent probes for H^+, K^+, and membrane potential. *J.Biol.Chem.* **270,** 4368-74

177. Rea, P.A., and Poole, R.J. (1986) Chromatographic resolution of H-translocating pyrophosphatase from h-translocating ATPase of higher plant tonoplast. *Plant Physiol.* **81,** 126-9

178. Zancani, M., Casolo, V., Vianello, A., and Macri, F. (1998) H^+/PP_i stoichiometry of a membrane-bound pyrophosphatase of plant mitochondria. *Physiol.Plantarum.* **103,** 304-11

179. Sosa, A., and Celis, H. (1995) H^+/PP_i stoichiometry of membrane-bound pyrophosphatase of *Rhodospirillum rubrum*. *Arch.Biochem.Biophys.* **316,** 421-7

180. Schmidt, A.L., and Briskin, D.P. (1993) Energy transduction in tonoplast vesicles from red beet (*Beta vulgaris* L.) storage tissue: H^+/substrate stoichiometries for the H^+-ATPase and H^+-PPase. *Arch.Biochem. Biophys.* **301,** 165-73

181. Huang, Y.T., Liu, T.H., Lin, S.M., Chen, Y.W., Pan, Y.J., Lee, C.H., Sun, Y.J., Tseng, F.G., and Pan, R.L. (2013) Squeezing at Entrance of Proton Transport Pathway in Proton-translocating Pyrophosphatase upon Substrate Binding. *J.Biol.Chem.* **288,** 19312-20

182. Chen, Y.W., Lee, C.H., Huang, Y.T., Pan, Y.J., Lin, S.M., Lo, Y.Y., Lee, C.H., Huang, L.K., Huang, Y.F., Hsu, Y.D., and Pan, R.L. (2014) Functional and fluorescence analyses of tryptophan residues in H^+-pyrophosphatase of *Clostridium tetani. J.Bioenerg.Biomembr.* **46,** 127-34

183. Gordon-Weeks, R., Parmar, S., Davies, T.G., and Leigh, R.A. (1999) Structural aspects of the effectiveness of bisphosphonates as competitive inhibitors of the plant vacuolar proton-pumping pyrophosphatase. *Biochem.J.* **337,** 373-7

184. Zhen, R.G., Baykov, A.A., Bakuleva, N.P., and Rea, P.A. (1994) Aminomethylenediphosphonate: A Potent Type-Specific Inhibitor of Both Plant and Phototrophic Bacterial H^+-Pyrophosphatases. *Plant Physiol.* **104,** 153-9

185. Baykov, A.A., Dubnova, E.B., Bakuleva, N.P., Evtushenko, O.A., Zhen, R.G., and Rea, P.A. (1993) Differential sensitivity of membrane-associated pyrophosphatases to inhibition by diphosphonates and fluoride delineates two classes of enzyme. *FEBS Lett.* **327,** 199-202

186. Fraichard, A., Magnin, T., Trossat, C., and Pugin, A. (1993) Properties of the proton pumping pyrophosphatase in tonoplast vesicles of *Acer pseudoplatanus*: Functional molecular mass and polypeptide composition. *Plant physiology and biochemistry.* **31,** 349-59

187. Marchesini, N., Luo, S., Rodrigues, C.O., Moreno, S.N., and Docampo, R. (2000) Acidocalcisomes and a vacuolar H^+-pyrophosphatase in malaria parasites. *Biochem.J.* **347,** 243-53

188. Kim, E.J., Zhen, R.G., and Rea, P.A. (1994) Heterologous expression of plant vacuolar pyrophosphatase in yeast demonstrates sufficiency of the substrate-binding subunit for proton transport. *Proc.Natl.Acad. Sci.U.S.A.* **91,** 6128-32

189. Cromartie, T.H., Fisher, K.J., and Grossman, J.N. (1999) The discovery of a novel site of action for herbicidal bisphosphonates. *Pestic.Biochem. Physiol.* **63,** 114-26

190. Ogliari, J., Freitas, S.P., Ramos, A.C., Bressan Smith, R.E., and Façanha, A.R. (2009) Proton Transport Primary Systems Used as Mechanisms of Mesotrione Detoxification in Corn Plants. *Planta daninha.* **27,** 799-807

191. Chanson, A., Fichmann, J., Spear, D., and Taiz, L. (1985) Pyrophosphate-driven proton transport by microsomal membranes of corn coleoptiles. *Plant Physiol.* **79,** 159-64

192. Sen, S.S., Bhuyan, N.R., and Bera, T. (2009) Characterization of plasma membrane bound inorganic pyrophosphatase from *Leishmania donovani* promastigotes and amastigotes. *Afr Health Sci.* **9,** 212-7

193. Schwarm, H.M., Vigenschow, H., and Knobloch, K. (1986) Kinetic characterization and partial purification of the membrane-bound inorganic pyrophosphatase from *Rhodopseudomonas palustris*. *Biol Chem Hoppe Seyler.* **367,** 127-33

194. Hirono, M., Mimura, H., Nakanishi, Y., and Maeshima, M. (2005) Expression of functional *Streptomyces coelicolor* H+-pyrophosphatase and characterization of its molecular properties. *J.Biochem.* **138,** 183-91

195. Hirono, M., Ojika, M., Mimura, H., Nakanishi, Y., and Maeshima, M. (2003) Acylspermidine derivatives isolated from a soft coral, *Sinularia* sp, inhibit plant vacuolar H^+-pyrophosphatase. *J.Biochem.* **133,** 811-6

196. Celis, H., Escobedo, S., and Romero, I. (1998) Triphenyltin as an inhibitor of membrane-bound pyrophosphatase of *Rhodospirillum rubrum*. *Arch.Biochem.Biophys.* **358,** 157-63

197. Kim, E.J., Zhen, R.G., and Rea, P.A. (1995) Site-directed mutagenesis of vacuolar H^+-pyrophosphatase. Necessity of Cys634 for inhibition by maleimides but not catalysis. *J.Biol.Chem.* **270,** 2630-5

198. Yang, S.J., Jiang, S.S., Van, R.C., Hsiao, Y.Y., and Pan, R. (2000) A lysine residue involved in the inhibition of vacuolar H^+-pyrophosphatase by fluorescein 5'-isothiocyanate. *Biochim.Biophys.Acta.* **1460,** 375-83

199. Yang, S.J., Jiang, S.S., Tzeng, C.M., Kuo, S.Y., Hung, S.H., and Pan, R.L. (1996) Involvement of tyrosine residue in the inhibition of plant vacuolar H^+-pyrophosphatase by tetranitromethane. *Biochim.Biophys. Acta.* **1294,** 89-97

200. Takasu, A., Nakanishi, Y., Yamauchi, T., and Maeshima, M. (1997) Analysis of the substrate binding site and carboxyl terminal region of vacuolar H^+-pyrophosphatase of mung bean with peptide antibodies. *J.Biochem.* **122,** 883-9

201. Bandani, A.R., Amiri, B., Butt, T.M., and Gordon-Weeks, R. (2001) Effects of efrapeptin and destruxin, metabolites of entomogenous fungi, on the hydrolytic activity of a vacuolar type ATPase identified on the brush border membrane vesicles of *Galleria mellonella* midgut and

on plant membrane bound hydrolytic enzymes. *Biochim.Biophys.Acta.* **1510,** 367-77

202. Matsuoka, K., Higuchi, T., Maeshima, M., and Nakamura, K. (1997) A vacuolar-type H^+-ATPase in a nonvacuolar organelle is required for the sorting of soluble vacuolar protein precursors in tobacco cells. *Plant Cell.* **9,** 533-46

203. White, P.J. (1994) Bafilomycin A1 is a non-competitive inhibitor of the tonoplast H^+-ATPase of maize coleoptiles. *J.Exp.Bot.* **45,** 1397-402

204. Hoffmann-Thoma, G., and Willenbrink, J. (1993) Differential Sensitivities towards Inhibitors and SH-Compounds of H^+-ATPase and H^+-Pyrophosphatase Associated with Intact Vacuoles from Sweet Sorghum (*Sorghum bicolor* [L.] Moench) Stem Parenchyma. *J.Plant Physiol.* **141,** 681-9

205. Okazaki, Y., Tazawa, M., Moriyama, Y., and Iwasaki, N. (1992) Bafilomycin Inhibits Vacuolar pH Regulation in a Fresh Water Charophyte, *Chara corallina. Botanica acta.* **105,** 421-6

206. Lai, S.P., Randall, S.K., and Sze, H. (1988) Peripheral and integral subunits of the tonoplast H^+-ATPase from oat roots. *J.Biol.Chem.* **263,** 16731-7

207. Nakayasu, T., Kawauchi, K., Hirata, H., and Shimmen, T. (1999) Cycloprodigiosin hydrochloride inhibits acidification of the plant vacuole. *Plant Cell Physiol.* **40,** 143-8

208. Pfeiffer, W. (1995) Effects of W-7, W-5, Verapamil and Diltiazem on vacuolar proton transport. Comparison of vacuolar H^+-ATPase and H^+-PPase from roots of *Zea mays. Physiol.Plantarum.* **94,** 284-90

209. Colombo, R., Cerana, R., and Lado, P. (1991) Effect of penconazole and flusilazol on the tonoplast of *Acer pseudoplatanus* cells. *Plant science.* **76,** 167-74

210. Strid, A., Nore, B.F., Nyren, P., and Baltscheffsky, M. (1987) Diethylstilbestrol is a potent inhibitor of the H^+-PPase but not of the H^+-ATPase of *Rhodospirillum rubrum* chromatophores. *Biochim.Biophys. Acta.* **892,** 236-44

211. Nurminsky, V.N., Ozolina, N.V., Sapega, J.G., Zheleznykh, A.O., Pradedova, E.V., Korzun, A.M., and Salyaev, R.K. (2009) The effect of dihydroquercetin on active and passive ion transport systems in plant vacuolar membrane. *Biology bulletin of the Russian Academy of Sciences.* **36,** 1-5

212. Pan, Y.J., Lee, C.H., Hsu, S.H., Huang, Y.T., Lee, C.H., Liu, T.H., Chen, Y.W., Lin, S.M., and Pan, R.L. (2011) The transmembrane domain 6 of vacuolar H^+-pyrophosphatase mediates protein targeting and proton transport. *Biochim.Biophys.Acta.* **1807,** 59-67

213. Lee, C.H., Chen, Y.W., Huang, Y.T., Pan, Y.J., Lee, C.H., Lin, S.M., Huang, L.K., Lo, Y.Y., Huang, Y.F., Hsu, Y.D., Yen, S.C., Hwang, J.K., and Pan, R.L. (2013) Functional Investigation of Transmembrane Helix 3 in H^+-Translocating Pyrophosphatase. *J.Membr.Biol.* **246,** 959-66

214. Schultz, A., and Baltscheffsky, M. (2003) Properties of mutated *Rhodospirillum rubrum* H^+-pyrophosphatase expressed in *Escherichia coli. Biochim.Biophys.Acta.* **1607,** 141-51

215. Mimura, H., Nakanishi, Y., and Maeshima, M. (2005) Disulfide-bond formation in the H^+-pyrophosphatase of *Streptomyces coelicolor* and its implications for redox control and enzyme structure. *FEBS Lett.* **579,** 3625-31

216. Hirono, M., Nakanishi, Y., and Maeshima, M. (2007) Essential amino acid residues in the central transmembrane domains and loops for energy coupling of *Streptomyces coelicolor* A3(2) H^+-pyrophosphatase. *Biochim.Biophys.Acta.* **1767,** 930-9

217. Huang, G., Bartlett, P.J., Thomas, A.P., Moreno, S.N., and Docampo, R. (2013) Acidocalcisomes of *Trypanosoma brucei* have an inositol 1,4,5-trisphosphate receptor that is required for growth and infectivity. *Proc.Natl.Acad.Sci.U.S.A.* **110,** 1887-92

218. Hsiao, Y.Y., Pan, Y.J., Hsu, S.H., Huang, Y.T., Liu, T.H., Lee, C.H., Lee, C.H., Liu, P.F., Chang, W.C., Wang, Y.K., Chien, L.F., and Pan, R.L. (2007) Functional roles of arginine residues in mung bean vacuolar H^+-pyrophosphatase. *Biochim.Biophys.Acta.* **1767,** 965-73

219. Zancani, M., Skiera, L.A., and Sanders, D. (2007) Roles of basic residues and salt-bridge interaction in a vacuolar H^+-pumping pyrophosphatase (AVP1) from *Arabidopsis thaliana. Biochim.Biophys.Acta.* **1768,** 311-6

220. Asaoka, M., Segami, S., and Maeshima, M. (2014) Identification of the critical residues for the function of vacuolar H^+-pyrophosphatase by mutational analysis based on the 3D structure. *J Biochem.* **156,** 333-44

221. Nakanishi, Y., Saijo, T., Wada, Y., and Maeshima, M. (2001) Mutagenic analysis of functional residues in putative substrate-binding site and acidic domains of vacuolar H^+-pyrophosphatase. *J.Biol.Chem.* **276,** 7654-60

222. Zhen, R.G., Kim, E.J., and Rea, P.A. (1997) Acidic residues necessary for pyrophosphate-energized pumping and inhibition of the vacuolar H^+-pyrophosphatase by *N,N'*-dicyclohexylcarbodiimide. *J.Biol.Chem.* **272,** 22340-8

223. Belogurov, G.A., Turkina, M.V., Penttinen, A., Huopalahti, S., Baykov, A.A., and Lahti, R. (2002) H^+-pyrophosphatase of *Rhodospirillum rubrum*. High yield expression in *Escherichia coli* and identification of the Cys residues responsible for inactivation by mersalyl. *J.Biol.Chem.* **277,** 22209-14

224. Malinen, A.M., Belogurov, G.A., Salminen, M., Baykov, A.A., and Lahti, R. (2004) Elucidating the role of conserved glutamates in H^+-pyrophosphatase of *Rhodospirillum rubrum. J. Biol. Chem.* **279,** 26811-6

225. Hirono, M., Nakanishi, Y., and Maeshima, M. (2007) Identification of amino acid residues participating in the energy coupling and proton transport of *Streptomyces coelicolor* A3(2) H^+-pyrophosphatase. *Biochim.Biophys.Acta.* **1767,** 1401-11

226. Serrano, A., Perez-Castineira, J., Baltscheffsky, H., and Baltscheffsky, M. (2004) Proton-pumping inorganic pyrophosphatases in some archaea and other extremophilic prokaryotes. *J.Bioenerg.Biomembr.* **36,** 127-33

227. Miroux, B., and Walker, J.E. (1996) Over-production of proteins in *Escherichia coli*: mutant hosts that allow synthesis of some membrane proteins and globular proteins at high levels. *J.Mol.Biol.* **260,** 289-98

228. Mimura, H., Nakanishi, Y., Hirono, M., and Maeshima, M. (2004) Membrane topology of the H^+-pyrophosphatase of *Streptomyces coelicolor* determined by cysteine-scanning mutagenesis. *J.Biol.Chem.* **279,** 35106-12

229. Kellosalo, J., Kajander, T., Palmgren, M.G., Lopéz-Marqués, R.L., and Goldman, A. (2011) Heterologous expression and purification of membrane-bound pyrophosphatases. *Protein Expr.Purif.* **79,** 25-34

230. Drozdowicz, Y.M., Shaw, M., Nishi, M., Striepen, B., Liwinski, H.A., Roos, D.S., and Rea, P.A. (2003) Isolation and characterization of TgVP1, a type I vacuolar H^+-translocating pyrophosphatase from *Toxoplasma gondii*. The dynamics of its subcellular localization and the cellular effects of a diphosphonate inhibitor. *J.Biol.Chem.* **278,** 1075-85

231. Ikeda, M., Umami, K., Hinohara, M., Tanimura, Y., Ohmae, A., Nakanishi, Y., and Maeshima, M. (2002) Functional expression of *Acetabularia acetabulum* vacuolar H^+-pyrophosphatase in a yeast VMA3-deficient strain. *J.Exp.Bot.* **53,** 2273-5

232. Drake, R., Serrano, A., and Perez-Castineira, J.R. (2010) N-terminal chimaeras with signal sequences enhance the functional expression and alter the subcellular localization of heterologous membrane-bound inorganic pyrophosphatases in yeast. *Biochem.J.* **426,** 147-57

233. Baltscheffsky, M., and Nyrén, P. (1986) Preparation and reconstitution of the proton-pumping membrane-bound inorganic pyrophosphatase from *Rhodospirillum rubrum*. *Meth.Enzymol.* **126,** 538-45

234. Nyrén, P., Hajnal, K., and Baltscheffsky, M. (1984) Purification of the membrane-bound proton-translocating inorganic pyrophosphatase from *Rhodospirillum rubrum. Biochim.Biophys.Acta.* **766,** 630-5

235. Baltscheffsky, M., and Nyrén, P. (1984) Membrane-bound inorganic pyrophosphatase. *Prog.Clin.Biol.Res.* **164,** 199-207

236. Nakamura, Y., Sakakibara, Y., Kobayashi, H., and Kasamo, K. (1997) Rapid reconstitution of tonoplast H^+-translocating pyrophosphatase from cultured rice cells into liposomes. *Plant Cell Physiol.* **38,** 371-4

237. Rao, P.V., and Keister, D.L. (1978) Energy-linked reactions in photosynthetic bacteria. X. Solubilization of the membrane-bound energy-linked inorganic pyrophosphatase of *Rhodospirillum rubrum. Biochem.Biophys.Res.Commun.* **84,** 465-73

238. Suzuki, Y., Kanayama, Y., Shiratake, K., and Yamaki, S. (1999) Vacuolar H^+-pyrophosphatase purified from pear fruit. *Phytochemistry.* **50,** 535-9

239. Perotti, E., and Chanson, A. (1993) Reconstitution into Liposomes of the Tonoplast ATP- and Pyrophosphate-Dependent Proton Pumps from *Rubus hispidus* Cell Cultures. *Botanica Acta.* **106,** 193-6

240. Nicholson, D.W., and McMurray, W.C. (1986) Triton solubilization of proteins from pig liver mitochondrial membranes. *Biochim.Biophys. Acta.* **856,** 515-25

241. Suzuki, Y., Maeshima, M., and Yamaki, S. (1999) Molecular cloning of vacuolar H^+-pyrophosphatase and its expression during the development of pear fruit. *Plant Cell Physiol.* **40,** 900-4

242. Becker, A., Canut, H., Lüttge, U., Maeshima, M., Marigo, G., and Ratajczak, R. (1995) Purification and immunological comparison of the tonoplast H^+-pyrophosphatase from cells of *Catharanthus roseus* and leaves from *Mesembryanthemum crystallinum* performing C3-photosynthesis and the obligate CAM-plant *Kalanchoe daigremontiana. J.Plant Physiol.* **146,** 88-94

243. Perotti, E., Gavin, O., Widmer, F., and Chanson, A. (1994) Purification and functional reconstitution of the tonoplast pyrophosphate-dependent proton pump from *Rubus hispidus* cell cultures. *Plant science.* **103,** 25-31

244. Drozdowicz, Y.M., and Rea, P.A. (2001) Vacuolar H^+ pyrophosphatases: from the evolutionary backwaters into the mainstream. *Trends Plant Sci.* **6,** 206-11

245. Seufferheld, M., Vieira, M.C., Ruiz, F.A., Rodrigues, C.O., Moreno, S.N., and Docampo, R. (2003) Identification of organelles in bacteria similar to acidocalcisomes of unicellular eukaryotes. *J.Biol.Chem.* **278,** 29971-8

246. Fang, J., Rohloff, P., Miranda, K., and Docampo, R. (2007) Ablation of a small transmembrane protein of *Trypanosoma brucei* (TbVTC1) involved in the synthesis of polyphosphate alters acidocalcisome biogenesis and function, and leads to a cytokinesis defect. *Biochem.J.* **407,** 161-70

247. Besteiro, S., Tonn, D., Tetley, L., Coombs, G.H., and Mottram, J.C. (2008) The AP3 adaptor is involved in the transport of membrane proteins to acidocalcisomes of *Leishmania. J.Cell.Sci.* **121,** 561-70

248. Huang, G., Fang, J., Sant'Anna, C., Li, Z.H., Wellems, D.L., Rohloff, P., and Docampo, R. (2011) Adaptor protein-3 (AP-3) complex mediates the biogenesis of acidocalcisomes and is essential for growth and virulence of *Trypanosoma brucei. J.Biol.Chem.* **286,** 36619-30

249. Luo, S., Marchesini, N., Moreno, S.N., and Docampo, R. (1999) A plant-like vacuolar H^+-pyrophosphatase in *Plasmodium falciparum. FEBS Lett.* **460,** 217-20

250. Rodrigues, C.O., Scott, D.A., Bailey, B.N., De Souza, W., Benchimol, M., Moreno, B., Urbina, J.A., Oldfield, E., and Moreno, S.N. (2000) Vacuolar proton pyrophosphatase activity and pyrophosphate (PP_i) in *Toxoplasma gondii* as possible chemotherapeutic targets. *Biochem.J.* **349,** 737-45

251. Sen, S.S., Bhuyan, N.R., Lakshman, K., Roy, A.K., Chakraborty, B., and Bera, T. (2009) Membrane bound pyrophosphatase and P-type adenosine triphosphatase of *Leishmania donovani* as possible chemotherapeutic targets: similarities and differences in inhibitor sensitivities. *Biochemistry (Mosc).* **74,** 1382-7

252. MacDonald, J.I., and Weeks, G. (1988) Evidence for a membrane-bound pyrophosphatase in *Dictyostelium discoideum. FEBS Lett.* **238,** 9-12

253. McIntosh, M.T., and Vaidya, A.B. (2002) Vacuolar type H^+ pumping pyrophosphatases of parasitic protozoa. *Int.J.Parasitol.* **32,** 1-14

254. Rodrigues, C.O., Scott, D.A., and Docampo, R. (1999) Presence of a vacuolar H^+-pyrophosphatase in promastigotes of *Leishmania donovani* and its localization to a different compartment from the vacuolar H^+-ATPase. *Biochem.J.* **340,** 759-66

255. Ruiz, F.A., Marchesini, N., Seufferheld, M., Govindjee, and Docampo, R. (2001) The polyphosphate bodies of *Chlamydomonas reinhardtii* possess a proton-pumping pyrophosphatase and are similar to acidocalcisomes. *J.Biol.Chem.* **276,** 46196-203

256. Robinson, D.G., Hoppenrath, M., Oberbeck, K., Luykx, P., and Ratajczak, R. (1998) Localization of pyrophosphatase and V-ATPase in *Chlamydomonas reinhardtii. Botanica acta.* **111,** 108-22

257. Kanehisa, M., and Goto, S. (2000) KEGG: kyoto encyclopedia of genes and genomes. *Nucleic Acids Res.* **28,** 27-30

258. Kanehisa, M., Goto, S., Sato, Y., Kawashima, M., Furumichi, M., and Tanabe, M. (2014) Data, information, knowledge and principle: back to metabolism in KEGG. *Nucleic Acids Res.* **42,** D199-205

259. Mitsuda, N., Enami, K., Nakata, M., Takeyasu, K., and Sato, M.H. (2001) Novel type *Arabidopsis thaliana* H^+-PPase is localized to the Golgi apparatus. *FEBS Lett.* **488,** 29-33

260. Shimaoka, T., Ohnishi, M., Sazuka, T., Mitsuhashi, N., Hara-Nishimura, I., Shimazaki, K., Maeshima, M., Yokota, A., Tomizawa, K., and Mimura, T. (2004) Isolation of intact vacuoles and proteomic analysis of tonoplast from suspension-cultured cells of *Arabidopsis thaliana. Plant Cell Physiol.* **45,** 672-83

261. Ellis, C.M., Ford, R.C., and Holzenburg, A. (1992) Detergent sensitivity of the tonoplast H^+-ATPase and its purification from *Beta vulgaris.. Biochim.Biophys.Acta.* **1136,** 319-26

262. Ni, M., and Beevers, L. (1991) Characterization of tonoplast polypeptides isolated from corn seedling roots. *Plant Physiol.* **97,** 264-72

263. Scherer, G.F., Vom Dorp, B., Schöllmann, C., and Volkmann, D. (1992) Proton-transport activity, sidedness, and morphometry of tonoplast and plasma-membrane vesicles purified by free-flow electrophoresis from roots of *Lepidium sativum* L. and hypocotyls of *Cucurbita pep*o L. *Planta.* **186,** 483-94

264. Hamamoto, S., Marui, J., Matsuoka, K., Higashi, K., Igarashi, K., Nakagawa, T., Kuroda, T., Mori, Y., Murata, Y., Nakanishi, Y., Maeshima, M., Yabe, I., and Uozumi, N. (2008) Characterization of a tobacco TPK-type K^+ channel as a novel tonoplast K^+ channel using yeast tonoplasts. *J.Biol.Chem.* **283,** 1911-20

265. Barkla, B.J., Vera-Estrella, R., and Pantoja, O. (2007) Enhanced separation of membranes during free flow zonal electrophoresis in plants. *Anal.Chem.* **79,** 5181-7

266. Liu, G., Sánchez-Fernández, R., Li, Z.S., and Rea, P.A. (2001) Enhanced multispecificity of arabidopsis vacuolar multidrug resistance-associated protein-type ATP-binding cassette transporter, AtMRP2. *J.Biol.Chem.* **276,** 8648-56

267. Sato, M.H., Nakamura, N., Ohsumi, Y., Kouchi, H., Kondo, M., Hara-Nishimura, I., Nishimura, M., and Wada, Y. (1997) The AtVAM3 encodes a syntaxin-related molecule implicated in the vacuolar assembly in *Arabidopsis thaliana. J.Biol.Chem.* **272,** 24530-5

268. Martinec, J., Feltl, T., Scanlon, C.H., Lumsden, P.J., and Macháckova, I. (2000) Subcellular localization of a high affinity binding site for D-myo-inositol 1,4,5-trisphosphate from *Chenopodium rubrum. Plant Physiol.* **124,** 475-83

269. Maeshima, M. (1992) Characterization of the major integral protein of vacuolar membrane. *Plant Physiol.* **98,** 1248-54

270. Sánchez-Nieto, S., García-Rubio, O., Pacheco-Moisés, F., Carballo, A., Rodríguez-Sotres, R., and Gavilanes-Ruíz, M. (1997) Purification of plasma membranes from dry maize embryos. *Physiol.Plantarum.* **101,** 157-64

271. Toll, E., Castillo, F.J., Crespi, P., Crevecoeur, M., and Greppin, H. (1995) Purification of plasma membranes from leaves of conifer and deciduous tree species by phase partitioning and free-flow electrophoresis. *Physiol. Plantarum.* **95,** 399-408

272. Paez-Valencia, J., Patron-Soberano, A., Rodriguez-Leviz, A., Sanchez-Lares, J., Sanchez-Gomez, C., Valencia-Mayoral, P., Diaz-Rosas, G., and Gaxiola, R. (2011) Plasma membrane localization of the type I H(+)-PPase AVP1 in sieve element-companion cell complexes from *Arabidopsis thaliana. Plant Sci.* **181,** 23-30

273. Siebers, B., Zaparty, M., Raddatz, G., Tjaden, B., Albers, S.V., Bell, S.D., Blombach, F., Kletzin, A., Kyrpides, N., Lanz, C., Plagens, A., Rampp, M., Rosinus, A., von Jan, M., Makarova, K.S., Klenk, H.P., Schuster, S.C., and Hensel, R. (2011) The complete genome sequence of *Thermoproteus tenax*: a physiologically versatile member of the Crenarchaeota. *PLoS One.* **6,** e24222

274. Schöcke, L., and Schink, B. (1998) Membrane-bound proton-translocating pyrophosphatase of *Syntrophus gentianae*, a syntrophically benzoate-degrading fermenting bacterium. *Eur J Biochem.* **256,** 589-94

275. Schöcke, L., and Schink, B. (1999) Energetics and biochemistry of fermentative benzoate degradation by *Syntrophus gentianae. Arch. Microbiol.* **171,** 331-7

276. Moreno, S.N., and Docampo, R. (2009) The role of acidocalcisomes in parasitic protists. *J.Eukaryot.Microbiol.* **56,** 208-13

277. Miranda, K., de Souza, W., Plattner, H., Hentschel, J., Kawazoe, U., Fang, J., and Moreno, S.N. (2008) Acidocalcisomes in Apicomplexan parasites. *Exp.Parasitol.* **118,** 2-9

278. Beutler, M., Milucka, J., Hinck, S., Schreiber, F., Brock, J., Mussmann, M., Schulz-Vogt, H.N., and de Beer, D. (2012) Vacuolar respiration of nitrate coupled to energy conservation in filamentous Beggiatoaceae. *Environ.Microbiol.* **14,** 2911-9

279. Sieber, J.R., Sims, D.R., Han, C., Kim, E., Lykidis, A., Lapidus, A.L., McDonnald, E., Rohlin, L., Culley, D.E., Gunsalus, R., and McInerney, M.J. (2010) The genome of *Syntrophomonas wolfei*: new insights into

syntrophic metabolism and biohydrogen production. *Environ.Microbiol.* **12,** 2289-301

280. García-Contreras, R., Celis, H., and Romero, I. (2004) Importance of *Rhodospirillum rubrum* H^+-pyrophosphatase under low-energy conditions. *J.Bacteriol.* **186,** 6651-5

281. Bäumer, S., Lentes, S., Gottschalk, G., and Deppenmeier, U. (2002) Identification and analysis of proton-translocating pyrophosphatases in the methanogenic archaeon *Methansarcina mazei*. *Archaea.* **1,** 1-7

282. Deppenmeier, U., Johann, A., Hartsch, T., Merkl, R., Schmitz, R.A., Martinez-Arias, R., Henne, A., Wiezer, A., Bäumer, S., Jacobi, C., Brüggemann, H., Lienard, T., Christmann, A., Bömeke, M., Steckel, S., Bhattacharyya, A., Lykidis, A., Overbeek, R., Klenk, H.P., Gunsalus, R.P., Fritz, H.J., and Gottschalk, G. (2002) The genome of *Methanosarcina mazei*: evidence for lateral gene transfer between bacteria and archaea. *J.Mol.Microbiol.Biotechnol.* **4,** 453-61

283. López-Marqués, R.L., Pérez-Castiñeira, J.R., Losada, M., and Serrano, A. (2004) Differential regulation of soluble and membrane-bound inorganic pyrophosphatases in the photosynthetic bacterium *Rhodospirillum rubrum* provides insights into pyrophosphate-based stress bioenergetics. *J.Bacteriol.* **186,** 5418-26

284. Klemme, J.H., and Gest, H. (1971) Regulatory properties of an inorganic pyrophosphatase from the photosynthic bacterium *Rhodospirillum rubrum. Proc.Natl.Acad.Sci.U.S.A.* **68,** 721-5

285. Romero, I., García-Contreras, R., and Celis, H. (2003) *Rhodospirillum rubrum* has a family I pyrophosphatase: purification, cloning, and sequencing. *Arch.Microbiol.* **179,** 377-80

286. Sosa, A., and Celis, H. (1993) Surface charge modifications do not affect the hydrolytic activity of membrane-bound pyrophosphatase of *Rhodospirillum rubrum. Biochem.Mol.Biol.Int.* **30,** 1135-41

287. Sarafian, V., Kim, Y., Poole, R.J., and Rea, P., A. (1992) Molecular cloning and sequence of cDNA encoding the pyrophosphate-energized vacuolar membrane proton pump of *Arabidopsis thaliana. Proc.Natl. Acad.Sci.U.S.A.* **89,** 1775-9

288. Marsh, K., González, P., and Echeverría, E. (2001) Partial characterization of H^+-translocating inorganic pyrophosphatase from 3 citrus varieties differing in vacuolar pH. *Physiol.Plantarum.* **111,** 519-26

289. Marsh, K., Gonzalez, P., and Echeverria, E. (2000) PP_i formation by reversal of the tonoplast-bound H^+-pyrophosphatase from 'Valencia' orange juice cells. *J.Am.Soc.Hort.Sci.* **125,** 420-4

290. Rea, P.A., and Poole, R.J. (1993) Vacuolar H^+-translocating pyrophosphatase. *Annu. Rev. Plant Physiol. Plant Mol. Biol.* **44,** 157-80

291. Kaestner, K.H., and Sze, H. (1987) Potential-dependent anion transport in tonoplast vesicles from oat roots. *Plant Physiol.* **83,** 483-9

292. Li, Z.S., Zhao, Y., and Rea, P.A. (1995) Magnesium Adenosine 5[prime]-Triphosphate-Energized Transport of Glutathione-S-Conjugates by Plant Vacuolar Membrane Vesicles. *Plant Physiol.* **107,** 1257-68

293. Schmidt, U.G., Endler, A., Schelbert, S., Brunner, A., Schnell, M., Neuhaus, H.E., Marty-Mazars, D., Marty, F., Baginsky, S., and Martinoia, E. (2007) Novel tonoplast transporters identified using a proteomic approach with vacuoles isolated from cauliflower buds. *Plant Physiol.* **145,** 216-29

294. Hasegawa, P.M. (2013) Sodium (Na^+) homeostasis and salt tolerance of plants. *Environ.Exp.Bot.* **92,** 19-31

295. Maeshima, M. (2001) Tonoplast transporters: organization and function. *Annu.Rev.Plant Physiol.Plant Mol.Biol.* **52,** 469-97

296. Maeshima, M., Nakanishi, Y., Matsuura-Endo, C., and Tanaka, Y. (1996) Proton pumps of the vacuolar membrane in growing plant cells. *J.Plant Res.* **109,** 119-25

297. Martinoia, E. (1992) Transport processes in vacuoles of higher plants. *Botanica acta.* **105,** 232-45

298. Gaxiola, R.A., Palmgren, M.G., and Schumacher, K. (2007) Plant proton pumps. *FEBS Lett.* **581,** 2204-2214

299. Davies, J.M. (1997) Vacuolar energization: Pumps, shunts and stress. *J.Exp.Bot.* **48,** 633-41

300. Yoshida, K., Ohnishi, M., Fukao, Y., Okazaki, Y., Fujiwara, M., Song, C., Nakanishi, Y., Saito, K., Shimmen, T., Suzaki, T., Hayashi, F., Fukaki, H., Maeshima, M., and Mimura, T. (2013) Studies on vacuolar membrane microdomains isolated from Arabidopsis suspension-cultured cells: local distribution of vacuolar membrane proteins. *Plant Cell Physiol.* **54,** 1571-84

301. Zingarelli, L., Anzani, P., and Lado, P. (1994) Enhanced K^+-stimulated pyrophosphatase activity in NaCl-adapted cells of *Acer pseudoplatanus*. *Physiol.Plantarum.* **91,** 510-6

302. Bolte, S., Lanquar, V., Soler, M.N., Beebo, A., Satiat-Jeunemaître, B., Bouhidel, K., and Thomine, S. (2011) Distinct lytic vacuolar compartments are embedded inside the protein storage vacuole of dry and germinating *Arabidopsis thaliana* seeds. *Plant Cell Physiol.* **52,** 1142-52

303. Jauh, G.Y., Phillips, T.E., and Rogers, J.C. (1999) Tonoplast intrinsic protein isoforms as markers for vacuolar functions. *Plant Cell.* **11,** 1867-82

304. Mimura, T., Ohnishi, M., Shimaoka, T., and Tomizawa, K. (2009) Proteomic analysis of the vacuolar membrane. *Plant Membrane and Vacuolar Transporters.* 301-43

305. Jiang, L., Phillips, T.E., Hamm, C.A., Drozdowicz, Y.M., Rea, P.A., Maeshima, M., Rogers, S.W., and Rogers, J.C. (2001) The protein storage vacuole: a unique compound organelle. *J.Cell Biol.* **155,** 991-1002

306. Hoh, B., Hinz, G., Jeong, B.K., and Robinson, D.G. (1995) Protein storage vacuoles form de novo during pea cotyledon development. *J.Cell.Sci.* **108,** 299-310

307. Tse, Y.C., Wang, J., Miao, Y., and Jiang, L. (2007) Biogenesis of the compound seed protein storage vacuole. *Seeds.* 112-9

308. Oberbeck, K., Drucker, M., and Robinson, D.G. (1994) V-type ATPase and pyrophosphatase in endomembranes of maize roots. *J.Exp.Bot.* **45,** 235-44

309. Viotti, C., Krüger, F., Krebs, M., Neubert, C., Fink, F., Lupanga, U., Scheuring, D., Boutté, Y., Frescatada-Rosa, M., Wolfenstetter, S., Sauer, N., Hillmer, S., Grebe, M., and Schumacher, K. (2013) The endoplasmic reticulum is the main membrane source for biogenesis of the lytic vacuole in *Arabidopsis*. *Plant Cell.* **25,** 3434-49

310. Ratajczak, R., Kemna, I., and Lüttge, U. (1994) Characteristics, partial purification and reconstitution of the vacuolar malate transporter of the CAM plant *Kalanchoe daigremontiana* Hamet et Perrier de la Bâthie. *Planta.* **195,** 226-36

311. Carqueijeiro, I., Noronha, H., Duarte, P., Gerós, H., and Sottomayor, M. (2013) Vacuolar transport of the medicinal alkaloids from *Catharanthus roseus* is mediated by a proton-driven antiport. *Plant Physiol.* **162,** 1486-96

312. Iwasaki, I., Arata, H., Kijima, H., and Nishimura, M. (1992) Two Types of Channels Involved in the Malate Ion Transport across the Tonoplast of a Crassulacean Acid Metabolism Plant. *Plant Physiol.* **98,** 1494-7

313. Szakiel, A., and Janiszowska, W. (2002) The mechanism of oleanolic acid monoglycosides transport into vacuoles isolated from *Calendula officinalis* leaf protoplasts. *Plant physiology and biochemistry.* **40,** 203-9

314. Fuglsang, A.T., Paez Valencia, J., and Gaxiola, R.A. (2011) Plant Proton Pumps: Regulatory Circuits Involving H^+-ATPase and H^+-PPase. *Signaling and Communication in Plants.* **7,** 39-64

315. Chanson, A. (1991) A Ca^{2+}/H^+ Antiport System Driven by the Tonoplast Pyrophosphate-Dependent Proton Pump from Maize Roots. *J.Plant Physiol.* **137,** 471-6

316. Kabala, K., Janicka-Russak, M., Reda, M., and Migocka, M. (2013) Transcriptional regulation of the V-ATPase subunit c and V-PPase isoforms in *Cucumis sativus* under heavy metal stress. *Physiol.Plant.* **150,** 32-45

317. Kawachi, M., Kobae, Y., Kogawa, S., Mimura, T., Krämer, U., and Maeshima, M. (2012) Amino acid screening based on structural modeling identifies critical residues for the function, ion selectivity and structure of *Arabidopsis* MTP1. *FEBS J.* **279,** 2339-56

318. Kawachi, M., Kobae, Y., Mimura, T., and Maeshima, M. (2008) Deletion of a histidine-rich loop of AtMTP1, a vacuolar Zn^{2+}/H^+ antiporter of *Arabidopsis thaliana*, stimulates the transport activity. *J.Biol.Chem.* **283,** 8374-83

319. Langhans, M., Ratajczak, R., Lützelschwab, M., Michalke, W., Wächter, R., Fischer-Schliebs, E., and Ullrich, C.I. (2001) Immunolocalization of plasma-membrane H^+-ATPase and tonoplast-type pyrophosphatase in the plasma membrane of the sieve element-companion cell complex in the stem of *Ricinus communis* L. *Planta.* **213,** 11-9

320. Davies, J.M., Poole, R.J., Rea, P.A., and Sanders, D. (1992) Potassium transport into plant vacuoles energized directly by a proton-pumping inorganic pyrophosphatase. *Proc.Natl.Acad.Sci.U.S.A.* **89,** 11701-5

321. Amemiya, T., Kawai, Y., Yarnaki, S., and Shiratake, K. (2005) Enhancement of vacuolar H^+-ATPase and H^+-pyrophosphatase expression by phytohormones in pear fruit. *J. Japan. Soc. Hort. Sci.* **74,** 353-60

322. Pfeiffer, W. (1998) Differential energization of the tonoplast in suspension cells and seedlings from *Picea abies. Trees.* **13,** 112-6

323. Kasai, M., Sasaki, M., Yamamoto, Y., and Matsumoto, H. (1993) *In vivo* Treatments That Modulate PP_i-Dependent H^+ Transport Activity of Tonoplast-Enriched Membrane Vesicles from Barley Roots. *Plant Cell Physiol.* **34,** 549-55

324. White, P.J., and Smith, A.C. (1992) Malate-Dependent Proton Transport in Tonoplast Vesicles Isolated from Orchid Leaves Correlates with the Expression of Crassulacean Acid Metabolism. *J.Plant Physiol.* **139,** 533-8

325. Pope, A.J., and Leigh, R.A. (1987) Some characteristics of anion transport at the tonoplast of oat roots, determined from the effects of anions on pyrophosphatedependent proton transport. *Planta.* **172,** 91-100

326. Ballesteros, E., Donaire, J.P., and Belver, A. (1996) Effects of salt stress on H^+-ATPase and H^+-PPase activities of tonoplast-enriched vesicles isolated from sunflower roots. *Physiol.Plantarum.* **97,** 259-68

327. Schumacher, K. (2006) Endomembrane proton pumps: connecting membrane and vesicle transport. *Curr.Opin.Plant Biol.* **9,** 595-600

328. Barkla, B.J., and Pantoja, O. (1996) Physiology of ion transport across the tonoplast of higher plants. *Annu.Rev.Plant Physiol.Plant Mol.Biol.* **47,** 159-84

329. Li, J., Yang, H., Peer, W.A., Richter, G., Blakeslee, J., Bandyopadhyay, A., Titapiwantakun, B., Undurraga, S., Khodakovskaya, M., Richards, E.L., Krizek, B., Murphy, A.S., Gilroy, S., and Gaxiola, R. (2005) *Arabidopsis* H^+-PPase AVP1 regulates auxin-mediated organ development. *Science.* **310,** 121-5

330. Harada, T., Satoh, S., Yoshioka, T., and Ishizawa, K. (2007) Anoxia-enhanced expression of genes isolated by suppression subtractive hybridization from pondweed (*Potamogeton distinctus* A. Benn.) turions. *Planta.* **226,** 1041-52

331. Brauer, D., Conner, D., and Tu, S.I. (1992) Effects of pH on proton transport by vacuolar pumps from maize roots. *Physiol.Plantarum.* **86,** 63-70

332. Verweij, W., Spelt, C., Di Sansebastiano, G.P., Vermeer, J., Reale, L., Ferranti, F., Koes, R., and Quattrocchio, F. (2008) An H^+-P-ATPase on the tonoplast determines vacuolar pH and flower colour. *Nat.Cell Biol.* **10,** 1456-62

333. Faraco, M., Spelt, C., Bliek, M., Verweij, W., Hoshino, A., Espen, L., Prinsi, B., Jaarsma, R., Tarhan, E., de Boer, A.H., Di Sansebastiano, G.P., Koes, R., and Quattrocchio, F.M. (2014) Hyperacidification of Vacuoles by the Combined Action of Two Different P-ATPases in the Tonoplast Determines Flower Color. *Cell Rep.* **6,** 32-43

334. Ward, J.M., and Sze, H. (1992) Subunit Composition and Organization of the Vacuolar H-ATPase from Oat Roots. *Plant Physiol.* **99,** 170-9

335. Brune, A., Muller, M., Taiz, L., Gonzalez, P., and Etxeberria, E. (2002) Vacuolar acidification in citrus fruit: Comparison between acid lime (*Citrus aurantifolia*) and sweet lime (*Citrus limmetioides*) juice cells. *J.Am.Soc.Hort.Sci.* **127,** 171-7

336. An, C.I., Fukusaki, E., and Kobayashi, A. (2001) Plasma-membrane H^+-ATPases are expressed in pitchers of the carnivorous plant *Nepenthes alata* Blanco. *Planta.* **212,** 547-55

337. Rybchenko, Z., and Palladina, T.O. (2012) [The action of adaptogenic preparations on vacuolar proton pumps activity in corn root cells under salt stress conditions]. *Ukr Biokhim Zh.* **84,** 88-94

338. Muto, Y., Segami, S., Hayashi, H., Sakurai, J., Murai-Hatano, M., Hattori, Y., Ashikari, M., and Maeshima, M. (2011) Vacuolar proton pumps and aquaporins involved in rapid internode elongation of deepwater rice. *Biosci.Biotechnol.Biochem.* **75,** 114-22

339. Yu, B.J., Lam, H.M., Shao, G.H., and Liu, Y.L. (2005) Effects of salinity on activities of H^+-ATPase, H^+-PPase and membrane lipid composition in plasma membrane and tonoplast vesicles isolated from soybean (*Glycine max* L.) seedlings. *J Environ Sci (China).* **17,** 259-62

340. Gordon-Weeks, R., Tong, Y., Davies, T., and Leggewie, G. (2003) Restricted spatial expression of a high-affinity phosphate transporter in potato roots. *J.Cell.Sci.* **116,** 3135-44

341. Terrier, N., Sauvage, F.X., Ageorges, A., and Romieu, C. (2001) Changes in acidity and in proton transport at the tonoplast of grape berries during development. *Planta.* **213,** 20-8

342. Newell, J.M., Leigh, R.A., and Hall, J.L. (1998) Vacuole development in cultured evacuolated oat mesophyll protoplasts. *J.Exp.Bot.* **49,** 817-27

343. Suzuki, Y., Shiratake, K., and Yamaki, S. (2000) Seasonal changes in the activities of vacuolar H^+-pumps and their gene expression in the developing Japanese pear fruit. *J. Japan. Soc. Hort. Sci.* **69,** 15-21

344. Shiratake, K., Hiroto, S., Yamaki, S., Kanayama, Y., and Maeshima, M. (2000) Changes in tonoplast and its proteins with the development of pear fruit. *Acta horticulturae.* **514,** 287-94

345. Terrier, N., Issaly, N., Sauvage, F., Ageorges, A., and Romieu, C. (2000) Aspects of grape berry development bioenergetics. *Acta horticulturae.* **526,** 331-8

346. Terrier, N., Deguilloux, C., Sauvage, F.X., Martinoia, E., and Romieu, C. (1998) Proton pumps and anion transport in *Vitis vinifera*: The inorganic pyrophosphatase plays a predominant role in the energization of the tonoplast. *Plant physiology and biochemistry.* **36,** 367-77

347. Milner, I.D., Ho, L.C., and Hall, J.L. (1995) Properties of proton and sugar transport at the tonoplast of tomato (*Lycopersicon esculentum*) fruit. *Physiol.Plantarum.* **94,** 399-410

348. McCarty, D., R., Keegstra, K., and Selman, B.R. (1984) Characterization and localization of the ATPase associated with pea chloroplast envelope membranes. *Plant Physiol.* **76,** 584-8

349. Darley, C.P., Skiera, L.A., Northrop, F.D., Sanders, D., and Davies, J.M. (1998) Tonoplast inorganic pyrophosphatase in *Vicia faba* guard cells. *Planta.* **206,** 272-7

350. Wisniewski, J.P., and Rogowsky, P.M. (2004) Vacuolar H^+-translocating inorganic pyrophosphatase (Vpp1) marks partial aleurone cell fate in cereal endosperm development. *Plant Mol.Biol.* **56,** 325-37

351. Segami, S., Makino, S., Miyake, A., Asaoka, M., and Maeshima, M. (2014) Dynamics of Vacuoles and H^+-Pyrophosphatase Visualized by Monomeric Green Fluorescent Protein in *Arabidopsis*: Artifactual Bulbs and Native Intravacuolar Spherical Structures. *Plant Cell.* **26,** 3416-34

352. Smart, L.B., Vojdani, F., Maeshima, M., and Wilkins, T.A. (1998) Genes involved in osmoregulation during turgor-driven cell expansion of developing cotton fibers are differentially regulated. *Plant Physiol.* **116,** 1539-49

353. Tsuchihira, A., Hanba, Y.T., Kato, N., Doi, T., Kawazu, T., and Maeshima, M. (2010) Effect of overexpression of radish plasma membrane aquaporins on water-use efficiency, photosynthesis and growth of Eucalyptus trees. *Tree Physiol.* **30,** 417-30

354. Maeshima, M., Hara-Nishimura, I., Takeuchi, Y., and Nishimura, M. (1994) Accumulation of Vacuolar H^+-Pyrophosphatase and H^+-ATPase during Reformation of the Central Vacuole in Germinating Pumpkin Seeds. *Plant Physiol.* **106,** 61-9

355. Krebs, M., Beyhl, D., Görlich, E., Al-Rasheid, K.A., Marten, I., Stierhof, Y.D., Hedrich, R., and Schumacher, K. (2010) Arabidopsis V-ATPase activity at the tonoplast is required for efficient nutrient storage but not for sodium accumulation. *Proc.Natl.Acad.Sci.U.S.A.* **107,** 3251-6

356. Pradedova, E.V., Ozolina, N.V., Salyaev, R.K., and Yushkevich, T.I. (1999) Dynamics of the hydrolytic activity of the tonoplast H^+-ATPase and H^+-pyrophosphatase in ontogenesis of red beetroot. *Doklady Akademii nauk.Rossijskaâ akademiâ nauk.* **364,** 835-8

357. Ueoka, H., and Hase, A. (1997) Tonoplast H^+ pumps are activated during callus formation of tuber tissues of Jerusalem artichoke (*Helianthus tuberosus*). *Physiol.Plantarum.* **100,** 91-101

358. Xiang, J.J., Zhang, G.H., Qian, Q., and Xue, H.W. (2012) Semi-rolled leaf1 encodes a putative glycosylphosphatidylinositol-anchored protein and modulates rice leaf rolling by regulating the formation of bulliform cells. *Plant Physiol.* **159,** 1488-500

359. Li, Y., Fan, C., Xing, Y., Yun, P., Luo, L., Yan, B., Peng, B., Xie, W., Wang, G., Li, X., Xiao, J., Xu, C., and He, Y. (2014) Chalk5 encodes a vacuolar H^+-translocating pyrophosphatase influencing grain chalkiness in rice. *Nat.Genet.* **46,** 398-404

360. Yoshida, K., Kawachi, M., Mori, M., Maeshima, M., Kondo, M., Nishimura, M., and Kondo, T. (2005) The involvement of tonoplast proton pumps and $Na^+(K^+)/H^+$ exchangers in the change of petal color during flower opening of Morning Glory, *Ipomoea tricolor* cv. Heavenly Blue. *Plant Cell Physiol.* **46,** 407-15

361. Suzuki, K., and Kasamo, K. (1993) Effects of aging on the ATP- and pyrophosphate-dependent pumping of protons across the tonoplast isolated from pumpkin cotyledons. *Plant Cell Physiol.* **34,** 613-9

362. Hsu, A.F.C., Rodenbach, S., and Tu, S.I. (1993) Separation of tonoplast vesicles enriched in atpase and pyrophosphatase activity from maize roots. *J.Plant Nutr.* **16,** 1179-92

363. Davies, J.M., Hunt, I., and Sanders, D. (1994) Vacuolar H^+-pumping ATPase variable transport coupling ratio controlled by pH. *Proc.Natl. Acad.Sci.U.S.A.* **91,** 8547-51

364. Kondoh, K., Koshiba, T., Hiraoka, A., and Sato, M. (1998) γ-irradiation damage to the tonoplast in cultured spinach cells. *Environ.Exp.Bot.* **39,** 97-104

365. Ozolina, N.V., Pradedova, E.V., Reutskaya, A.M., and Salyaev, R.K. (2000) Identification of auto-inhibitory domain in tonoplast H^+-ATPase. *Membr Cell Biol.* **17,** 238-40

366. Pérez-Castiñeira, J.R., Hernández, A., Drake, R., and Serrano, A. (2011) A plant proton-pumping inorganic pyrophosphatase functionally complements the vacuolar ATPase transport activity and confers bafilomycin resistance in yeast. *Biochem.J.* **437,** 269-78

367. Davies, J.M., Darley, C.P., and Sanders, D. (1997) Energetics of the plasma membrane pyrophosphatase. *Trends Plant Sci.* **2,** 9-10

368. Fischer-Schliebs, E., Ratajczak, R., Weber, P., Tavakoli, N., Ullrich, C.I., and Lüttge, U. (1998) Concordant time-dependent patterns of activities and enzyme protein amounts of V-PPase and V-ATPase in induced (flowering and CAM or tumour) and non-induced plant tissues. *Botanica acta.* **111,** 130-6

369. Macrì, F., Zancani, M., Petrussa, E., Dell'Antone, P., and Vianello, A. (1995) Pyrophosphate and H^+-pyrophosphatase maintain the vacuolar proton gradient in metabolic inhibitor-treated *Acer pseudoplatanus* cells. *Biochimica et Biophysica Acta.* **1229,** 323-8

370. Ohnishi, M., Mimura, T., Tsujimura, T., Mitsuhashi, N., Washitani-Nemoto, S., Maeshima, M., and Martinoia, E. (2007) Inorganic phosphate uptake in intact vacuoles isolated from suspension-cultured cells of *Catharanthus roseus* (L.) G. Don under varying P_i status. *Planta.* **225,** 711-8

371. Yang, H., Knapp, J., Koirala, P., Rajagopal, D., Peer, W.A., Silbart, L.K., Murphy, A., and Gaxiola, R.A. (2007) Enhanced phosphorus nutrition in monocots and dicots over-expressing a phosphorus-responsive type I H^+-pyrophosphatase. *Plant Biotechnol J.* **5,** 735-45

372. Gaxiola, R.A., Sanchez, C.A., Paez-Valencia, J., Ayre, B.G., and Elser, J.J. (2012) Genetic manipulation of a "vacuolar" H^+-PPase: from salt tolerance to yield enhancement under phosphorus-deficient soils. *Plant Physiol.* **159,** 3-11

373. Vicente, J.A., and Vale, M.G. (1991) Differentiation between Several Types of Phosphohydrolases in Light Microsomes of Corn Roots. *Plant Physiol.* **96,** 1345-53

374. Drozdowicz, Y.M., Kissinger, J.C., and Rea, P.A. (2000) AVP2, a sequence-divergent, K^+-insensitive H^+-translocating inorganic pyrophosphatase from *Arabidopsis. Plant Physiol.* **123,** 353-62

375. Choura, M., and Rebai, A. (2005) Identification and characterization of new members of vacuolar H^+-pyrophosphatase family from *Oryza sativa* genome. *Russian journal of plant physiology.* **52,** 821-5

376. Lerchl, J., König, S., Zrenner, R., and Sonnewald, U. (1995) Molecular cloning, characterization and expression analysis of isoforms encoding tonoplast-bound proton-translocating inorganic pyrophosphatase in tobacco. *Plant Mol.Biol.* **29,** 833-40

377. Wang, Y., Xu, H., Zhang, G., Zhu, H., Zhang, L., Zhang, Z., Zhang, C., and Ma, Z. (2009) Expression and responses to dehydration and salinity stresses of V-PPase gene members in wheat. *J Genet Genomics.* **36,** 711-20

378. Kranewitter, W., Gehwolf, R., Nagl, M., Pfeiffer, W., and Bentrup, F.W. (1999) Heterogeneity of the vacuolar pyrophosphatase protein from *Chenopodium rubrum. Protoplasma.* **209,** 68-76

379. Kim, Y., Kim, E.J., and Rea, P.A. (1994) Isolation and characterization of cDNAs encoding the vacuolar H^+-pyrophosphatase of *Beta vulgaris*. *Plant Physiol.* **106,** 375-82

380. Segami, S., Nakanishi, Y., Sato, M.H., and Maeshima, M. (2010) Quantification, Organ-Specific Accumulation and Intracellular Localization of Type II H -Pyrophosphatase in Arabidopsis thaliana. *Plant Cell Physiol.* **51,** 1350-60

381. Paez-Valencia, J., Sanchez-Lares, J., Marsh, E., Dorneles, L.T., Santos, M.P., Sanchez, D., Winter, A., Murphy, S., Cox, J., Trzaska, M., Metler, J., Kozic, A., Facanha, A.R., Schachtman, D., Sanchez, C.A., and Gaxiola, R.A. (2013) Enhanced proton translocating pyrophosphatase activity improves nitrogen use efficiency in romaine lettuce. *Plant Physiol.* **161,** 1557-69

382. Benderradji, L., Brini, F., Amar, S.B., Kellou, K., Azaza, J., Masmoudi, K., Bouzerzour, H., and Hanin, M. (2011) Sodium transport in the seedlings of two bread wheat (*Triticum aestivum* L.) genotypes showing contrasting salt stress tolerance. *Australian Journal of Crop Science.* **5,** 233-8

383. Hirata, T., Nakamura, N., Omote, H., Wada, Y., and Futai, M. (2000) Regulation and reversibility of vacuolar H^+-ATPase. *J.Biol.Chem.* **275,** 386-9

384. Blumwald, E., Aharon, G.S., and Apse, M.P. (2000) Sodium transport in plant cells. *Biochim.Biophys.Acta.* **1465,** 140-51

385. Qiu, Q.S., Guo, Y., Quintero, F.J., Pardo, J.M., Schumaker, K.S., and Zhu, J.K. (2004) Regulation of vacuolar Na^+/H^+ exchange in *Arabidopsis thaliana* by the salt-overly-sensitive (SOS) pathway. *J.Biol.Chem.* **279,** 207-15

386. Gaxiola, R.A., Li, J., Undurraga, S., Dang, L.M., Allen, G.J., Alper, S.L., and Fink, G.R. (2001) Drought- and salt-tolerant plants result from overexpression of the AVP1 H^+-pump. *Proc.Natl.Acad.Sci.U.S.A.* **98,** 11444-9

387. Colmes, T.D., and Fan, T.W.M. (1994) Interactions of Ca^{2+} and NaCl stress on the ion relations and intracellular pH of *Sorghum bicolor* root tips: An *in vivo*^{31}P-NMR study. *J.Exp.Bot.* **45,** 1037-44

388. Queirós, F., Fontes, N., Silva, P., Almeida, D., Maeshima, M., Gerós, H., and Fidalgo, F. (2009) Activity of tonoplast proton pumps and Na^+/H^+ exchange in potato cell cultures is modulated by salt. *J.Exp.Bot.* **60,** 1363-74

389. Fukuda, A., Yazaki, Y., Ishikawa, T., Koike, S., and Tanaka, Y. (1998) Na^+/H^+ antiporter in tonoplast vesicles from rice roots. *Plant Cell Physiol.* **39,** 196-201

390. Silva, P., Façanha, A.R., Tavares, R.M., and Gerós, H. (2010) Role of Tonoplast Proton Pumps and Na^+/H^+ Antiport System in Salt Tolerance of *Populus euphratica* Oliv. *J.Plant Growth Regul.* **29,** 23-34

391. Silva, P., and Gerós, H. (2009) Regulation by salt of vacuolar H^+-ATPase and H^+-pyrophosphatase activities and Na^+/H^+ exchange. *Plant Signal Behav.* **4,** 718-26

392. del Martínez-Ballesta, M.C., Silva, C., López-Berenguer, C., Cabañero, F.J., and Carvajal, M. (2006) Plant aquaporins: New perspectives on water and nutrient uptake in saline environment. *Plant Biol (Stuttg).* **8,** 535-46

393. Mansour, M.M.F., Salama, K.H.A., and Al-Mutawa, M.M. (2003) Transport proteins and salt tolerance in plants. *Plant science.* **164,** 891-900

394. Nakamura, Y., Ogawa, T., Kasamo, K., Sakata, M., and Ohta, E. (1992) Changes in the Cytoplasmic and Vacuolar pH in Intact Cells of Mung Bean Root-Tips under High-NaCl Stress at Different External Concentrations of Ca^{2+} Ions. *Plant Cell Physiol.* **33,** 849-58

395. Katsuhara, M., Kuchitsu, K., Takeshige, K., and Tazawa, M. (1989) Salt Stress-Induced Cytoplasmic Acidification and Vacuolar Alkalization in *Nitellopsis obtusa* Cells : *In Vivo* P-Nuclear Magnetic Resonance Study. *Plant Physiol.* **90,** 1102-7

396. Zhao, F.G., and Qin, P. (2004) Protective effect of exogenous polyamines on root tonoplast function against salt stress in barley seedlings. *Plant growth regulation.* **42,** 97-103

397. Undurraga, S.F., Santos, M.P., Paez-Valencia, J., Yang, H., Hepler, P.K., Facanha, A.R., Hirschi, K.D., and Gaxiola, R.A. (2012) *Arabidopsis* sodium dependent and independent phenotypes triggered by H^+-PPase up-regulation are SOS1 dependent. *Plant Sci.* **183,** 96-105

398. Bille, J., Weiser, T., and Bentrup, F.W. (1992) The lysolipid sphingosine modulates pyrophosphatase activity in tonoplast vesicles and isolated vacuoles from a heterotrophic cell suspension culture of *Chenopodium rubrum. Physiol.Plantarum.* **84,** 250-4

399. Xu, C.X., Liu, Y.L., Zheng, Q.S., and Liu, Z.P. (2006) Silicate improves growth and ion absorption and distribution in aloe vera under salt stress. *Journal of plant physiology and molecular biology.* **32,** 73-8

400. Liu, H., Liu, Y., Yu, B., Liu, Z., and Zhang, W. (2004) Increased polyamines conjugated to tonoplast vesicles correlate with maintenance

of the H^+-ATPase and H^+-PPase activities and enhanced osmotic stress tolerance in wheat. *J.Plant Growth Regul.* **23,** 156-65

401. Zhang, W.H., Chen, Q., and Liu, Y.L. (2002) Relationship between tonoplast H^+-ATPase activity, ion uptake and calcium in barley roots under NaCl stress. *Acta Botanica Sinica.* **44,** 667-72

402. Nakamura, Y., Kasamo, K., Sakata, M., and Ohta, E. (1992) Stimulation of the Extrusion of Protons and H^+-ATPase Activities with the Decline in Pyrophosphatase Activity of the Tonoplast in Intact Mung Bean Roots under High-NaCl Stress and Its Relation to External Levels of Ca^{2+} Ions. *Plant Cell Physiol.* **33,** 139-49

403. Ueda, A., Kathiresan, A., Bennett, J., and Takabe, T. (2006) Comparative transcriptome analyses of barley and rice under salt stress. *Theor.Appl. Genet.* **112,** 1286-94

404. Tanaka, Y., Chiba, K., Maeda, M., and Maeshima, M. (1993) Molecular cloning of cDNA for vacuolar membrane proton-translocating inorganic pyrophosphatase in *Hordeum vulgare. Biochem.Biophys.Res.Commun.* **190,** 1110-4

405. Gao, F., Gao, Q., Duan, X., Yue, G., Yang, A., and Zhang, J. (2006) Cloning of an H^+-PPase gene from *Thellungiella halophila* and its heterologous expression to improve tobacco salt tolerance. *J.Exp.Bot.* **57,** 3259-70

406. Colombo, R.C., and Cerana, R. (1993) Enhanced activity of tonoplast pyrophosphatase in NaCl-grown cells of *Daucus carota*. *J.Plant Physiol.* **142,** 226-9

407. Zhang, M., Fang, Y., Liang, Z., and Huang, L. (2012) Enhanced expression of vacuolar H^+-ATPase subunit E in the roots is associated with the adaptation of *Broussonetia papyrifera* to salt stress. *PLoS One.* **7,** e48183

408. Zhang, W., Diao, F., Yu, B., and Lin, Y. (1998) H^+-ATPase and H^+-transport activities in tonoplast vesicles from barley roots under salt stress and influence of calcium and abscisic acid. *J.Plant Nutr.* **21,** 447-58

409. Hörtensteiner, S., Martinoia, E., and Amrhein, N. (1994) Factors affecting the re-formation of vacuoles in evacuolated protoplasts and the expression of the two vacuolar proton pumps. *Planta.* **192,** 395-403

410. Kabala, K., and Klobus, G. (2008) Modification of vacuolar proton pumps in cucumber roots under salt stress. *J.Plant Physiol.* **165,** 1830-7

411. Otoch, M.L.O., Sobreira, A.C.M., de Aragão, M. E. F., Orellano, E.G., Lima, M.G.S., and de Melo, D.F. (2001) Salt modulation of vacuolar H^+-ATPase and H^+-pyrophosphatase activities in *Vigna unguiculata. J.Plant Physiol.* **158,** 545-51

412. Brini, F., Gaxiola, R.A., Berkowitz, G.A., and Masmoudi, K. (2005) Cloning and characterization of a wheat vacuolar cation/proton antiporter and pyrophosphatase proton pump. *Plant Physiol.Biochem.* **43,** 347-54

413. Löw, R., and Rausch, T. (1996) In suspension-cultured *Daucus carota* cells salt stress stimulates H^+-transport but not ATP hydrolysis of the V-ATPase. *J.Exp.Bot.* **47,** 1725-32

414. Yi, X., Sun, Y., Yang, Q., Guo, A., Chang, L., Wang, D., Tong, Z., Jin, X., Wang, L., Yu, J., Jin, W., Xie, Y., and Wang, X. (2014) Quantitative proteomics of *Sesuvium portulacastrum* leaves revealed that ion transportation by V-ATPase and sugar accumulation in chloroplast played crucial roles in halophyte salt tolerance. *J Proteomics.* **99,** 84-100

415. Guo, S., Yin, H., Zhang, X., Zhao, F., Li, P., Chen, S., Zhao, Y., and Zhang, H. (2006) Molecular cloning and characterization of a vacuolar H^+-pyrophosphatase gene, SsVP, from the halophyte *Suaeda salsa* and its overexpression increases salt and drought tolerance of *Arabidopsis. Plant Mol.Biol.* **60,** 41-50

416. Epimashko, S., Fischer-Schliebs, E., Christian, A.L., Thiel, G., and Lüttge, U. (2006) Na^+/H^+-transporter, H^+-pumps and an aquaporin in light and heavy tonoplast membranes from organic acid and NaCl accumulating vacuoles of the annual facultative CAM plant and halophyte *Mesembryanthemum crystallinum* L. *Planta.* **224,** 944-51

417. Parks, G.E., Dietrich, M.A., and Schumaker, K.S. (2002) Increased vacuolar Na^+/H^+ exchange activity in *Salicornia bigelovii* Torr. in response to NaCl. *J.Exp.Bot.* **53,** 1055-65

418. Wang, B., Lüttge, U., and Ratajczak, R. (2001) Effects of salt treatment and osmotic stress on V-ATPase and V-PPase in leaves of the halophyte *Suaeda salsa. J.Exp.Bot.* **52,** 2355-65

419. Hamada, A., Shono, M., Xia, T., Ohta, M., Hayashi, Y., Tanaka, A., and Hayakawa, T. (2001) Isolation and characterization of a Na^+/H^+ antiporter gene from the halophyte *Atriplex gmelini. Plant Mol.Biol.* **46,** 35-42

420. Barkla, B.J., Zingarelli, L., Blumwald, E., and Smith, J. (1995) Tonoplast Na^+/H^+ Antiport Activity and Its Energization by the Vacuolar H^+-ATPase in the Halophytic Plant *Mesembryanthemum crystallinum* L. *Plant Physiol.* **109,** 549-56

421. Zhang, J.L., and Shi, H. (2013) Physiological and molecular mechanisms of plant salt tolerance. *Photosynthesis Res.* **115,** 1-22

422. Nogueira de Oliveira, L. M., de Menezes Sobreira, A. C., Costa, J.H., Otoch, M.L.O., Maeshima, M., and de Melo, D.F. (2011) Chilling-induced changes of vacuolar proton pumps in hypocotyls of *Vigna unguiculata. Plant growth regulation.* **64,** 211-9

423. Ghasernnezhad, M., Marsh, K., Shilton, R., Babalar, M., and Woolf, A. (2008) Effect of hot water treatments on chilling injury and heat damage in 'satsuma' mandarins: Antioxidant enzymes and vacuolar ATPase, and pyrophosphatase. *Postharvest Biol.Technol.* **48,** 364-71

424. Darley, C.P., Davies, J.M., and Sanders, D. (1995) Chill-Induced Changes in the Activity and Abundance of the Vacuolar Proton-Pumping Pyrophosphatase from Mung Bean Hypocotyls. *Plant Physiol.* **109,** 659-65

425. Ozolina, N.V., Kolesnikova, E.V., Nurminsky, V.N., Nesterkina, I.S., Dudareva, L.V., Tretyakov, A.V., and Salyaev, R.K. (2011) Redox-Dependence of Transport Activity of Tonoplast Proton Pumps: Effects of Nitrogen Oxide Exposure in the Course of Ontogenesis and of Hypo- and Hyper-Osmotic Stress. *Biologicheskie membrany.* **28,** 284-9

426. Chiu, F.S., Hsu, S.H., Chen, J.H., Hsiao, Y.Y., Pan, Y.J., Van, R.C., Huang, Y.T., Tseng, F.G., Chou, W.M., Shih, K.F., and Pan, R.L. (2006) Differential response of vacuolar proton pumps to osmotica. *Functional plant biology.* **33,** 195-206

427. Wang, T., Li, J., Guo, S.R., Gao, H.B., and Wang, S.P. (2005) [Effects of exogenous polyamines on the growth and activities of H^+-ATPase and H^+-PPase in cucumber seedling roots under hypoxia stress]. *Journal of plant physiology and molecular biology.* **31,** 637-42

428. Li, X., Guo, C., Gu, J., Duan, W., Zhao, M., Ma, C., Du, X., Lu, W., and Xiao, K. (2014) Overexpression of VP, a vacuolar H^+-pyrophosphatase gene in wheat (*Triticum aestivum* L.), improves tobacco plant growth under P_i and N deprivation, high salinity, and drought. *J.Exp.Bot.* **65,** 683-96

429. Kabala, K., Janicka-Russak, M., and Klobus, G. (2010) Different responses of tonoplast proton pumps in cucumber roots to cadmium and copper. *J.Plant Physiol.* **167,** 1328-35

430. Ruan, H.H., Shen, W.B., and Xu, L.L. (2004) Nitric oxide modulates the activities of plasma membrane H^+-ATPase and PPase in wheat seedling roots and promotes the salt tolerance against salt stress. *Acta Botanica Sinica.* **46,** 415-22

431. Pradedova, E.V., Sapega, J.G., Jeleznich, A.O., Ozolina, N.V., and Salyaev, R.K. (2006) Effects of redox agents on the activity of V-ATPase and H^+-pyrophosphatase in red beet root. *Biologicheskie membrany.* **23,** 364-9

432. Sikora, A., Hillmer, S., and Robinson, D.G. (1998) Sucrose starvation causes a loss of immunologically detectable pyrophosphatase and V-ATPase in the tonoplast of suspension-cultured tobacco cells. *J.Plant Physiol.* **152,** 207-12

433. Toll, E., Crespi, P., Greppin, H., and Castillo, F.J. (1998) Effect of ozone and sulphur dioxide on membrane enzyme activities of *Pinus sylvestris* needles. *Trees.* **13,** 13-8

434. Kasai, M., Nakamura, T., Kudo, N., Sato, H., Maeshima, M., and Sawada, S. (1998) The activity of the root vacuolar H^+-pyrophosphatase in rye plants grown under conditions deficient in mineral nutrients. *Plant Cell Physiol.* **39,** 890-4

435. Schneider, T., Schellenberg, M., Meyer, S., Keller, F., Gehrig, P., Riedel, K., Lee, Y., Eberl, L., and Martinoia, E. (2009) Quantitative detection of changes in the leaf-mesophyll tonoplast proteome in dependency of a cadmium exposure of barley (*Hordeum vulgare* L.) plants. *Proteomics.* **9,** 2668-77

436. Martins, V., Hanana, M., Blumwald, E., and Gerós H. (2012) Copper transport and compartmentation in grape cells. *Plant Cell Physiol.* **53,** 1866-80

437. Zhang, Y., Han, X., Chen, X., Jin, H., and Cui, X. (2009) Exogenous nitric oxide on antioxidative system and ATPase activities from tomato seedlings under copper stress. *Scientia horticulturae.* **123,** 217-23

438. Santos, L.A., Bucher, C.A., de Souza, S.R., and Fernandes, M.S. (2009) Effects of Nitrogen Stress on Proton-Pumping and Nitrogen Metabolism in Rice. *J.Plant Nutr.* **32,** 549-64

439. Ramos, A.C., Martins, M.A., Okorokova-Façanha, A.L., Olivares, F.L., Okorokov, L.A., Sepúlveda, N., Feijó, J.A., and Façanha, A.R. (2009) Arbuscular mycorrhizal fungi induce differential activation of the plasma membrane and vacuolar H^+ pumps in maize roots. *Mycorrhiza.* **19,** 69-80

440. Ramos, A.C., Martins, M.A., and Facanha, A.R. (2005) Atpase and pyrophosphatase activities in corn root microsomes colonized with arbuscular mycorrhizal fungi. *Rev. Bras. Ciênc. Solo.* **29,** 207-13

441. Yang, S., Maeshima, M., Tanaka, Y., and Komatsu, S. (2003) Modulation of vacuolar H^+-pumps and aquaporin by phytohormones in rice seedling leaf sheaths. *Biol.Pharm.Bull.* **26,** 88-92

442. Grebe, M. (2005) Plant biology. Enhanced: growth by auxin: when a weed needs acid. *Science.* **310,** 60-1

443. Fukuda, A., and Tanaka, Y. (2006) Effects of ABA, auxin, and gibberellin on the expression of genes for vacuolar H^+-inorganic pyrophosphatase, H^+-ATPase subunit A, and Na^+/H^+ antiporter in barley. *Plant Physiol Biochem.* **44,** 351-8

444. Pradedova, E.V., Ozolina, N.V., and Salyaev, R.K. (2004) Effect of phytohormones on the activity of H^+-ATPase and H^+-pyrophosphatase of red beet root tonoplast *Beta vulgaris* L. under conditions of different buffer systems. *Biologicheskie membrany.* **21,** 15-8

445. Salyaev, R.K., Ozolina, N.V., and Pradedova, E.V. (1999) Effects of exogenous phytohormones and kinetin on the hydrolytic activity of proton pumps in the tonoplast of red beet at different stages of plant development. *Russian journal of plant physiology.* **46,** 1-4

446. Ozolina, N.V., Pradedova, E.V., and Salyaev, R.K. (1996) Phytohormone effects on hydrolytic activity of phosphohydrolases in red beet (*Beta vulgaris* L) tonoplasts. *Plant growth regulation.* **19,** 189-91

447. Wang, Z.N., You, R.L., and Chen-Zhu, X.Z. (2001) Effects of colchicine on the accumulation of vacuolar H^+-pyrophosphatase and H^+-ATPase in germinating *Acacia mangium* seeds and the recovery effects by sucrose, indole butyric acid and 6-benzyladenine. *Plant growth regulation.* **34,** 293-303

448. Kasai, M., Yamamoto, Y., and Matsumoto, H. (1994) *In Vivo* Treatment of Barley Roots with Vanadate Increases Vacuolar H^+-Translocating ATPase Activity of the Tonoplast-Enriched Membrane Vesicles and the Level of Endogenous ABA. *Plant Cell Physiol.* **35,** 291-5

449. Kasai, M., Yamamoto, Y., Maeshima, M., and Matsumoto, H. (1993) Effects of *in vivo* Treatment with Abscisic Acid and/or Cytokinin on Activities of Vacuolar H^+ Pumps of Tonoplast-Enriched Membrane Vesicles Prepared from Barley Roots. *Plant Cell Physiol.* **34,** 1107-15

450. Park, M.Y., Chung, M.S., Koh, H.S., Lee, D.J., Ahn, S.J., and Kim, C.S. (2009) Isolation and functional characterization of the *Arabidopsis* salt-tolerance 32 (AtSAT32) gene associated with salt tolerance and ABA signaling. *Physiol.Plantarum.* **135,** 426-35

451. Gamboa, M.C., Baltierra, F., Leon, G., and Krauskopf, E. (2013) Drought and salt tolerance enhancement of transgenic Arabidopsis by overexpression of the vacuolar pyrophosphatase 1 (EVP1) gene from *Eucalyptus globulus. Plant Physiol.Biochem.* **73,** 99-105

452. Pradedova, E.V., Ozolina, N.V., Korzun, A.M., and Salyaev, R.K. (2002) Effect of epibrassinolide on activities of the tonoplast H^+-ATPase and H^+-pyrophosphatase under conditions of high and low KCl concentrations. *Biologiceskie membrany.* **19,** 216-20

453. Rizhong, Z., Cuifang, D., Xiaoyuan, L., Weimin, T., and Zhiyi, N. (2009) Vacuolar-type inorganic pyrophosphatase located on the rubber particle in the latex is an essential enzyme in regulation of the rubber biosynthesis in *Hevea brasiliensis. Plant science.* **176,** 602-7

454. Li, Z., Zhou, M., Hu, Q., Reighard, S., Yuan, S., Yuan, N., San, B., Li, D., Jia, H., and Luo, H. (2012) Manipulating expression of tonoplast transporters. *Methods Mol.Biol.* **913,** 359-69

455. Qin, H., Gu, Q., Kuppu, S., Sun, L., Zhu, X., Mishra, N., Hu, R., Shen, G., Zhang, J., Zhang, Y., Zhu, L., Zhang, X., Burow, M., Payton, P., and Zhang, H. (2013) Expression of the *Arabidopsis* vacuolar H^+-pyrophosphatase gene AVP1 in peanut to improve drought and salt tolerance. *Plant Biotechnology Reports.* **7,** 345-55

456. Khoudi, H., Maatar, Y., Brini, F., Fourati, A., Ammar, N., and Masmoudi, K. (2013) Phytoremediation potential of *Arabidopsis thaliana*, expressing ectopically a vacuolar proton pump, for the industrial waste phosphogypsum. *Environ.Sci.Pollut.Res.Int.* **20,** 270-80

457. Khoudi, H., Maatar, Y., Gouiaa, S., and Masmoudi, K. (2012) Transgenic tobacco plants expressing ectopically wheat H^+-pyrophosphatase (H^+-PPase) gene TaVP1 show enhanced accumulation and tolerance to cadmium. *J.Plant Physiol.* **169,** 98-103

458. Bao, A.K., Wang, S.M., Wu, G.Q., Xi, J.J., Zhang, J.L., and Wang, C.M. (2009) Overexpression of the Arabidopsis H^+-PPase enhanced resistance to salt and drought stress in transgenic alfalfa (*Medicago sativa* L.). *Plant science.* **176,** 232-40

459. Lv, S.L., Lian, L.J., Tao, P.L., Li, Z.X., Zhang, K.W., and Zhang, J.R. (2009) Overexpression of *Thellungiella halophila* H^+-PPase (TsVP) in cotton enhances drought stress resistance of plants. *Planta.* **229,** 899-910

460. Lv, S., Zhang, K., Gao, Q., Lian, L., Song, Y., and Zhang, J. (2008) Overexpression of an H^+-PPase gene from *Thellungiella halophila* in cotton enhances salt tolerance and improves growth and photosynthetic performance. *Plant Cell Physiol.* **49,** 1150-64

461. Li, B., Wei, A., Song, C., Li, N., and Zhang, J. (2008) Heterologous expression of the TsVP gene improves the drought resistance of maize. *Plant Biotechnol J.* **6,** 146-59

462. D'yakova, E.V., Rakitin, A.L., Kamionskaya, A.M., Baikov, A.A., Lahti, R., Ravin, N.V., and Skryabin, K.G. (2006) A Study of the Effect of Expression of the Gene Encoding the Membrane H^+-Pyrophosphatase of *Rhodospirillum rubrum* on Salt Resistance of Transgenic Tobacco Plants. *Doklady. Biological sciences.* **409,** 346-8

463. Park, S., Li, J., Pittman, J.K., Berkowitz, G.A., Yang, H., Undurraga, S., Morris, J., Hirschi, K.D., and Gaxiola, R.A. (2005) Up-regulation of a H^+-pyrophosphatase (H^+-PPase) as a strategy to engineer drought-resistant crop plants. *Proc.Natl.Acad.Sci.U.S.A.* **102,** 18830-5

464. Wang, J.W., Wang, H.Q., Xiang, W.W., and Chai, T.Y. (2014) A *Medicago truncatula* H^+-pyrophosphatase gene, MtVP1, improves sucrose accumulation and anthocyanin biosynthesis in potato (*Solanum tuberosum* L.). *Genetics and molecular research.* **13,** 3615-26

465. Zhang, H., Shen, G., Kuppu, S., Gaxiola, R., and Payton, P. (2011) Creating drought- and salt-tolerant cotton by overexpressing a vacuolar pyrophosphatase gene. *Plant.Signal.Behav.* **6,** 861-3

466. Pasapula, V., Shen, G., Kuppu, S., Paez-Valencia, J., Mendoza, M., Hou, P., Chen, J., Qiu, X., Zhu, L., Zhang, X., Auld, D., Blumwald, E., Zhang, H., Gaxiola, R., and Payton, P. (2011) Expression of an *Arabidopsis* vacuolar H^+-pyrophosphatase gene (AVP1) in cotton improves drought- and salt tolerance and increases fibre yield in the field conditions. *Plant Biotechnol J.* **9,** 88-99

467. Duan, X.G., Yang, A.F., Gao, F., Zhang, S.L., and Zhang, J.R. (2007) Heterologous expression of vacuolar H^+-PPase enhances the electrochemical gradient across the vacuolar membrane and improves tobacco cell salt tolerance. *Protoplasma.* **232,** 87-95

468. Zhang, J., Li, J., Wang, X., and Chen, J. (2011) OVP1, a vacuolar H^+-translocating inorganic pyrophosphatase (V-PPase), overexpression improved rice cold tolerance. *Plant Physiol Biochem.* **49,** 33-8

469. Schulze, W.X., Schneider, T., Starck, S., Martinoia, E., and Trentmann, O. (2012) Cold acclimation induces changes in *Arabidopsis* tonoplast protein abundance and activity and alters phosphorylation of tonoplast monosaccharide transporters. *Plant J.* **69,** 529-41

470. Gouiaa, S., Khoudi, H., Leidi, E.O., Pardo, J.M., and Masmoudi, K. (2012) Expression of wheat Na^+/H^+ antiporter TNHXS1 and H^+-pyrophosphatase TVP1 genes in tobacco from a bicistronic transcriptional unit improves salt tolerance. *Plant Mol.Biol.* **79,** 137-55

471. Wei, A., He, C., Li, B., Li, N., and Zhang, J. (2011) The pyramid of transgenes TsVP and BetA effectively enhances the drought tolerance of maize plants. *Plant Biotechnol J.* **9,** 216-29

472. Meng, X., Xu, Z., and Song, R. (2011) Molecular cloning and characterization of a vacuolar H^+-pyrophosphatase from *Dunaliella viridis. Mol.Biol.Rep.* **38,** 3375-82

473. Yagisawa, F., Nishida, K., Kuroiwa, H., Nagata, T., and Kuroiwa, T. (2007) Identification and mitotic partitioning strategies of vacuoles in the unicellular red alga *Cyanidioschyzon merolae*. *Planta.* **226,** 1017-29

474. Ikeda, M., Satoh, S., Maeshima, M., Mukohata, Y., and Moritani, C. (1991) A vacuolar ATPase and pyrophosphatase in *Acetabularia acetabulum*. *Biochim.Biophys.Acta.* **1070,** 77-82

475. Berkelman, T., and Lagarias, J.C. (1990) Calcium Transport in the Green Alga *Mesotaenium caldariorum*: Preliminary Characterization and Subcellular Distribution. *Plant Physiol.* **93,** 748-57

476. Sasaki, T., Pronina, N.A., Maeshima, M., Iwasaki, I., Kurano, N., and Miyachi, S. (1999) Development of vacuoles and vacuolar H^+-ATPase

activity under extremely high CO_2 conditions in *Chlorococcum littorale* cells. *Plant biology.* **1,** 68-75

477. Faraday, C.D., Spanswick, R.M., and Bisson, M.A. (1996) Plasma membrane isolation from freshwater and salt-tolerant species of *Chara*: antibody cross-reactions and phosphohydrolase activities. *J.Exp.Bot.* **47,** 589-94

478. Nakanishi, Y., Matsuda, N., Aizawa, K., Kashiyama, T., Yamamoto, K., Mimura, T., Ikeda, M., and Maeshima, M. (1999) Molecular cloning and sequencing of the cDNA for vacuolar H^+-pyrophosphatase from *Chara corallina*. *Biochim.Biophys.Acta.* **1418,** 245-50

479. McIntosh, M.T., Drozdowicz, Y.M., Laroiya, K., Rea, P.A., and Vaidya, A.B. (2001) Two classes of plant-like vacuolar-type H^+-pyrophosphatases in malaria parasites. *Mol.Biochem.Parasitol.* **114,** 183-95

480. Kirk, K. (2004) Channels and transporters as drug targets in the Plasmodium-infected erythrocyte. *Acta Trop.* **89,** 285-98

481. Rohloff, P., Montalvetti, A., and Docampo, R. (2004) Acidocalcisomes and the contractile vacuole complex are involved in osmoregulation in *Trypanosoma cruzi*. *J.Biol.Chem.* **279,** 52270-81

482. Mallo, N., Lamas, J., Piazzon, C., and Leiro, J.M. (2014) Presence of a plant-like proton-translocating pyrophosphatase in a scuticociliate parasite and its role as a possible drug target. *Parasitology.* **14,** 1-14

483. Hill, J.E., Scott, D.A., Luo, S., and Docampo, R. (2000) Cloning and functional expression of a gene encoding a vacuolar-type proton-translocating pyrophosphatase from *Trypanosoma cruzi*. *Biochem.J.* **351,** 281-8

484. Pérez-Castiñeira, J.R., Gómez-García, R., López-Marqués, R.L., Losada, M., and Serrano, A. (2001) Enzymatic systems of inorganic pyrophosphate bioenergetics in photosynthetic and heterotrophic protists: remnants or metabolic cornerstones?. *Int Microbiol.* **4,** 135-42

485. Luo, S., Ruiz, F.A., and Moreno, S.N. (2005) The acidocalcisome Ca^{2+}-ATPase (TgA1) of *Toxoplasma gondii* is required for polyphosphate storage, intracellular calcium homeostasis and virulence. *Mol.Microbiol.* **55,** 1034-45

486. Saliba, K.J., Allen, R.J., Zissis, S., Bray, P.G., Ward, S.A., and Kirk, K. (2003) Acidification of the malaria parasite's digestive vacuole by a H^+-ATPase and a H^+-pyrophosphatase. *J.Biol.Chem.* **278,** 5605-12

487. Scott, D.A., de Souza, W., Benchimol, M., Zhong, L., Lu, H.G., Moreno, S.N., and Docampo, R. (1998) Presence of a plant-like proton-pumping pyrophosphatase in acidocalcisomes of *Trypanosoma cruzi*. *J.Biol. Chem.* **273,** 22151-8

488. Docampo, R., Ulrich, P., and Moreno, S.N. (2010) Evolution of acidocalcisomes and their role in polyphosphate storage and osmoregulation in eukaryotic microbes. *Philos Trans R Soc Lond B Biol Sci.* **365,** 775-84

489. Sheiner, L., and Soldati-Favre, D. (2008) Protein trafficking inside *Toxoplasma gondii*. *Traffic.* **9,** 636-46

490. Docampo, R., de Souza, W., Miranda, K., Rohloff, P., and Moreno, S.N. (2005) Acidocalcisomes - conserved from bacteria to man. *Nat Rev Microbiol.* **3,** 251-61

491. de Souza, W., and da Cunha-e-Silva, N.L. (2003) Cell fractionation of parasitic protozoa: a review. *Mem Inst Oswaldo Cruz.* **98,** 151-70

492. Docampo, R., and Moreno, S.N. (2001) The acidocalcisome. *Mol. Biochem.Parasitol.* **114,** 151-9

493. Rodrigues, C.O., Scott, D.A., and Docampo, R. (1999) Characterization of a vacuolar pyrophosphatase in *Trypanosoma brucei* and its localization to acidocalcisomes. *Mol.Cell.Biol.* **19,** 7712-23

494. Luo, S., Vieira, M., Graves, J., Zhong, L., and Moreno, S.N. (2001) A plasma membrane-type Ca^{2+}-ATPase co-localizes with a vacuolar H^+-pyrophosphatase to acidocalcisomes of *Toxoplasma gondii*. *EMBO J.* **20,** 55-64

495. Miranda, K., Docampo, R., Grillo, O., Franzen, A., Attias, M., Vercesi, A., Plattner, H., Hentschel, J., and de Souza, W. (2004) Dynamics of polymorphism of acidocalcisomes in *Leishmania* parasites. *Histochem. Cell Biol.* **121,** 407-18

496. Rodrigues, C.O., Ruiz, F.A., Rohloff, P., Scott, D.A., and Moreno, S.N. (2002) Characterization of isolated acidocalcisomes from *Toxoplasma gondii* tachyzoites reveals a novel pool of hydrolyzable polyphosphate. *J.Biol.Chem.* **277,** 48650-6

497. Docampo, R., Jimenez, V., King-Keller, S., Li, Z.H., and Moreno, S.N. (2011) The role of acidocalcisomes in the stress response of *Trypanosoma cruzi*. *Adv Parasitol.* **75,** 307-24

498. Liu, J., Pace, D., Dou, Z., King, T., Guidot, D., Li, Z., Carruthers, V., and Moreno, S.N.J. (2014) A vacuolar-H^+ -pyrophosphatase (TgVP1) is required for microneme secretion, host cell invasion, and extracellular survival of *Toxoplasma gondii*. *Mol.Microbiol.* **93,** 698-712

499. Rohloff, P., Miranda, K., Rodrigues, J.C., Fang, J., Galizzi, M., Plattner, H., Hentschel, J., and Moreno, S.N. (2011) Calcium Uptake and Proton Transport by Acidocalcisomes of *Toxoplasma gondii*. *PLoS One.* **6,** e18390

500. Soares Medeiros, L.C., Moreira, B.L., Miranda, K., de Souza, W., Plattner, H., Hentschel, J., and Barrabin, H. (2005) A proton pumping pyrophosphatase in acidocalcisomes of *Herpetomonas* sp. *Mol.Biochem. Parasitol.* **140,** 175-82

501. van Schalkwyk, D.A., Chan, X.W., Misiano, P., Gagliardi, S., Farina, C., and Saliba, K.J. (2010) Inhibition of *Plasmodium falciparum* pH regulation by small molecule indole derivatives results in rapid parasite death. *Biochem.Pharmacol.* **79,** 1291-9

502. Martinez, R., Wang, Y., Benaim, G., Benchimol, M., de Souza, W., Scott, D.A., and Docampo, R. (2002) A proton pumping pyrophosphatase in the Golgi apparatus and plasma membrane vesicles of *Trypanosoma cruzi*. *Mol.Biochem.Parasitol.* **120,** 205-13

503. van Schalkwyk, D.A., Saliba, K.J., Biagini, G.A., Bray, P.G., and Kirk, K. (2013) Loss of pH control in *Plasmodium falciparum* parasites subjected to oxidative stress. *PLoS One.* **8,** e58933

504. Schoijet, A.C., Miranda, K., Girard-Dias, W., de Souza, W., Flawiá, M.M., Torres, H.N., Docampo, R., and Alonso, G.D. (2008) A *Trypanosoma cruzi* phosphatidylinositol 3-kinase (TcVps34) is involved in osmoregulation and receptor-mediated endocytosis. *J.Biol.Chem.* **283,** 31541-50

505. Bentley, S.D., Chater, K.F., Cerdeño-Tárraga, A.M., Challis, G.L., Thomson, N.R., James, K.D., Harris, D.E., Quail, M.A., Kieser, H., Harper, D., Bateman, A., Brown, S., Chandra, G., Chen, C.W., Collins, M., Cronin, A., Fraser, A., Goble, A., Hidalgo, J., Hornsby, T., Howarth, S., Huang, C.H., Kieser, T., Larke, L., Murphy, L., Oliver, K., O'Neil, S., Rabbinowitsch, E., Rajandream, M.A., Rutherford, K., Rutter, S., Seeger, K., Saunders, D., Sharp, S., Squares, R., Squares, S., Taylor, K., Warren, T., Wietzorrek, A., Woodward, J., Barrell, B.G., Parkhill, J., and Hopwood, D.A. (2002) Complete genome sequence of the model actinomycete *Streptomyces coelicolor* A3(2). *Nature.* **417,** 141-7

506. Bradford, M.M. (1976) A rapid and sensitive method for the quantitation of microgram quantities of protein utilizing the principle of protein-dye binding. *Anal.Biochem.* **72,** 248-54

507. Towbin, H., Staehelin, T., and Gordon, J. (1979) Electrophoretic transfer of proteins from polyacrylamide gels to nitrocellulose sheets: procedure and some applications. *Proc.Natl.Acad.Sci.U.S.A.* **76,** 4350-4

508. Schneider, C.A., Rasband, W.S., and Eliceiri, K.W. (2012) NIH Image to ImageJ: 25 years of image analysis. *Nat Methods.* **9,** 671-5

509. Baykov, A.A., and Avaeva, S.M. (1981) A simple and sensitive apparatus for continuous monitoring of orthophosphate in the presence of acid-labile compounds. *Anal.Biochem.* **116,** 1-4

510. Casadio, R. (1991) Measurements of transmembrane pH differences of low extents in bacterial chromatophores. *European Biophysics Journal.* **19,** 189-201

511. Altschul, S.F., Gish, W., Miller, W., Myers, E.W., and Lipman, D.J. (1990) Basic local alignment search tool. *J.Mol.Biol.* **215,** 403-10

512. Edgar, R.C. (2004) MUSCLE: multiple sequence alignment with high accuracy and high throughput. *Nucleic Acids Res.* **32,** 1792-7

513. Ronquist, F., and Huelsenbeck, J.P. (2003) MrBayes 3: Bayesian phylogenetic inference under mixed models. *Bioinformatics.* **19,** 1572-4

514. Stamatakis, A. (2014) RAxML version 8: a tool for phylogenetic analysis and post-analysis of large phylogenies. *Bioinformatics.* **30,** 1312-3

515. Schlegel, K., Leone, V., Faraldo-Gómez, J.D., and Müller, V. (2012) Promiscuous archaeal ATP synthase concurrently coupled to Na^+ and H^+ translocation. *Proc.Natl.Acad.Sci.U.S.A.* **109,** 947-52

516. Laubinger, W., and Dimroth, P. (1989) The sodium ion translocating adenosinetriphosphatase of *Propionigenium modestum* pumps protons at low sodium ion concentrations. *Biochemistry (N.Y.).* **28,** 7194-8